BEST AVAILABLE IMAGES

Defective images within this document are accurate representations of the original documents submitted by the applicant.

Defects in the images may include (but are not limited to):

- BLACK BORDERS
- TEXT CUT OFF AT TOP, BOTTOM OR SIDES
- FADED TEXT
- ILLEGIBLE TEXT
- SKEWED/SLANTED IMAGES
- COLORED PHOTOS
- BLACK OR VERY BLACK AND WHITE DARK PHOTOS
- GRAY SCALE DOCUMENTS

IMAGES ARE BEST AVAILABLE COPY.

As rescanning documents *will not* correct images, please do not report the images to the Image Problem Mailbox.

REMARKS

In the Office Action of November 25, 2003, the Examiner rejected claims 109-142 under 35 U.S.C. § 112, first paragraph, for lack of enablement. The Examiner also raised a double patenting objection against claims 106-142.

Applicants respectfully traverse these rejections and request that the Examiner consider the following remarks in response to the Office Action.

Claim Rejections:

35 U.S.C. 112, First Paragraph

Applicants thank the Examiner for withdrawing the rejection of claims 106-108 under 35 U.S.C. § 112, first paragraph for lack of enablement. Specifically, the Examiner noted that page 31 of the specification provides an alternative utility for expression of a protein *in vivo,* namely monitoring cell migration. Based on this alternative utility, the Examiner has withdrawn the rejection of claims 106-108. While Applicants agree that claims 106-108 are supported by this alternative utility, Applicants maintain that claims 106-108 are supported by the therapeutic utility relied on throughout prosecution of this application.

The Examiner has maintained rejection of claims 109-142 under 35 U.S.C. § 112, first paragraph for lack of enablement. Specifically, the Examiner dismisses as irrelevant the data set forth in the Declaration of Elizabeth G. Nabel, M.D. (hereafter the "Nabel Declaration") filed with the response submitted July 30, 2003. The Nabel Declaration demonstrates that the expression of therapeutic levels of the p27 protein, achieved using the claimed methods, effects treatment of a cardiovascular condition. More specifically, the Nabel Declaration demonstrates that porcine vascular smooth muscle cells (VSMCs) transformed to express p27, and then instilled into the pig from which they originated, have the therapeutic utility of reducing intimal hyperplasia.

Nonetheless, the Examiner has dismissed the p27 data in the Nabel declaration because p27 was allegedly not known until 1994. In rejecting the data, the Examiner argues that enablement is to be judged as of the filing date, March 31, 1989 in this case, and concludes that the p27 data is not sufficient to support enablement. More specifically, the Examiner argues, based on *In re Glass,* 181 USPQ 31 (CCPA 1974), that "if a disclosure is insufficient as of the time it is filed, it cannot be made sufficient, while the application is still pending by later publications or evidence which add to the knowledge of the art so that the disclosure, supplemented by such publications, would suffice to enable the practice of the invention."

Despite the quoted passage from *In re Glass*, the Examiner's arguments are not based on the sufficiency of the disclosure in the present application. As the Examiner notes, numerous proteins are disclosed that could be used in the claimed invention. The Examiner also notes that the working examples demonstrate that the claimed method can be used to achieve detectable expression levels of the β-gal gene product. However, the Examiner argues that there is no data demonstrating that achieving expression of a therapeutic protein using the claimed method would result in treatment of any disease or condition. Such reasoning appears directed to the operativeness of the claimed invention. Where a dispute involves a device disclosed in sufficient detail that one of ordinary skill in the art could construct it, but operativeness is challenged, the courts do not prohibit operativeness from being demonstrated by actual reduction to practice at any time. *See In re Langer*, 503 F.2d 1380, 1391, 183 USPQ 288, 297 (CCPA 1974).

The Nabel declaration supplies data demonstrating that the claimed method is operative, and therefore, should be considered. It is irrelevant that this data uses a therapeutic protein discovered after the filing of the application. The Examiner's challenge is to the *claimed* method, not to any specific protein used with that method. Moreover, the claimed method is not limited to use with any specific protein. In fact, at page 26, the specification states that the "range of recombinant proteins which may be expressed in these cells is broad and varied." Therefore, in demonstrating that the

claimed invention is enabled, Applicants are neither required to use, nor limited to using, only those proteins disclosed in the specification, or those known in the art at the time the application was filed, to demonstrate a therapeutic effect. *See Quigg v. Gould,* 822 F.2d 1074, 1078, 3 USPQ2d 1302, 1305 (Fed. Cir. 1987) (post-filing evidence is relevant to enablement if it proves that the invention works as broadly as claimed).

In any event, even if the Examiner rejects the relevancy of the data in the Nabel declaration, the claimed invention is still enabled. The Examiner's rejection is based on the contention that there is no data, either in the specification or made of record, demonstrating that a *therapeutic* protein achieves a therapeutic effect when used in the vicinity of where such an effect is desired. In *In re Strahilevitz,* 668 F.2d 1229, 212 USPQ 561 (CCPA 1982), the examiner and Board of Patent Appeals and Interferences made similar rejections, alleging that claims to methods and devices for removing a hapten, antigen, or antibody from the blood of a living mammal were not enabled because no dialysis or absorption data were presented in the specification. *Id.* at 563. Relying on both the specification and various articles indicating what was known in the art, the court reversed the examiner and the Board and found that the specification at issue was enabling. *Id.* at 565. Similar to *In re Strahilevitz,* in the present situation when various art references are considered in combination with the specification, the specification enables one of ordinary skill in the art to practice the claimed invention.

First, the specification discloses and demonstrates that cells transformed to express β-gal and subsequently implanted using the methods described in the specification expressed the β-gal protein for at least six weeks following transplantation. Specification at pages 37-39. Moreover, Applicants demonstrated that this expression is in the vicinity of neointimal cells, which proliferate in response to catheter injury. Specification at p. 39-41. Based on this disclosure and information in the art, one of skill in the art would appreciate that no undue experimentation would be needed to achieve transplantation of cells transformed to express a therapeutic protein, such that expression of the therapeutic protein in the vicinity of proliferating neointimal cells would exert a therapeutic effect.

In this regard, St. Louis *et al.* describe the *ex vivo* transformation of mouse fibroblast cells with retroviruses containing human factor IX cDNA. These transformed cells were reintroduced to a syngeneic mouse. Following reintroduction, the transfected protein, human factor IX, was secreted from the reintroduced cells. The transfected cells were viable and continued to synthesize human factor IX for 28 days following reintroduction. *See* St. Louis *et al.,* "An alternative approach to somatic cell gene therapy," *Proc. Natl. Acad. Sci. USA,* 1988. 85:3150-3154.

As another example, Selden *et al.* report that murine fibroblasts transfected with a human growth hormone (hGH) fusion gene can be implanted at various locations in mice and following implantation, the fibroblasts synthesize and secrete hGH at detectable levels. Specifically, fibroblasts transfected to express hGH and implanted intraperitoneally secreted detectable levels of hGH for up to 7 days; those implanted subcutaneously secreted detectable levels for up to 10 days; those implanted under the renal capsule secreted detectable levels for up to 10 days; and those implanted intrahepatically, intraportally, or into the inferior vena cava all expressed hGH for 7-11 days. *See* Selden *et al.,* "Implantation of genetically engineered fibroblasts into mice: implications for gene therapy." *Science,* 1987. 236(4802):714-18. Selden *et al.* also report that if the mice were immunosuppressed, then hGH was expressed in the serum for longer periods of time, up to three months. Thus, one of skill in the art at the time of the invention would know that the method described in the present application could be used to achieve stable expression of a therapeutic protein.

The inventor of the present invention has also reported that fibroblast growth factor expression *in vivo* exhibits therapeutic effects relating to vascularization. Specifically, Nabel *et al.,* report that *in vivo* FGF-1 expression induced intimal thickening in porcine arteries 21 days after gene transfer. *Nature* 1993. 362:844-46. Nabel *et al.* also report that where there was substantial intimal hyperplasia, neocapillary formation was detected in the expanded intima.

Leiden, U.S. Patent No. 5,661,133, filed January 23, 1995, which is a continuation of U.S. Application Serial No. 789,983, filed November 21, 1991, demonstrates that direct injection of a plasmid encoding FGF-5 produces sufficient protein to achieve a therapeutic benefit, namely to achieve stimulation of collateral blood vessel formation and induction of angiogenesis. *See* Figure 5.

The skilled artisan would also appreciate that various other therapeutic proteins, described in the present specification, could be used to achieve a therapeutic effect. For example, skilled artisans knew that tumor necrosis factor α (TNF-α) injected into mice had the therapeutic effect of preventing or prolonging development of diabetes. Jacob *et al.,* "Prevention of diabetes in nonobese diabetic mice by tumor necrosis factor (TNF): Similarities between TNF-α and interleukin 1," *Proc. Natl. Acad. Sci. USA,* 1990. 87:968-972. *See also* Cuevas *et al.,* "Basic Fibroblast Growth Factor (FGF) Promotes Cartilage Repair *In Vivo." Biochem Biophys Res Commun.* 1988; 156 (2):611-8 and Hayek *et al.,* "An *In Vivo* Model for the Study of the Angiogenic Effects of Basic Fibroblast Growth Factor." *Biochem Biophys Res Commun.* 1987. 147(2):876-80. As another example, transforming growth factor ß (TGF- ß1) could be used to differentially modulate extracellular matrix production and cellular proliferation in the arterial wall *in vivo*. *See* Nabel *et al. Proc. Natl. Acad. Sci. USA* 1993. 90:10759-10763. *See Hormone Research Found. v. Genentech, Inc.*, 904 F.2d 1558, 15 USPQ2d 1039 (Fed. Cir. 1990) (Court found that inventor's assertion that he was able to use the disclosed method to synthesize the invention was supported by evidence, including journal articles published as much as 17 months after filing date).

Thus, one skilled in the art, at the time the application was filed knew that various therapeutic proteins, disclosed in the specification (at pages 27-31), achieve therapeutic effects when administered to subjects in the form of protein or nucleic acids (*i.e.* by direct gene transfer). Skilled artisans also knew that it was possible to transfect a cell *ex vivo* and then implant that cell into a syngeneic host and achieve expression of the transfected gene. The specification also demonstrated that the claimed method achieved expression of a marker gene. Thus, the disclosure set forth in the

specification, along with the knowledge of one skilled in the art as shown by the references discussed above, clearly demonstrates that the claimed invention was enabled as of the filing date.

An analysis of the *Wands* factors, taken with the above information, more clearly demonstrates that the present invention is enabled because it is neither unpredictable, nor would undue experimentation be required to practice the claimed method. "The quantity of experimentation needed to be performed by one skilled in the art is only one factor involved in determining whether 'undue experimentation' is required to make and use the invention. '[A]n extended period of experimentation may not be undue if the skilled artisan is given sufficient direction or guidance.' *In re Colianni,* 561 F.2d 220, 224, 195 USPQ 150, 153 (CCPA 1977)." MPEP § 2164.06. Moreover, ""[t]he test is not merely quantitative, since a considerable amount of experimentation is permissible, if it is merely routine, or ***if the specification in question provides a reasonable amount of guidance with respect to the direction in which the experimentation should proceed.***"" MPEP 2164.06 *quoting In re Wands,* 858 F.2d 731, 737, 8 USPQ2d 1400, 1404 (Fed. Cir. 1988). Some of the many factors to consider when determining whether any experimentation that is necessary is undue include, but are not limited to:

1) the breadth of the claims;

The claims are not overly broad, but rather are commensurate with the scope of enablement. Specifically, the claims are directed to a method of treating a human patient comprising the step of site-specific instillation of transformed cells into the patient, wherein the cells originate from the patient or are syngeneic to the patient and are selected from the group consisting of endothelium, smooth muscle, and parencyhmal cells.

2) the nature of the invention;

The invention is based on a novel method of treating a human patient. The method uses the knowledge of those skilled in the art relating to various therapeutic proteins

that might be used to treat various conditions, and combines that knowledge with the method of the invention to achieve a therapeutic effect in the human patient.

3) the state of the prior art;

The state of the art is advanced with regard to knowledge about what proteins have therapeutic effects. The state of the art is also advanced with respect to gene transfer and cell transformation. Moreover, analysis of the art as of the effective filing date of the present invention shows that skilled artisans were able to achieve therapeutic levels and effects of various therapeutic proteins *disclosed in the specification,* using direct injection techniques. *See supra* at 5-6. In addition, the art shows that skilled artisans were able to achieve stable expression of marker proteins in transplanted and/or transformed cells. *See* pages 37-39 of the specification.

4) the level of one of ordinary skill in the art;

The level of skill in the art is advanced.

5) the level of predictability in the art;

When an asserted scope of enablement is questionable because the art seems or is alleged to be unpredictable, additional factors, such as teachings in pertinent references, may be used to substantiate that the asserted scope of enablement is in fact commensurate with the scope of protection sought. *In re Marzocchi*, 429 F.2d 220, 223-24, 169 USPQ 367, 369-70 (CCPA 1971). The Examiner asserts that the art of gene therapy is unpredictable. However, Applicants have demonstrated that their disclosed method successfully achieves expression a marker gene from transplanted transformed cells for at least six weeks. Specification at pages 37-39. In addition, Applicants have demonstrated that their disclosed method successfully achieves expression of a therapeutic gene, and results in the therapeutic effect of reducing or preventing neointimal hyperplasia. *See* Nabel Declaration. Moreover, the art references discussed above indicate that therapeutic effects of the proteins disclosed in the specification were known at the time of invention. *See* specification at p. 10, 27-31; *See also supra* at 9. Hence, contrary to the Examiner's contention, given these

significant disclosures, those of skill in the art would predict achievement of a therapeutic effect when using the presently claimed method with a therapeutic protein.

6) the amount of direction provided by the inventor;

Applicants have provided a significant amount of guidance in the specification. For example, in addition to the working example described below, from pages 12 – 16 of the specification, Applicants describe the introduction of normal or genetically altered cells into a blood vessel. From pages 16 – 20, Applicants describe direct injection of recombinant genes into the wall of a blood vessel. From pages 20-28, Applicants describe how to obtain the cells used in practicing the claimed invention, as well as how to select therapeutic and marker proteins that might be expressed by the cells used in practicing various embodiments of the claimed invention.

7) the existence of working examples; and

At pages 37-39, the specification describes in detail a working example of endothelial cells transformed to express the marker protein β-gal when instilled into a denuded iliac artery.

8) the quantity of experimentation needed to make or use the invention based on the content of the disclosure.

Based on the significant disclosure of the present specification, the level of skill in the art, and the state of the art, undue experimentation would not be required to practice the claimed invention. Significantly, even a "considerable amount of experimentation is permissible, if it is merely routine or if the specification provides a reasonable amount of guidance with respect to the direction in which the experimentation should proceed." *In re Wands,* 858 F.2d 731, 737 (Fed. Cir. 1988).

The Examiner also argues that the single example provided (which demonstrates that the expression of p27 inhibits neointimal hyperplasia) does not provide a scope of enablement that correlates with the breadth of Applicant's claimed methods, which read on treatment of any type of disease in a patient.

As discussed above, Applicants disclose a general method that is effective for achieving treatment of a disease or symptom where expression of a therapeutic protein provides a therapeutic benefit. Applicants also disclose various proteins that might be used to treat various diseases. *See* specification at p. 10, 27-31.

In addition, one of ordinary skill in the art at the time the application was filed would know that the various proteins disclosed in the specification might be used with the method disclosed in the present application to treat a variety of diseases or symptoms. For example, as discussed above, in the 1990 issue of *Proc. Natl. Acad. Sci. USA,* 87:968-972, Jacob *et al.* report tumor necrosis factor α (TNF-α) (disclosed at page 27 of the specification) injected into mice has the therapeutic effect of preventing or prolonging development of diabetes. Cuevas *et al.* teach that intraarticular administration of basic fibroblast growth factor (bFGF) (disclosed at page 30 of the specification) can elicit a repair response at the site of injury. *See* Cuevas *et al.,* "Basic Fibroblast Growth Factor (FGF) Promotes Cartilage Repair *In Vivo." Biochem Biophys Res Commun.* 1988; 156 (2):611-8 (FGF promotes healing of intra-chondrial lesions by stimulating chrondrocyte proliferation and the formation of extracellular matrix). Wilson *et al.* teach that hyperlipidemia can be treated by transplanting hepatocytes that are genetically modified to include a functional human low density lipoprotein receptor gene. Wilson *et al., Proc. Natl. Acad. Sci. USA* 1990. 87(21):8437-41. Leiden *et al.* report that implanted myoblast cells, transformed to express human growth hormone (hGH) secrete physiological levels of hGH. Leiden *et al.* "Systemic Delivery of Recombinant Proteins by Genetically Modified Myoblasts," *Science* 1991. 254:1507-09. *See also* Hayek *et al.,* "An *In Vivo* Model for the Study of the Angiogenic Effects of Basic Fibroblast Growth Factor." *Biochem Biophys Res Commun.* 1987. 147(2):876-80. Hence, one of skill in the art would be enabled to select the appropriate therapeutic protein to achieve treatment of the desired disease or symptom using the claimed method.

For all of these reasons, Applicants have overcome rejection of claims 109-142 under 35 U.S.C. § 112, and therefore, respectfully request that this rejection be withdrawn.

Double Patenting Rejection

The Examiner has rejected claims 106-109, 114-118, 121-131, 136, and 142 in light of U.S. Patent No. 6,203,991 for double patenting. Specifically, the Examiner alleges that the '991 claims are both broader and narrower than the present claims and that the limitations of the '991 claims render obvious the present claims. While Applicants disagree, to expedite prosecution and without prejudice, Applicants will file a terminal disclaimer upon allowance of the present claims.

SUMMARY

Pending Claims 106-142 are patentable. Applicants respectfully request the Examiner grant allowance of this application. The Examiner is invited to contact the undersigned attorney for the Applicant via telephone if such communication would expedite this application.

Respectfully submitted,

C. Noel Kaman

C. Noel Kaman
Registration No. 51,857
Attorney for Applicant

BRINKS HOFER GILSON & LIONE
P.O. BOX 10395
CHICAGO, ILLINOIS 60610
(312) 321-4200

Recombinant fibroblast growth factor-1 promotes intimal hyperplasia and angiogenesis in arteries *in vivo*

Elizabeth G. Nabel*, Zhi-yong Yang*, Gregory Plautz*, Reza Forough†, Xi Zhan†, Christian C. Haudenschild‡, Thomas Maciag† & Gary J. Nabel*

* Departments of Internal Medicine and Biological Chemistry, Howard Hughes Medical Institute, University of Michigan Medical Center, Ann Arbor, Michigan 48109-0650, USA
Departments of † Molecular Biology and ‡ Experimental Pathology, Holland Laboratory, American Red Cross, Rockville, Maryland 20855, USA

THE prototype members of the heparin-binding fibroblast growth factor (FGF) family[1–6], acidic FGF (FGF-1) and basic FGF (FGF-2), are among the growth factors that act directly on vascular cells to induce endothelial cell growth and angiogenesis. *In vivo*, the role of the FGF prototypes in vascular pathology has been difficult to determine. We report here the introduction, by direct gene transfer into porcine arteries, of a eukaryotic expression vector encoding a secreted form of FGF-1. This somatic transgenic model defines gene function in the arterial wall *in vivo*. FGF-1 expression induced intimal thickening in porcine arteries 21 days after gene transfer, in contrast to control arteries transduced with an *Escherichia coli* β-galactosidase gene. Where there was substantial intimal hyperplasia, neocapillary formation was detected in the expanded intima. These findings suggest that FGF-1 induces intimal hyperplasia in the arterial wall *in vivo* and, through its ability to stimulate angiogenesis in the neointima, FGF-1 could stimulate neovascularization of atherosclerotic plaques. Potentially, gene transfer of FGF-1 could also be used as a genetic intervention to improve blood flow to ischaemic tissues in selected clinical settings.

The FGF prototypes lack a classic signal sequence[1] (ss) for secretion, making it difficult to study their biological effects as extracellular polypeptides. It is now possible, however, to deliver recombinant genes directly into vascular cells at specific sites *in vivo*[7–12] to determine their effects in the arterial wall. A secreted form of the FGF-1 gene was derived by ligation of the signal sequence from the hst/KS3 (FGF-4) gene to the 5′ end of the open reading frame of FGF-1 (ref. 13) in the pMEX neo eukaryotic expression vector[14]. The pMEX neo-ss-hsk/KS3:FGF-1 expression vector plasmid was transfected into porcine iliofemoral arteries by direct gene transfer[8,15,16], and controls were transfected with the *E. coli* β-galactosidase gene. The presence of the ss-hst/KS:FGF-1 plasmid was confirmed using polymerase chain reaction (PCR) in transfected iliofemoral arterial segments (Fig. 1*a*, lanes 1 and 2) but not in nontransfected carotid artery segments from the same pig (data not shown), and the presence of its messenger RNA was confirmed by reverse transcription PCR (Fig. 1*b*, lane 4). Expression of recombinant FGF-1 protein was confirmed by immunohistochemistry in transduced arterial segments. Porcine arteries transfected with ss-hst/KS:FGF-1 had immunoreactive protein primarily in the intima, including the endothelium, 21 days after transfection, whereas no FGF-1 protein was detected in arteries transduced with the β-galactosidase expression vector (Fig. 2*a–c*).

To evaluate the response of the arterial wall to expression of ss-hst/KS:FGF-1, the transfected artery segments were examined by light microscopy 21 days after gene transfer. Animals transduced with β-galactosidase showed minimal intimal thickening in iliofemoral artery segments, in contrast to the ss-hst/KS:FGF-1-transduced arteries (compare Fig. 3*a* and *b*). By quantitative morphometry, the intimal to medial ratio was more than sixfold greater in FGF-1 than β-galactosidase-transduced vessels (0.27 ± 0.06 versus 0.04 ± 0.01, $P = 0.003$). Finally, in several experimental subjects, expression of ss-hst/KS:FGF-1 induced the formation of capillaries in the neointima (Fig. 4*a*, *b*), an effect not observed with the control.

Thus expression of secreted recombinant FGF-1 induced significant intimal proliferation and angiogenesis *in vivo*. Angiogenic factors[1,2,6] have been classified previously into two categories: those that act directly on vascular endothelial cells to stimulate locomotion and mitosis and those that act indirectly to induce host cells to release growth factors that target the endothelial cell. In addition, because the FGF prototypes lack a classic signal sequence for secretion, their normal mode of release is not fully understood. They are detected after arterial

injury[17,18] and can be found in the subendothelial matrix[19]. Indeed, NIH 3T3 cells can release FGF-1 *in vitro* in response to heat shock[20]. In an injury model *in vivo*, systemically administered FGF-2 is a potent mitogen for vascular smooth muscle cells[21], but it has not previously been possible to determine the function of the FGF prototypes in the normal arteries. Analysis of tissue sections in this study suggests that mitotic activity is induced by FGF-1 in the vessel wall, although it remains possible that FGF-1 affects cell migration, as suggested for platelet-derived growth factor (PDGF)[22].

Several recombinant genes induce intimal smooth muscle hyperplasia, including PDGF[16] or TGF-β1 (E.G.N. *et al.*, unpublished results). In contrast, FGF-1 stimulates intimal hyperplasia and also induces the formation of new blood vessels in the expanded intima. These data therefore suggest that smooth muscle hyperplasia alone is not sufficient for the formation of new capillaries. Luminal endothelial cells in the iliofemoral

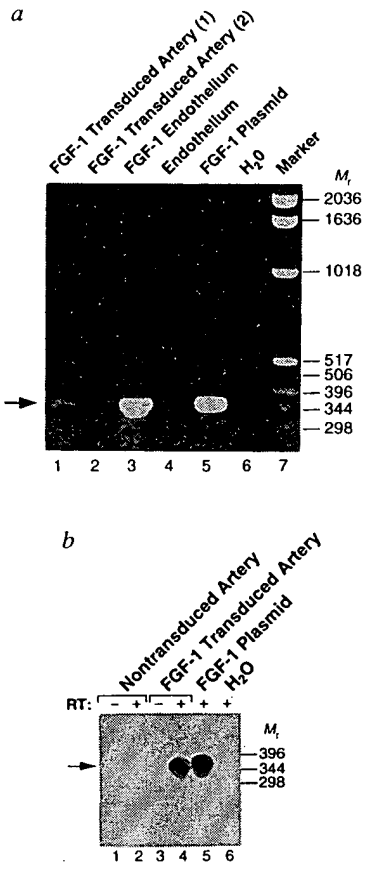

FIG. 1 Presence of ss-hst/KS:FGF-1 plasmid DNA (*a*) and mRNA (*b*) in porcine arteries after direct gene transfer *in vivo*. *a*, Recombinant ss-hst/KS:FGF-1 DNA was transfected into porcine right (lane 1) and left (lane 2) iliofemoral arteries and was detected by PCR 7 days after direct gene transfer using ethidium staining of agarose gels. *In vitro* transfected porcine endothelial cells (FGF-1 endothelium) (lane 3) compared with nontransduced porcine endothelial cells (Endothelium) (lane 4) were analysed as positive and negative controls. Additional controls included the recombinant FGF-1 plasmid (lane 5) and water (lane 6). *b*, The presence of ss-hst/KS:FGF-1 mRNA was detected using reverse transcription PCR by methods described previously[16]. The presence of recombinant FGF-1 mRNA was analysed by Southern blotting of PCR-amplified complementary DNA in nontransduced or transduced arteries treated with or without the addition of reverse transcriptase (RT) as indicated for lanes 1–4. Recombinant FGF-1 plasmid (lane 5) and water (lane 6) were included as positive and negative controls, respectively.

METHODS. Recombinant FGF-1 gene transfer in arterial segments was analysed by PCR of genomic DNA as previously described[15]. To conduct PCR analysis of recombinant FGF-1 transfected vessels, primers were synthesized from the cDNA sequence[20] which generated a 364 base pair (bp) fragment: sense (25 mer): CAA ACT CCT CTA CTG TAG CAA CGG G; antisense (25 mer): TTG CTT TCT GGC CAT AGT GAG TCC G. The sense primer was selected from a region 50 bp upstream to the transcription start site. Samples were analysed by ethidium bromide staining on a 1% agarose gel. The ss-hst/KS:FGF-1 chimaera was prepared and inserted into the pMEX neo expression vector as previously described[20]. Primary porcine endothelial muscle cell cultures were established as previously described and transfected with Lipofectin (BRL)[15] to test the expression of the ss-hst/KS:FGF-1 vector. Transduced endothelial cells were assayed for secretion of recombinant FGF-1 into culture supernatants with a colorimetric proliferation assay by standard methods[24].

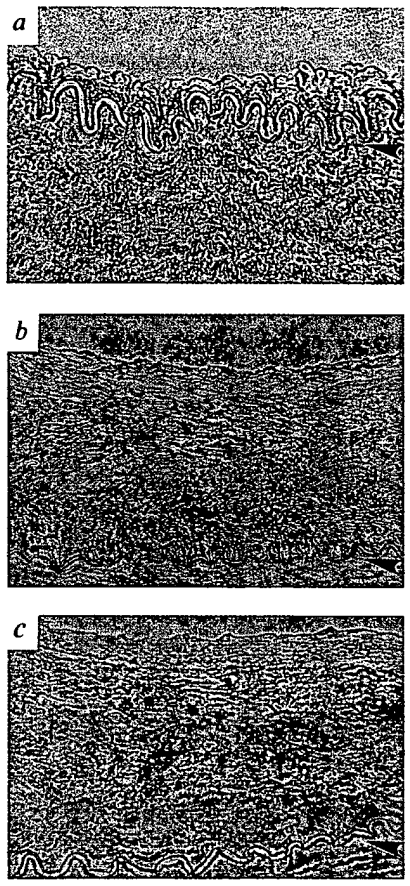

FIG. 2 Expression of recombinant ss-hst/KS:FGF-1 protein in porcine artery cells after direct gene transfer. Immunohistochemical staining of porcine arteries transduced with the *E. coli* β-galactosidase gene (*a*), or recombinant ss-hst/KS:FGF-1 gene (*b*, *c*) at 21 days using a control purified rabbit IgG antibody (*b*), or an affinity-purified rabbit antibody to FGF-1 (*a*, *c*). Arrow denotes the internal elastic lamina. (Magnification ×300).

METHODS. Recombinant FGF-1 protein expression was analysed by immunohistochemistry of artery segments transduced with the recombinant ss-hst/KS:FGF-1 or *E. coli* β-galactosidase genes. Artery segments embedded in Tissue-Tek OCT compound (Miles, Elkhart, IN) were sectioned (6 μm) and were incubated in 10 mM Tris–Cl pH 7.5, 150 mM NaCl, 1 mM EDTA (TNE), and 1% fetal bovine serum with 1:150 dilution of an affinity-purified rabbit anti-human FGF-1 antibody for 1 h at room temperature. Endogenous peroxidase activity was blocked by preincubation in TNE with 0.1% H_2O_2 for 45 min[25]. Peroxidase-conjugated goat anti-rabbit IgG (H+L) antibody (Vector Laboratories, Burlingame, CA) (1:400) was added for 30 min at room temperature and samples were stained in 50 μM sodium acetate (pH 5.0), 20 μg ml^{-1} 3-amino-9-ethyl-carbazole, and 0.015% H_2O_2 for 15 min. FGF-1-transduced arterial segments were also analysed with a control first antibody, purified rabbit IgG, and peroxidase conjugated goat anti-rabbit IgG (1:400) (Vector Laboratories).

FIG. 3 Intimal hyperplasia in porcine arteries 21 days after direct gene transfer of ss-hst/KS:FGF-1 and *E. coli* β-galactosidase. Vessels were transduced with an *E. coli* β-galactosidase (negative control) (*a*) or ss-hst/KS:FGF-1 (*b*) gene. Arrow denotes internal elastic lamina. (Magnification ×54, haematoxylin-eosin stain).

METHODS. Direct intra-arterial gene transfer was done *in vivo* in 12 pigs, 6 with the recombinant ss-hst/KS:FGF-1 gene and 6 with a control reporter gene, *E. coli* β-galactosidase. A double balloon intravascular catheter (C. R. Baid Inc., Billerica, MA) was inserted in porcine iliofemoral arteries as previously described[8]. The arterial segment isolated by the catheter was flushed with 5 ml saline and 5 ml Opti-MEM (BRL) to rinse blood from the vessel. The DNA liposome conjugates were prepared 10 min before transfection. Lipofectin (5 μl) was diluted into 0.2 ml of Opti-MEM at room temperature, and 2–5 μg plasmid DNA (stock concentration >1 mg ml^{-1}) was added. The solution remained at room temperature for 5–10 min, and 0.5 ml Opti-MEM was added. DNA liposomes were instilled into the arterial segment between the two balloons at 150 mm Hg in the left and right iliofemoral arteries and incubated for 20 min. Four of the twelve pigs were killed at one week, and eight pigs were killed at three weeks. Previous studies established that recombinant genes are stably expressed in vascular cells *in vivo* at 2–3 weeks[8,15], and intimal thickening induced by arterial manipulation is observed at this time point[26]. Morphometric measurements of intimal and medial thickness were done in a blinded manner (by C.C.H.). Intimal-to-medial ratios were determined ($n=12$, $n=6$ *E. coli* β-galactosidase gene, $n=6$ FGF-1 gene) as previously described[16]. Intima-to-media ratios are expressed as a mean ±s.e.m. Comparisons between ss-hst/KS:FGF-1 gene-transduced vessels and control vessels transduced with a reporter gene were made by two-tailed unpaired *t*-test.

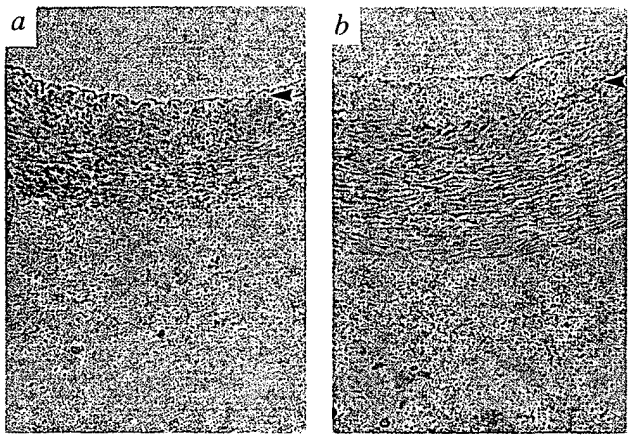

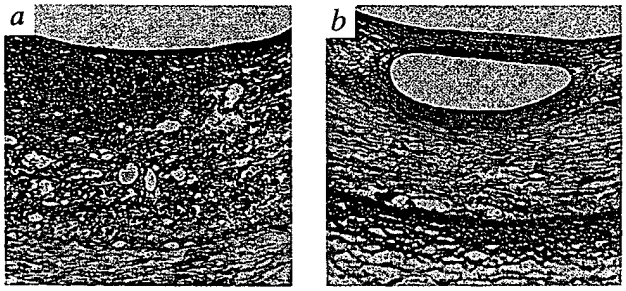

FIG. 4 Angiogenesis in the neointima of arterial segments after ss-hst/KS:FGF-1 gene transfer. Vessels were transduced with ss-hst/KS:FGF-1 and sections representing formation of multiple capillaries (*a*) or a larger intimal capillary (*b*) are shown. Arrow, Internal elastic lamina. (Magnification ×212 (*a*), ×106 (*b*), haematoxylin-eosin stain).

artery do not contain factor VIII, in contrast to those of the small capillaries in the adventitia. Endothelial cells lining the new intimal capillary beds are negative for von Willebrand factor (data not shown), suggesting that the FGF-1-induced capillaries arise from adjacent luminal endothelial cells. These findings are most consistent with a model in which FGF-1 acts locally on endothelial cells, perhaps through mitotic and locomotive effects. These angiogenic effects of FGF-1 could be mediated directly on endothelial cells and/or indirectly through the induction of other endogenous growth factors. In either case, the effects of FGF-1 are specific because they are not observed with other recombinant growth factor genes[15,16]. This model will aid the definition of such factors and the design of potential inhibitors of vascular cell proliferation.

The elaboration of FGF *in vivo* represents a potential mechanism to provide a blood supply to the hyperplastic intima. Such angiogenesis is observed in atherosclerotic plaques[23], and mechanisms to explain this observation have been lacking. Direct gene transfer of this FGF-1 or related genes *in vivo* could provide a method to stimulate collateral blood flow which would be beneficial for the treatment of ischaemic cardiovascular diseases. □

Received 21 October 1992; accepted 18 February 1993.

1. Burgess, W. H. & Maciag, T. *A. Rev. Biochem.* **58**, 575–606 (1989).
2. Ausprunk, D. H. & Folkman, J. *Microvasc. Res.* **14**, 53–65 (1977).
3. Abraham, J. A. *et al. Science* **233**, 545–548 (1986).
4. Gospodarowicz, D., Chen, J., Lui, G. M., Baird, A. & Bohlent, P. *Proc. natn. Acad. Sci. U.S.A.* **81**, 6963–6967 (1984).
5. Thomas, K. A. *et al. Proc. natn. Acad. Sci. U.S.A.* **82**, 6409–6413 (1985).
6. Yanagisawa-Miwa, A. *et al. Science* **257**, 1401–1403 (1992).
7. Nabel, E. G., Plautz, G., Boyce, F. M., Stanley, J. C. & Nabel, G. J. *Science* **244**, 1342–1344 (1989).
8. Nabel, E. G., Plautz, G. & Nabel, G. J. *Science* **249**, 1285–1288 (1990).
9. Plautz, G., Nabel, E. G. & Nabel, G. J. *Circulation* **83**, 578–583 (1991).
10. Lim, C. S. *et al. Circulation* **83**, 2007–2011 (1991).
11. Chapman, G. D. *et al. Circ. Res.* **71**, 27–33 (1992).
12. Leclerc, G., Gal, D., Takeshita, S., Nikol, S., Weir, L. & Isner, J. M. *J. clin. Invest.* **90**, 936–944 (1992).
13. Forough, R. *et al. J. biol. Chem.* **268**, 2960–2968 (1993).
14. Martin-Zanca, D., Oskam, R., Mitra, G., Copeland, T. & Barbacid, M. *Molec. cell. Biol.* **9**, 24–33 (1989).
15. Nabel, E. G., Plautz, G. & Nabel, G. J. *Proc. natn. Acad. Sci. U.S.A.* **89**, 5157–5161 (1992).
16. Nabel, E. G. *et al. J. clin. Invest* **91**, 1822–1829 (1993).
17. Gajdusek, C. M. & Carbon, S. *J. Cell Physiol.* **139**, 570–579 (1989).
18. McNeil, P. L., Muthukrishnan, L., Warder, E. & D'Amore, P. A. *J. Cell Biol.* **109**, 811–822 (1989).
19. Vlodavsky, I., Folkman, J., Sullivan, R., Friedman, R. & Ishai-Michaeli, R. *Proc. natn. Acad. Sci. U.S.A.* **84**, 2292–2296 (1987).
20. Jackson, A. *et al. Proc. natn. Acad. Sci. U.S.A.* **99**, 10691–10695 (1992).
21. Lindner, V., Lappi, D. A., Baird, A., Majack, R. A. & Reidy, M. A. *Circ. Res.* **68**, 106–113 (1991).
22. Jawien, A., Bowen-Pope, D. F., Lindner, V., Schwartz, S. M. & Clowes, A. *J. clin. Invest.* **89**, 507–511 (1992).
23. Barger, A. C., Beeuwkes, R. III, Lainey, L. L. & Silverman, K. J. *N. Engl. J. Med.* **310**, 175–177 (1984).
24. Mosmann, T. *J. immun. Meth.* **65**, 55–63 (1983).
25. Ellis, S. *J.*, Taylor, C. & McMichael, A. *Hum. Immun.* **5**, 49–59 (1982).
26. Clowes, A. W., Clowes, M. M. & Reidy, M. A. *Lab Invest.* **54**, 295–303 (1986).

ACKNOWLEDGEMENTS. We thank D. Gordon for comments and advice, C. Enger for providing catheters and D. Gschwend for secretarial assistance. These studies were supported by grants from the NIH and the American Heart Association.

Proc. Natl. Acad. Sci. USA
Vol. 85, pp. 3150–3154, May 1988
Medical Sciences

An alternative approach to somatic cell gene therapy

(human factor IX/retroviral vector/skin fibroblast/collagen implant)

DANIEL ST. LOUIS AND INDER M. VERMA*

Molecular Biology and Virology Laboratory, The Salk Institute, P.O. Box 85800, San Diego, CA 92138

Communicated by Renato Dulbecco, December 18, 1987 (received for review November 17, 1987)

ABSTRACT **Mouse primary skin fibroblasts were infected with a recombinant retrovirus containing human factor IX cDNA. Bulk infected cells capable of synthesizing and secreting biologically active human factor IX protein were embedded in collagen, and the implant was grafted under the epidermis. Sera from the transplanted mice contain human factor IX protein for at least 10–12 days. Loss of immunoreactive human factor IX protein in the mouse serum is not due to graft rejection. Instead, the mouse serum contains anti-human factor IX antibodies, which react with the protein. We suggest that retroviral-infected primary skin fibroblasts offer an alternative approach to somatic cell gene therapy.**

The concept of human gene therapy involves the introduction of a functionally active gene into somatic cells of an affected individual to correct the defect. To ensure lifelong supply of the replaced gene product, it is essential to introduce and express the gene in cells that proliferate during the entire adult life of the recipient. Because pluripotent stem cells in bone marrow have both self-renewal capacity as well as ability to give rise to all hematopoietic lineages, they are a popular target for introducing functionally active genes (1–4). Recently, hepatocytes have been used as target cells for introducing functionally active genes (5, 6).

Murine retroviruses efficiently infect many fibroblast cell lines, including immortalized and normal human diploid fibroblasts (7–10) and human keratinocytes (11). This approach to gene transfer offers several advantages: (*i*) primary skin fibroblasts are readily accessible by skin biopsy and easily cultured and manipulated *in vitro*; (*ii*) efficient infection of primary cultures by retroviral vectors reduces the *in vitro* culturing period; (*iii*) use of fibroblasts as target cells for gene transfer overcomes inefficient gene expression by retroviral vectors in other target tissues, such as bone marrow; (*iv*) because skin fibroblasts reside in a highly vascularized compartment of the dermis, infected cells have direct access to the circulatory system; (*v*) use of syngeneic primary cultures obviates problems of graft rejection; and (*vi*) the implanted skin fibroblasts can be conveniently removed. We report the development and characterization of an alternative approach of gene product delivery using mouse skin fibroblasts.

MATERIALS AND METHODS

Construction and Infection by Recombinant Factor IX Retroviruses. The recombinant pAFFIXSVNeo is based on a retroviral construct pAFVXM generated by Kriegler *et al.* (12). A human factor IX cDNA was linked directly to the 5' long terminal repeat (LTR) by inserting a 1.6-kilobase (kb) *Bam*HI/*Hin*dIII fragment from the clone CVI between the *Bgl* II and *Hin*dIII sites of pAFVXM (13). The entire expression unit from the neomycin phosphotransferase expression plasmid (pKoNeo) was excised by partial *Hin*dIII digestion and inserted into the *Hin*dIII site of the above factor IX viral construct (Fig. 1*a*). "Helper-free" recombinant ecotropic virus in Ψ2 cells was generated as described (14, 15). The titers of recombinant retrovirus expressed from drug-resistant clones were done essentially as described (14).

Primary mouse embryo fibroblasts (MEF) were obtained from day-17 embryos of C57BL/6J mice (16). The BL/6 line is an immortalized skin cell line derived from x-ray irradiated skin fibroblasts obtained from C57BL/6J mice. The skin fibroblast cell line BL/6 and NIH 3T3 TK$^-$ cells were infected with recombinant retroviruses from the cell line, ΨFIXNeo 4, at a multiplicity-of-infection (moi) of 1–2 in the presence of Polybrene at 8 μg/ml; MEF cells were infected at a moi of 5.

Implantation of Infected Mouse Fibroblasts in Mouse. Infected BL/6 and MEF cells were cultured in an artificial extracellular matrix composed of rat tail type I collagen (1 mg/ml; Sigma) and Dulbecco's modified Eagle's medium (DMEM) supplemented with 10% fetal bovine serum in a 5-cm dish (17, 18). The cells were cultured at 37°C for 3 days during which the collagen lattice contracted to a tissue-like structure (1/25th the area of the original gel). Once contracted, two artificial tissues containing ≈4 × 10^6 infected fibroblasts were grafted into the loose connective tissue of the dermis in the mid-back of a recipient C57BL/6 mouse. To ensure rapid vascularization of the grafted tissue, a 2-mm^2 piece of Gelfoam (Upjohn) containing 2 μg of basic fibroblast growth factor was inserted into the loose connective tissue along with each graft. Serum samples were drawn at 2-day intervals and analyzed for the presence of human factor IX by ELISA.

Analysis of Secreted Factor IX. Levels of antigenic factor IX were assayed by ELISA as described by Anson *et al.* (19). Biologically active human factor IX was immunoaffinity-purified using A7 antibody (19, 20). The amount of biologically active protein was determined by a one-step clotting assay using canine factor IX-deficient plasma (21). This assay is based on the ability of the sample to decrease the prolonged activated partial thromboplastin time of congenital factor IX-deficient plasma. Purified human factor IX was used as a control.

RESULTS

Transduction of Neomycin Resistance and Expression of Human Factor IX. The titers of helper-free ΨFIXNeo virus produced in the various cell lines ranged from 3 × 10^5 to 7 × 10^5 G418-resistant colony forming units per ml when assayed on NIH 3T3 TK$^-$ cells. As measured by ELISA, all virus-producing cell lines secreted essentially the same levels of factor IX into the culture media (≈200 ng/ml). All infected and drug-resistant cell lines were also found to secrete factor

The publication costs of this article were defrayed in part by page charge payment. This article must therefore be hereby marked "*advertisement*" in accordance with 18 U.S.C. §1734 solely to indicate this fact.

Abbreviations: MEF, mouse embryo fibroblasts; LTR, long terminal repeat; moi, multiplicity of infection.

*To whom reprint requests should be sent.

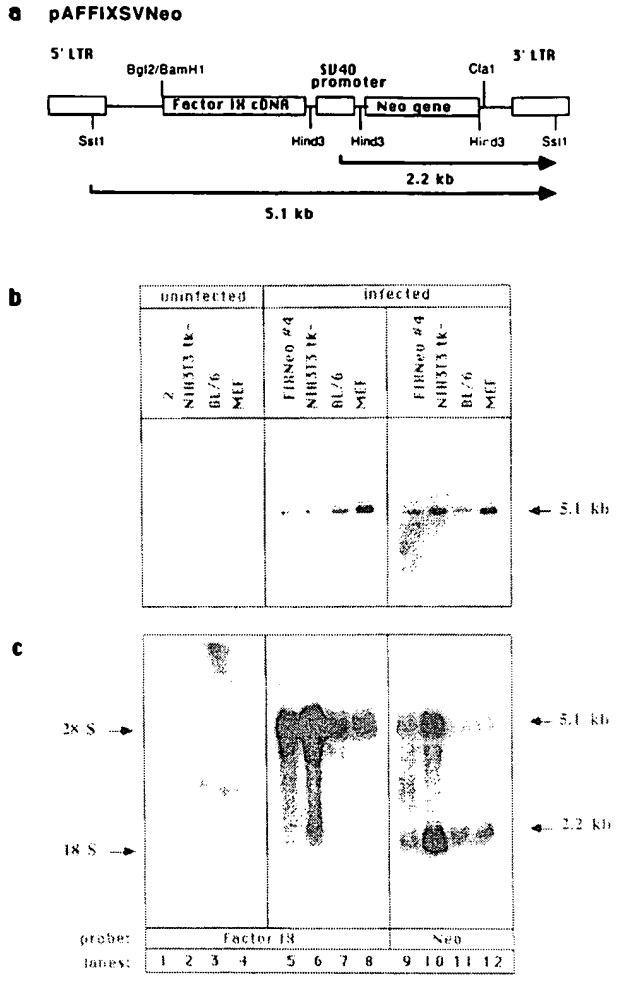

FIG. 1. Analysis of recombinant human factor IX retrovirus. (*a*) pAFFIXSVNeo. Arrows indicate transcripts that initiate at either the promoter in the 5' LTR or the simian virus 40 early promoter between the two LTRs and terminate at the polyadenylylation signal in the 3' LTR. Bars indicate the putative initiation site of transcription. The restriction endonuclease cleavage sites *Sst* I, *Hin*dIII, *Bam*HI, *Bgl* II, and *Cla* I are diagnostic sites used during the construction of the vector or subsequent characterization of the provirus in the genome of infected cell lines. (*b*) Proviral DNA. Genomic DNA isolated from either uninfected or infected ΨFIXNeo 4, NIH 3T3 TK$^-$, BL/6, MEF cells, and from the virus-producing cell line ΨFIXNeo 4 was digested with Sst I, fractionated by agarose gel electrophoresis, transferred onto a nitrocellulose membrane, and hybridized to either a nick-translated 1.6-kb factor IX cDNA probe (lanes 1–8) or 1.4-kb *Hin*dIII to *Bam*HI Neo DNA probe (lanes 9–12). Under these conditions of hybridization, human factor IX cDNA does not hybridize to mouse DNA. (*c*) RNA transcripts. Total RNA (10 μg) isolated from uninfected and infected cells and cell lines was subjected to RNA blot analysis.

IX into the culture media, albeit at different levels (see Fig. 2).

We determined the organization of the integrated recombinant retrovirus in the virus-producing cell line by Southern blot analysis of *Sst* I-digested (*Sst* I cleaves once in each LTR to generate a 5.1-kb DNA fragment (Fig. 1*b*) genomic DNA. All infected cells displayed a single band of the expected size of ≈5.1 kb, which hybridizes to both the factor IX cDNA and the Neo probe, therefore ruling out any detectable rearrangements. Furthermore, the size of this band in infected NIH 3T3 TK$^-$, BL/6, and MEF cells is identical to that found in the virus-producing cell line ΨFIXNeo 4 (compare lanes 5 and 9 to other lanes).

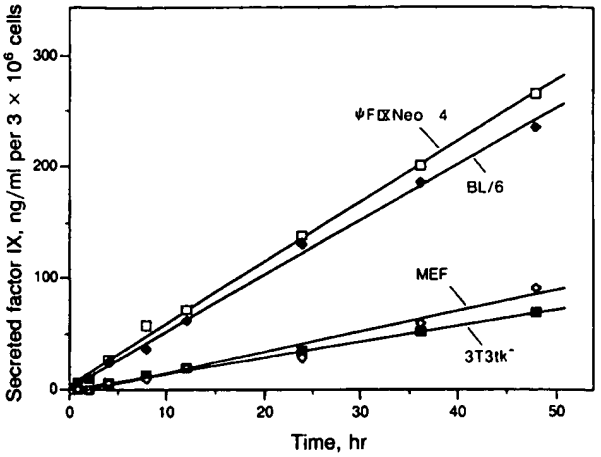

FIG. 2. Secretion of human factor IX. Rate of secretion of human factor IX by the virus-producing cell line ΨFIXNeo 4 (□) and by infected NIH 3T3 TK$^-$ cells (■), BL/6 cells (◆), and MEF cells (◇). Cells were seeded at 3 × 10^6 cells per 5-cm dish in 4 ml of medium. At each indicated time point 100 μl of medium was removed and assayed for human factor IX by enzyme-linked immunoabsorbant assay (ELISA) (19). The mouse anti-human monoclonal antibody, FXC008, generated by Bajaj *et al.* (22) was used as the primary antibody, whereas pooled normal human sera were used as a standard. Each time point was done in triplicate and thus represents an average amount of factor IX secreted over a 48-hr period. Curves were corrected for the slight increase in cell number over this period.

The RNA blot analysis of the RNA isolated from ΨFIXNeo 4, infected NIH 3T3 TK$^-$, BL/6, and MEF is shown in Fig. 1*c*. When hybridized to factor IX probe, only one major transcript of the expected size of 5.1 kb, corresponding to full-length viral RNA, could be detected in the infected cells. Hybridization with Neo probe reveals an additional 2.2-kb transcript that is the predicted size of the mRNA species, the synthesis of which is initiated from the simian virus 40 early promoter and is terminated in the 3' LTR (Fig. 1*c*). Ratios of the steady-state levels of the 5.1-kb and the 2.2-kb transcripts varied within the different infected cell types. From results shown in Fig. 1, we conclude that the ΨFIXNeo recombinant retrovirus is properly integrated and expressed in the infected cells.

Secretion of Factor IX Protein. Because human factor IX is a secretory protein we wanted to verify whether it is secreted into the medium of the infected cells. Fig. 2 shows that both rate and extent of antigenic factor IX released into the medium is dependent on cell type rather than on relative amounts of the factor IX transcripts. For instance, steady-state levels of factor IX transcript in infected NIH 3T3 TK$^-$ cells is much higher than in BL/6 cells (Fig. 1*c*); yet, the rate and amount of factor IX secreted in the latter cell type is much higher. Both the virus-producing cell line ΨFIXNeo 4 and infected skin fibroblast cell line BL/6 secreted antigenic factor IX at similar rates—≈5.7 ng per ml/hr for 3 × 10^6 cells and 5.0 ng per ml/hr for 3 × 10^6 cells, respectively. This rate was almost 3-fold higher than the rate of factor IX secretion seen for infected MEF (1.75 ng per ml/hr for 3 × 10^6 cells) and infected NIH 3T3 cells (1.65 ng per ml/hr for 3 × 10^6 cells). These results indicate that the rate of synthesis and/or secretion may be a property of the cell type, rather than the levels of expression.

Secreted Human Factor IX Protein Is Biologically Active. The primary translation product of factor IX gene undergoes extensive post-translational modification, which include addition of sialic carbohydrates (23, 24), vitamin K-dependent conversion of glutamic acid residues to γ-carboxy/glutamic

acid, (25) and β-hydroxylation of aspartic acid residue 64 (26). The γ-carboxylation of factor IX is essential for clotting activity, and this modification generally occurs in the liver, the primary source of factor IX synthesis in the body. We took two different approaches to assess biological activity of human factor IX secreted from cells in culture: (*i*) the infected mouse embryo fibroblasts were cultured in factor IX-deficient canine serum obtained from hemophiliac dogs, supplemented with epidermal growth factor (10 ng/ml) and vitamin K (25 ng/ml). Media harvested after 48-hr incubation was monitored for activity by a one-step assay (21). Conditioned media from MEF cells contained biologically active human factor IX at 210 ng/ml, which is similar to the levels seen with ELISA assays (Fig. 4). (*ii*) Because BL/6 cells did not attach to the tissue culture dish in canine sera, we had to resort to a different approach. Infected BL/6 cells were grown in 10% fetal calf serum supplemented with vitamin K (25 ng/ml), and the media harvested after 48-hr incubation was applied to an immunoaffinity column containing human factor IX monoclonal antibody A-7 (19, 20). This monoclonal antibody recognizes the calcium-binding domain of human factor IX protein, thus discriminating between carboxyl-lacking factor IX and biologically active γ-carboxyl human factor IX. One-hundred and sixty milliliters of the media obtained from BL/6 cells containing 32 μg of antigenic human factor IX (determined by ELISA) was passed through the column. Nearly 3.5 μg of the biologically active material was recovered from the column. This represents over 10% of the total antigenic factor IX in the starting sample. No biologically active factor IX could be identified from uninfected MEF or BL/6 cells. Despite lack of information on the extent of γ-carboxylation or other post-translational modifications, we conclude that the infected cells used for subsequent implantation studies synthesize biologically active human factor IX.

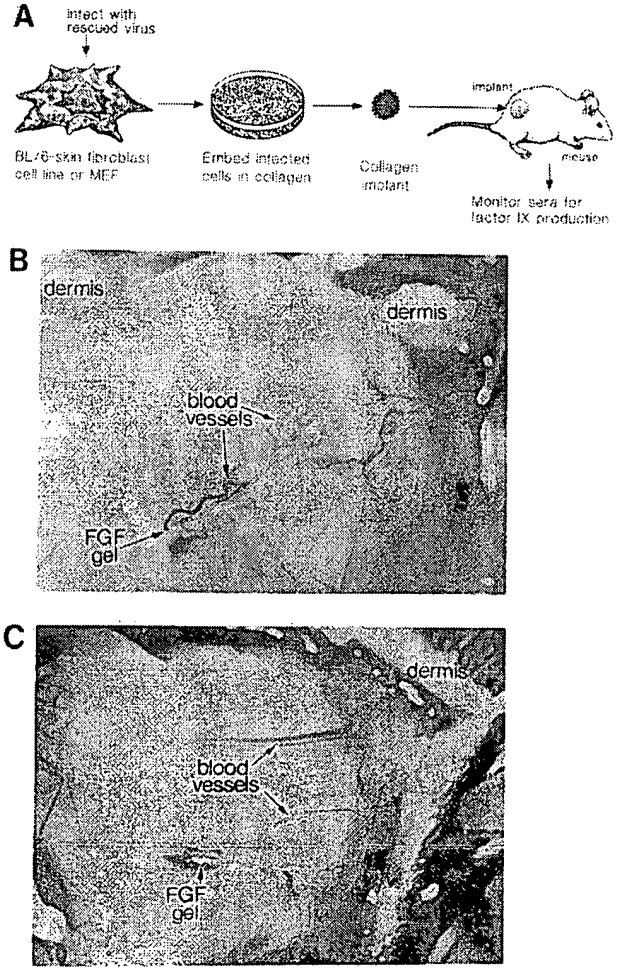

FIG. 3. Embedding and implantation. (*A*) Schematic representation of the protocol used to generate and graft the collagen implants into the loose connective tissue of the skin of the mouse model system. (*B* and *C*) View of both MEF (*B*) and BL/6 (*C*) collagen implants at day 14. The grafts (white area) and the high degree of vascularization are clearly visible. The implant is 0.75 cm in diameter. FGF, fibroblast growth factor.

Detection of Human Factor IX in Mice Grafted with Infected Fibroblasts. Infected MEF cells and BL/6 cells were cultured in an artificial extracellular matrix, composed of collagen, before grafting. We chose a tumor cell line, BL/6, in addition to MEF because it has an advantage in growth and vascularization and thus would increase our chances of detecting secreted factor IX in the sera. Attachment of the cells to the collagen resulted in a three-dimensional array of cells stacked on top of one another. After the primary fibroblast cells (MEF) or the tumor cell line BL/6 contracted in the collagen gel, the cells were grafted onto the loose connective tissue of the mid-back dermis of a recipient syngenic C57BL/6 mouse (Fig. 3*A*). Fig. 3*B* shows that the inserted implants were extensively vascularized by day 14. A similar extent of vascularization was also detected in 28-day implants (data not shown).

The serum levels of the human clotting factor were measured in engrafted mice by ELISA over a 34-day period. Fig. 4 shows that the average levels of human factor IX in three mice progressively increased from 20 ng/ml at day 2 to a peak of 97 ng/ml 7 days after grafting the BL/6 cells into the mice. The four mice grafted with the infected MEF fibroblasts showed a similar pattern of increase, in which an average peak of 25 ng/ml of factor IX was detected at day 9. This rise was followed by a rapid decline to near nondetectable levels of serum human factor IX at day 16 in both the BL/6 and MEF grafts. A minor peak of factor IX was seen at day 20 in mice with either graft, which was followed by loss of any detectable factor IX antigen. In parallel experiments, 10^7 infected BL/6 or MEF cells were injected directly into the peritoneal cavity of the recipient C57BL/6 mice. Serum levels of human factor IX in the injected

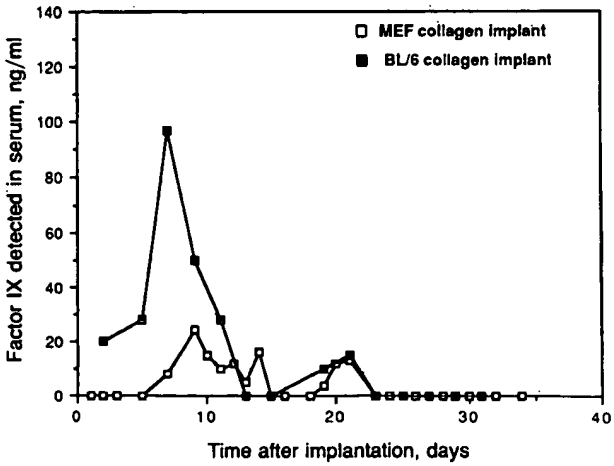

FIG. 4. Factor IX in human sera. Average (four mice for MEF; three mice for BL/6) amount of human factor IX detected in the sera of mice that received two collagen implants containing ≈4 × 10^6 cells each. Sera was drawn from each animal at the indicated times. Levels of circulating human factor IX were determined by ELISA; levels of factor IX fluctuated 2- to 3-fold between experiments.

Table 1. Amount of antigenic factor IX secreted from cells explanted from grafts

Days after implantation	Collagen explants, ng/ml	
	BL/6	MEF
14	180	40
21	210	27
28	150	11

Tissue explanted from the grafts at times indicated after implantation were cultured *in vitro*. When cells were confluent, medium was replaced; after 48 hr, levels of factor IX secreted into the culture were assayed by ELISA.

animals followed a similar profile as that seen with the grafts (data not shown).

Explanted Grafts Make Factor IX. The decline in serum levels of antigenic human factor IX in animals that were either grafted or injected i.p. was not associated with necrosis of cells in the grafts. BL/6 cells in the collagen matrix grew as an aggressive tumor at the site of the graft; the tumor continued to grow until animals were sacrificed at day 32. Mice with grafts containing infected MEF were visibly vascularized upon gross inspection until day 28; however, by day 120 the extent of vascularization was reduced, but the implant was still viable (data not shown). Additionally, cells explanted at various times during the course of the experiment produced factor IX when grown in culture (Table 1). The explanted BL/6 cells grew well in culture and secreted antigenic factor IX at levels similar to that before grafting. The MEF cells explanted from the grafts at days 14 and 21 grew well in culture, but produced slightly lower levels of factor IX. Cells explanted at day 28 did not grow well, and the low level of factor IX secreted from these cells is, perhaps, a consequence of this poor growth.

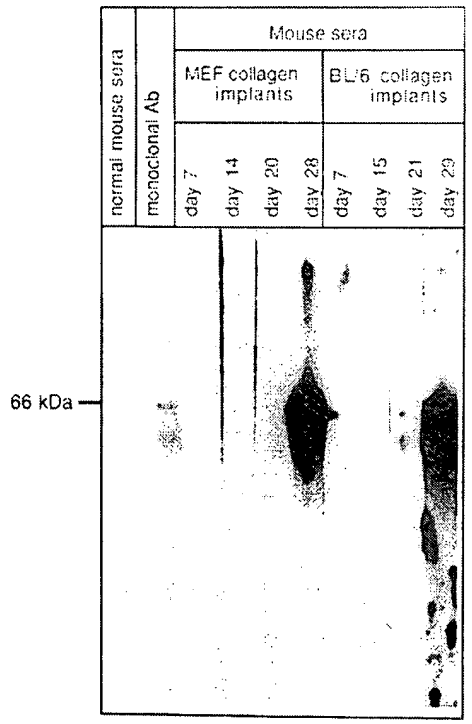

FIG. 5. Detection of mouse anti-human factor IX antibodies in mice grafted with collagen implants. Purified human factor IX was subjected to PAGE under denaturing conditions and then transferred onto nitrocellulose as described (27). The nitrocellulose strips were treated with blocking solution for 2 hr followed by 1:100 dilution of naive normal mouse serum (lane 1); 1:100 dilution mouse monoclonal anti-factor IX antibody FXC008 (lane 2); 1:100 dilution of serum from mouse harboring grafts containing infected MEF cells drawn at day 7, day 14, day 20, and day 28 (lanes 3–6); 1:100 dilution of serum from mouse harboring grafts containing infected BL/6 cells drawn at day 7, day 15, day 21, and day 29 (lanes 7–10). After overnight incubation at 37°C the strips were washed, incubated with ^{125}I-labeled goat anti-mouse IgG antibody, and then subjected to autoradiography as described (31).

Detection of Serum Anti-Factor IX Antibodies. To further investigate the decline of serum levels of human factor IX we reasoned that the recipient animal mounted an immunological response against the highly immunogenic human factor IX protein. To test whether mice bearing grafts with infected BL/6 or MEF cells are generating anti-factor IX IgG antibodies, pooled serum samples were used to probe immunologic blots containing purified human factor IX protein (Fig. 5). The levels of anti-human factor IX IgG antibodies were not detectable in mice with MEF grafts at day 7 to day 21. Slightly higher levels of serum antibodies were detected in mice with BL/6 grafts during this period—presumably because they are releasing more factor IX. Maximum levels of anti-human factor IX antibodies were detected at day 28 in mice with either graft. The mice with BL/6 grafts exhibited the highest level of xenoantibodies. Pooled serum drawn from mice 28 days after i.p. injection with infected MEF also showed anti-factor IX IgG antibodies, albeit at much lower levels. Naive animals, which have not been exposed to infected BL/6 or MEF cells, do not make anti-human factor IX antibodies. These observations would suggest that human factor IX is continuously produced in grafted mice but is not detectable due to a large pool of mouse anti-human factor IX antibodies.

DISCUSSION

We present the development and characterization of a different approach of gene product delivery into an animal model system. The BL/6 cells and MEF cells infected with a helper-free recombinant retroviral vector containing the human clotting factor IX cDNA secrete partially biologically active clotting factor at a rate 10-fold higher than seen with another retroviral vector containing the human clotting factor cDNA (19). In addition, we have demonstrated that these genetically modified cells can be reintroduced into the loose connective tissue of the dermis of a syngeneic mouse. Grafts are quickly vascularized in the presence of angiogenic factor, fibroblast growth factor, and remain vascularized for at least 28 days. Grafts containing the BL/6 cells grow as aggressive tumors over this period, while the size of the grafts containing MEF cells does not increase over the same period. The clotting factor secreted from the infected cells in the graft is accessible to the circulatory compartment and can easily be detected in serum of the recipient. Functional status of the infected cells in the grafts can be measured by monitoring serum levels of human factor IX or by the ability of explanted cells to continue secreting the human protein. However, C57BL/6 mice recognize the human blood clotting factor as foreign and thus mount a strong humoral immune response against it. Although a humoral response against factor IX clearly exists, there does not appear to be a major cell-mediated response against the cells in the grafts. The cells in the graft are still viable after 28 days of implantation and continue to synthesize factor IX protein.

Recently two groups have used mouse fibroblasts to introduce and express foreign genes in mice (28, 29). One group implanted mice with DNA-transfected cell line and showed that the recipient mice made the gene product (growth hormone) and maintained the graft only if the mice are immunosuppressed (28). The other group using retroviral vectors containing α_1-antitrypsin gene generated a cell line

and then transplanted them into the peritoneal cavity of nude mice (29). In both cases cell lines were generated that would potentially be tumorigenic in mice. Neither study addresses the issue of cell maintenance in grafted mice without the use of harsh immunosuppressive agents. Moreover, because of their potential tumorigenicity it is not advisable to generate syngenic human diploid cell lines and use them for introducing foreign genes. The method we have described obviates the need for cell lines and instead essentially uses the cells of recipient mice, minimizing the possibility of rejection. Culturing the cells in collagen matrix circumvents the problem of necrosis that would ensue following s.c. injection (30). The high efficiency of retroviral infection and expression in fibroblasts (>80%) simplifies the overall endeavor of introduction of foreign genes. Clinical examples for this type of treatment would include hemophilia, endocrine deficiency, α_1-antitrypsin, etc. Even though the data presented here was obtained from mouse embryo fibroblasts, we wish to add that we have extended these observations by infecting adult hemophiliac dog fibroblasts with factor IX retrovirus.

Further advances toward application of this approach would require the following: (*i*) increased levels of factor IX proteins. In normal individuals levels of factor IX protein are $\approx$5 μg/ml of plasma. Although the levels reported here are lower by several orders of magnitude, we note that individuals containing 0.5 μg of biologically active factor IX per ml in plasma do not show the symptoms of hemophilia. The low levels of factor IX can be increased either by making improved vectors capable of generating large amounts of factor IX proteins or, alternatively, by grafting more cells. According to the data presented here, we can generate up to 25 ng of factor IX per hr from an implant containing 4×10^6 cells (Fig. 4). In larger animals multiple grafts of up to 10^8 cells can be easily implanted, increasing the levels of factor IX protein to that required to alleviate the deficiency. (*ii*) Improved culturing conditions—culturing infected cells in a defined medium (without fetal bovine serum) and improved technology for reconstitution of living skin would also increase the efficiency of the system (30). Moreover, improved surgical skills may ensure that the implant would lay flat in the dermal compartment of the mouse skin to allow more uniform vascular development and hence improve cell viability during the brief period required for vascularization. Although the extent of cell viability has not yet been determined in grafts containing MEF cells, experiments in rats have shown that transplanted fibroblasts persist for at least 13 months (30).

In conclusion, we have shown that skin fibroblasts can be used as a viable mode of introduction and expression of foreign genes in animals. The process of manipulation of genetically engineered fibroblasts appears to be both less complex and cumbersome than the widely accepted use of bone marrow transplantation for somatic cell gene therapy.

We are grateful to Drs. G. G. Brownlee, D. Anson, P. Bajaj, K. Smith, S. Maki, and A. Baird for reagents. We are particularly indebted to Drs. K. Brinkhous and D. McCord for performing clotting assays. We thank Dr. J. Rhinewald, Dr. D. Anson, and B. Malone for their interest and P. McClintock for preparing the text. D.S.L. was supported by a postdoctoral fellowship from the National Cancer Institute, Canada. This work was supported by grants from the National Institutes of Health to I.M.V.

1. Miller, A. D., Eckner, R. J., Jolly, D. J., Friedmann, T. & Verma, I. M. (1984) *Science* **225**, 630–632.
2. Williams, D. A., Lemischka, I. R., Nathans, D. G. & Mulligan, R. C. (1984) *Nature (London)* **310**, 476–480.
3. Keller, G., Paige, C., Gilboa, E. & Wagner, E. F. (1985) *Nature (London)* **318**, 149–154.
4. Dick, J. E., Magli, M. C., Huszar, D. H., Phillips, R. A. & Bernstein, A. (1985) *Cell* **42**, 71–79.
5. Ledley, F. D., Darlington, G. J., Hahn, T. & Woo, S. L. C. (1987) *Proc. Natl. Acad. Sci. USA* **84**, 5335–5339.
6. Wolfe, J. A., Yee, J.-K., Skelly, H. F., Moores, J. C., Respess, J. G., Friedmann, T. & Leffert, H. (1987) *Proc. Natl. Acad. Sci. USA* **84**, 3344–3348.
7. Ledley, F. D., Grenett, H. E., McGinnis-Shelnutt, M. & Woo, S. L. C. (1986) *Proc. Natl. Acad. Sci. USA* **83**, 409–413.
8. Sorge, J., Kuhl, W., West, C. & Beutler, E. (1987) *Proc. Natl. Acad. Sci. USA* **84**, 906–909.
9. Palmer, T. D., Hock, R. A., Osborne, W. R. A. & Miller, A. D. (1987) *Proc. Natl. Acad. Sci. USA* **84**, 1055–1059.
10. Garver, R. I., Jr., Chytil, A., Courtney, M. & Crystal, R. G. (1987) *Science* **237**, 762–764.
11. Morgan, J. R., Barrandon, Y., Green, H. & Mulligan, R. C. (1987) *Science* **237**, 1476–1479.
12. Kriegler, M., Perez, C. F., Hardy, C. & Botchan, M. (1984) *Cell* **38**, 483–491.
13. Anson, D. S., Choo, K. H., Rees, D. J. G., Gianelli, F., Goald, K., Huddleston, J. A. & Brownlee, G. G. (1984) *EMBO J.* **3**, 1053–1060.
14. Miller, A. D. & Buttimore, C. (1986) *Mol. Cell. Biol.* **6**, 2895–2902.
15. Mann, R., Mulligan, R. C. & Baltimore, D. (1983) *Cell* **33**, 153–159.
16. Todaro, G. J. & Green, H. J. (1963) *J. Cell Biol.* **17**, 299–313.
17. Elsdale, T. & Bard, J. (1972) *J. Cell Biol.* **54**, 626–637.
18. Bell, E., Ivarsson, B. & Merrill, C. (1979) *Proc. Natl. Acad. Sci. USA* **76**, 1274–1278.
19. Anson, D. S., Hock, R. A., Austen, D., Smith, K. J., Brownlee, G. G., Verma, I. M. & Miller, A. D. (1987) *Mol. Biol. Med.* **4**, 11–20.
20. Smith, K. J., Singaraju, C. & Smith, L. F. (1987) *Am. J. Clin. Pathol.* **87**, 370–376.
21. Goldsmith, J. C., Chung, K. S. & Roberts, H. R. (1978) *Thromb. Res.* **12**, 497–502.
22. Bajaj, S. P., Rapaport, S. I. & Maki, S. L. (1985) *J. Biol. Chem.* **260**, 11574–11580.
23. Chavin, S. I. & Weidner, S. M. (1984) *J. Biol. Chem.* **259**, 3387–3390.
24. Fournel, M. A., Newgren, J., Madanat, M. & Pancham, N. (1985) *Thromb. Haemostasis* **54**, 147 (abstr.).
25. Suttie, J. W. (1980) *CRC Crit. Rev. Biochem.* **8**, 191–223.
26. Ferlund, P. & Stenflo, J. (1983) *J. Biol. Chem.* **258**, 12509–12512.
27. Towbin, H., Staehelin, T. & Gordon, J. (1979) *Proc. Natl. Acad. Sci. USA* **76**, 4350–4354.
28. Selden, R. F., Skoskiewicz, M. J., Howie, K. B., Russell, P. S. & Goodman, H. M. (1987) *Science* **236**, 714–718.
29. Garver, R. I., Jr., Chytil, A., Karlsson, S., Fells, G. A., Brantley, M. L., Courtney, M., Kantoff, P. W., Nienhuis, A. W., Anderson, W. F. & Crystal, R. G. (1987) *Proc. Natl. Acad. Sci. USA* **84**, 1050–1054.
30. Bell, S., Sher, S., Hall, B., Merrill, C., Rosen, S., Chamson, A., Asselinean, D., Dubertret, L., Coulomb, B., Capiere, C., Nusgens, B. & Nevewe, Y. (1983) *J. Invest. Dermatol.* **81**, 25–103.
31. Glenney, J. (1986) *J. Anal. Biochem.* **156**, 315–319.

Proc. Natl. Acad. Sci. USA
Vol. 85, pp. 8241–8245, November 1988
Medical Sciences

Expression of the human growth hormone variant gene in cultured fibroblasts and transgenic mice

(anterior pituitary/transient expression/metallothionein)

RICHARD F SELDEN*†, THOMAS E. WAGNER‡, SANDRA BLETHEN§, JEUNG S. YUN‡, MARY ELLEN ROWE*†, AND HOWARD M. GOODMAN*†

*Department of Molecular Biology, Massachusetts General Hospital, Boston, MA 02114; †Department of Genetics, Harvard Medical School, Boston, MA 02114; ‡Edison Animal Biotechnology Center, Ohio University, Athens, OH 45701; and §Department of Pediatric Endocrinology, Long Island Jewish Medical Center, New Hyde Park, NY 11042

Communicated by Robert L. Letsinger, June 30, 1988

ABSTRACT **The nucleotide sequence of the human growth hormone variant gene, one of the five members of the growth hormone gene family, predicts that it encodes a growth hormone-like protein. As a first step in determining whether this gene is functional in humans, we have expressed a mouse metallothionein I/human growth hormone variant fusion gene in mouse L cells and in transgenic mice. The growth hormone variant protein expressed in transiently transfected L cells is distinct from growth hormone itself with respect to reactivity with anti-growth hormone monoclonal antibodies, behavior during column chromatography, and isoelectric point. Transgenic mice expressing the growth hormone variant protein are 1.4- to 1.9-fold larger than nontransgenic controls, suggesting that the protein has growth-promoting properties.**

Structure–function relationships within the human growth hormone (hGH) gene family are likely to play critical roles in growth and development. The hGH gene family consists of five highly homologous members (1–3), which are encoded within 50 kilobases (kb) on band q22-q24 of chromosome 17 (4, 5) and are categorized based on their resemblance to hGH or to chorionic somatomammotropin (CS). The *GHA* gene (now designated *GH1*) encodes pituitary hGH and is expressed in the somatotrophs of the anterior pituitary (6). The hGH variant gene (*GHB*; now designated *GH2*) also encodes a GH-like polypeptide (3, 7, 8), and recent evidence suggests that low levels of GHB mRNA are present in term placenta (9). Two of the CS-like genes (*CSA* and *CSB*; now designated *CSH1* and *CSH2*) express identical forms of CS in the placental syncitium (7), and the third (*CSHP1*) is a pseudogene (2, 3). Any two of the five genes in the family are at least 92% homologous, suggesting a relatively recent series of gene duplications (2, 3). The hGH gene family members are also related to the prolactin gene (10), with hGH and prolactin sharing ≈35% amino acid homology.

Of the five members of the hGH gene family, only the function of hGH itself (the product of the *GHA* gene) has been well characterized. The GHA protein (hGH) has both growth-promoting properties and a variety of metabolic properties (11–13), and a homozygous deletion of only the *GHA* gene has been reported to cause isolated hGH deficiency type IA (14, 15). CS may play a role in both intermediary metabolism and mammary gland development (16), but individuals with homozygous deletions of the genes for CS appear normal (17). It is possible that the structural homology of the hGH gene family members allows for some functional overlap.

An important step towards understanding the molecular biology and physiology of the hGH gene family is to determine the function(s) of the hGH variant and its morphological and developmental pattern of expression in the body. Hamer and coworkers (18, 19) have shown that the *GHB* gene can be expressed in monkey kidney cells infected by simian virus 40/*GHB* recombinants and that the protein produced resembles hGH, based in part on one-dimensional tryptic maps. We have extended these results by producing GHB in transiently transfected cells and have studied the function of GHB by generating a series of transgenic mice. In this report, we present further characterization of the protein and demonstrate that transgenic mice expressing *GHB* grow to almost twice the size of control mice.

MATERIALS AND METHODS

Plasmid Constructions. The *Mt-1/GHB* fusion gene was constructed by ligating a 1.8-kb *Eco*RI–*Bgl* II fragment containing promoter sequences from the mouse metallothionein I gene, *Mt-1*, (20) to a 2.1-kb *Bam*HI–*Eco*RI *GHB* gene fragment (prepared by using a partial *Bam*HI digestion), which contains structural sequences from the start of transcription at the *Bam*HI site to ≈500 base pairs (bp) past the poly(A) addition site (3). The ligated material was digested with *Eco*RI and inserted into the *Eco*RI site of the plasmid vector pUC12 (21). The resulting plasmid is referred to as pXGH4. The *Mt-1/GHA* fusion gene was constructed as described (22) and is referred to as pXGH5. Standard techniques of molecular cloning utilized to construct and isolate these plasmids were performed as described (23).

Tissue Culture and Transfections. Mouse L cell fibroblasts were grown in Dulbecco's modified Eagle's medium supplemented with 10% (vol/vol) calf serum. L cells (≈5×10^5) were plated on 10-cm tissue culture dishes and allowed to grow for 3 days to ≈30% confluence. DEAE-dextran-mediated transfections were performed essentially as described (22, 24). Briefly, the medium was aspirated from the dish, and the cells were washed once with phosphate-buffered saline (PBS). The desired amount of DNA was precipitated with ethanol and resuspended in 60 μl of Tris-buffered saline (0.15 M NaCl/5 mM KCl/1.5 mM Na_2HPO_4/2.5 mM Tris base/1 mM $CaCl_2$/0.5 mM $MgCl_2$, pH 7.5; the $CaCl_2$ and $MgCl_2$ were prepared together as a 100× stock solution, which was added slowly to the other components to avoid precipitation) and then added to 120 μl of warm (30–40°C) Tris-buffered saline containing DEAE-dextran at 5 mg/ml. This mixture was then combined with 3 ml of 10% Nu-Serum (Collaborative Research, Waltham, MA) and added to the plate. After incubation for 4 hr at 37°C in 5% CO_2/95% air, the DNA–DEAE-dextran–Nu-Serum was removed and replaced by 5 ml of 10% (vol/vol) dimethyl sulfoxide in PBS. This was incubated for 1 min at room

The publication costs of this article were defrayed in part by page charge payment. This article must therefore be hereby marked "*advertisement*" in accordance with 18 U.S.C. §1734 solely to indicate this fact.

Abbreviations: GH, growth hormone; hGH, human GH; CS, chorionic somatomammotropin; nt, nucleotides.

temperature, the dimethyl sulfoxide was aspirated, and 10 ml of the appropriate medium was added to the dish. The cells were incubated at 37°c in 5% CO_2/95% air for several days, and aliquots of the medium were collected at various times as described in the text. Total RNA was prepared from mouse L cells, and blot-hybridization analysis was carried out as described (25). The resulting nitrocellulose filter was prehybridized overnight and then hybridized to a ^{32}P-labeled *Mt-1/GHB* genomic probe (an 802-bp *Sac* I fragment from position −211 to +591 with respect to the transcriptional start site; see Fig. 1).

Protein Analyses. GH levels were measured with a two-site radioimmunoassay under the conditions recommended by the manufacturer (Hybritech, San Diego, CA). Radiolabeling of L cells transiently transfected (as above) was performed as follows: 5 days after transfection, medium was removed and replaced with 7.5 ml of methionine-free minimal essential medium containing 2% calf serum; 2 hr later, 5 ml of the identical medium supplemented with 0.2 mCi (1 Ci = 37 GBq) of [^{35}S]methionine was added to each plate, and aliquots of medium were collected 23 hr later. Fifty microliters of each sample was electrophoresed on a denaturing 12% polyacrylamide gel. Radioimmunoassays using affinity-purified iodinated GHA were performed as follows (S.B., unpublished data): 100 μl of standard or unknown was incubated with 100 μl of monoclonal antibody (mAb) 352, 033, or 665 [ref. 26; diluted 1:2 × 10^6 (mAB 352), 1:3.2 × 10^6 (mAB 033), and 1:3 × 10^6 (mAB 665) in PBS, pH 7.0/0.2% bovine serum albumin] for 2 hr at 37°C; ^{125}I-labeled GHA (≈4000 cpm) was added, the mixture was incubated overnight at 4°C, and bound radiolabel was separated by using a solid-phase goat anti-mouse IgG (Immunobeads, Bio-Rad). Interassay variability was 12%, and intraassay variability was 7%. Human, bovine, and murine GH were purified by A. F. Parlow of Harbor–University of California, Los Angeles, Medical Center and distributed by the National Hormone and Pituitary Program. Gel filtration was performed with 1.6 × 70 cm columns of Sephadex G-75 in PBS (pH 7.0). Samples of 2 ml were applied to the column, and 2.5-ml fractions were collected and assayed for GH immunoreactivity with antibody 665. Isoelectric focusing was performed as described (27).

Transgenic Mice. A 2.8-kb *Kpn* I–*Eco*RI fragment containing the *Mt-1/GHB* fusion gene was isolated from pXGH4 sequences by preparative gel electrophoresis and electroelution. Fertilized mouse eggs for microinjection were recovered *in cumulus* from the oviducts of (C57BL/6 × C3H)F_1 females that had mated with (C57BL/6 × C3H)F_1 males several hours earlier. Approximately 1000 copies of the fusion gene fragment were microinjected into the male pronucleus of each fertilized egg. Microinjected eggs were implanted into the oviducts of 1-day pseudopregnant ICR foster mothers and were carried to term (28). Total genomic DNA was prepared from mouse tails as described (29). Total cellular RNA was isolated from tissue samples by the guanidinium isothiocyanate/CsCl technique (30). For RNA blot analysis, 10 μg of total RNA from each sample was subjected to electrophoresis on a 1.2% agarose/formaldehyde denaturing gel and transferred to nitrocellulose filters. The filter was then prehybridized, hybridized to a ^{32}P-labeled 802-bp *Sac* I fragment from within the *Mt-1/GHB* fusion gene, washed, and exposed to x-ray film.

RESULTS

Production and Characterization of the GHB Protein. We have demonstrated (22) that hGH (GHA) and several other secreted proteins can be produced in large quantities by transiently transfected mouse L cells. To express the GHA and GHB proteins, appropriate fusion genes were constructed (Fig. 1); the plasmid containing the *Mt-1/GHB* fusion gene is pXGH4, and the *Mt-1/GHA*-containing plasmid is pXGH5.

Total cellular RNA was prepared 4 days after transient transfection of L cells with 10 μg of either pXGH4 or pXGH5 by the DEAE-dextran method. The RNA was then subjected to blot-hybridization analysis (Fig. 2 *Left*). RNA prepared from cells transfected with either plasmid contained a hybridizing band of ≈900–950 nucleotides (nt), which corresponds to the expected fusion mRNAs [predicted to contain 64 nt of *Mt-1* 5′ untranslated region, 817 nt of *GHA* or *GHB*, and a poly(A) tail]. Based on this result, we conclude that similar amounts of GHA and GHB fusion mRNAs are produced in L cells transiently transfected with equal amounts of the plasmids. This similarity in mRNA levels can be attributed to the presence of the identical *Mt-1* promoter in both fusion genes and to the high homology between the GHA and GHB mRNAs. It also suggests that the transcriptional rates of the fusion genes are approximately the same and that the stabilities of the fusion mRNAs are also comparable. Both RNA samples contain an additional hybridizing band of ≈1500 nt. The origin of this band may be due to an upstream promoter or to aberrant or partial processing of a correctly initiated transcript.

To determine if the fusion mRNAs could direct synthesis and secretion of GHA and GHB, aliquots of medium were taken daily from dishes of L cells transiently transfected with 1 μg of either pXGH4 or pXGH5. The level of GHA or GHB secreted into the medium was determined with a commercially available radioimmunoassay in which the amount of hGH specifically bound by a first mAb is measured by using a second, ^{125}I-labeled mAb directed against a different hGH epitope. GHA production (solid line in Fig. 2 *Center*) was first detectable at ≈24 hr after transfection and accumulated rapidly in the medium during the next 3 days. GHB expression (dashed line in Fig. 2 *Center*) could not be detected by this assay. Since the *Mt-1/GHB* fusion gene is properly transcribed, this result suggests that, if GHB is synthesized and secreted properly, it does not bind efficiently to one or both of the anti-GHA mAbs used in this assay.

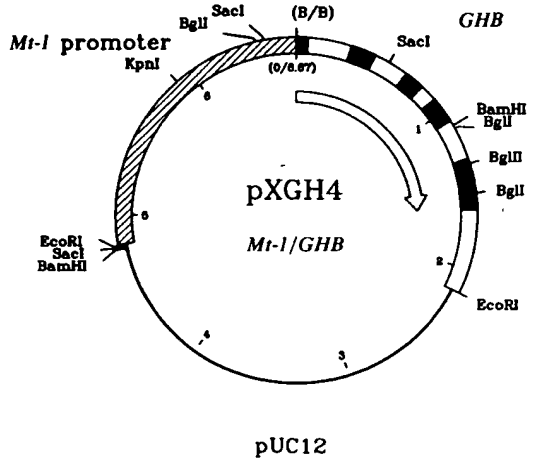

FIG. 1. Structure of plasmid containing the *Mt-1/GHB* (pXGH4) fusion gene. The hatched box in the plasmid represents the promoter and 5′ flanking sequences of the mouse *Mt-1* gene, and the black and white boxes represent the exons and introns respectively of the human *GHB* gene. B/B is the site at which the *Mt-1 Bgl* II site was ligated to the *GHB Bam* HI site (and which now cannot be cut with either enzyme). Numbers inside the plasmid represent the distance in kb from B/B, and the clockwise arrows indicate the predicted start site and direction of transcription of the fusion gene.

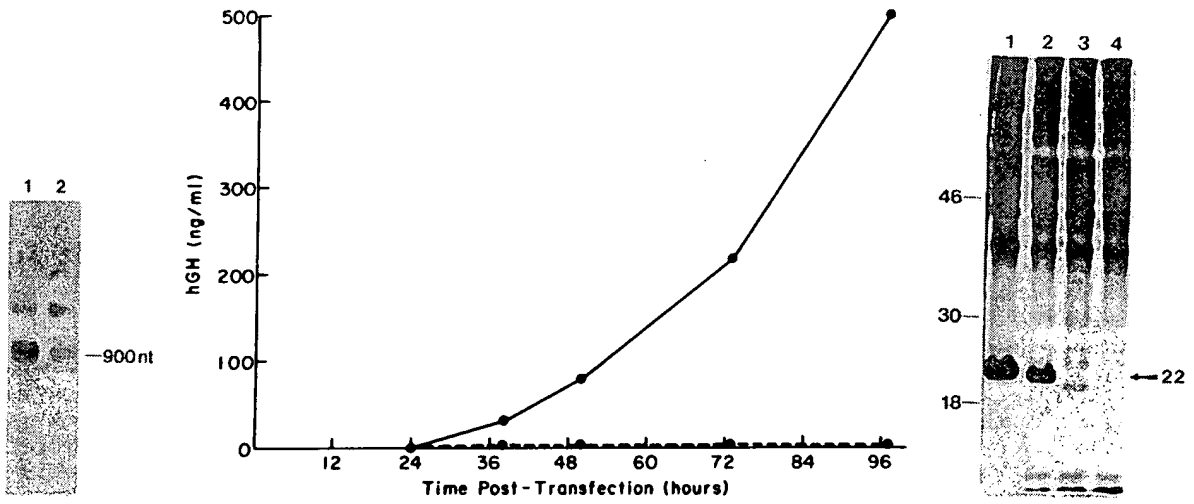

FIG. 2. (*Left*) Blot-hybridization analysis of total cellular RNA prepared from transiently transfected cells. Mouse L cells were transfected with 10 μg of pXGH4 or pXGH5 using the DEAE-dextran protocol, and RNA was prepared 4 days later, separated on a 1.2% agarose/formaldehyde gel, transferred to nitrocellulose, and hybridized with an 802-bp *Sac* I fragment of the *Mt-1/GHB* gene as described. Lanes contained 10 μg of total RNA prepared from cells transfected with pXGH4 (lane 1) or pXGH5 (lane 2). In this experiment the hybridizing bands are ≈900 nt, although in other experiments (not shown), the bands are closer to 950 nt; this minor discrepancy may be due to small differences in the quality of RNA preparations but most likely reflects typical experiment-to-experiment variability in electrophoresis. (*Center*) Detection of GHA (—) and GHB (- - -) in the medium of transiently transfected cells. Mouse L cells were transfected with 1 μg of pXGH4 or pXGH5 as in *Left*, and aliquots of the medium were taken at the indicated times after transfection and assayed by using a commercially available radioimmunoassay. (*Right*) Radiolabeling of transiently expressed GHA and GHB. Mouse L cells were mock-transfected (lane 4) or were transfected with 10 μg of pXGH4 (lane 3) or pXGH5 (lane 2) and were radiolabeled as described. Rat GH4 cells, a well-characterized pituitary tumor cell line known to secrete a 22-kDa rat GH (arrow), were radiolabeled as above but were not transfected (lane 1). Aliquots of medium were electrophoresed on a denaturing 12% polyacrylamide gel, and size markers (in kDa) are indicated.

The ability of the GHB fusion mRNA to direct translation of a secreted product was investigated by performing a radiolabeling experiment. L cells transiently transfected with 10 μg of either pXGH4 or pXGH5 were cultured in the presence of [^{35}S]methionine for ≈1 day. Aliquots of medium from both transfections were collected and analyzed by sodium dodecyl sulfate (SDS)/polyacrylamide gel electrophoresis followed by autoradiography (Fig. 2 *Right*). Medium from cells transfected with either pXGH4 or pXGH5 contained a radiolabeled protein that was not present in the medium of mock-transfected L cells treated as above.

The radiolabeled pXGH4- and pXGH5-derived bands differed with respect to apparent molecular mass and intensity. The pXGH5-derived band had an apparent molecular mass of 22 kDa and was ≈10-fold more intense than the pXGH4-derived band, which had an apparent molecular mass of 21 kDa. Mature GHA and GHB were both predicted to have molecular masses of 22 kDa, and the difference in their observed mobility most likely reflected differences in their isoelectric points (see below) and SDS-binding capacities. The 10-fold difference in accumulation between GHA and GHB (as determined by densitometry) might reflect less efficient synthesis or secretion of GHB or a greater instability of GHB in the medium as compared with GHA. In any case, the *GHB* fusion gene does direct synthesis and secretion of a protein product consistent with its DNA sequence.

Medium from cells transfected with the *GHB* fusion gene was tested with a battery of three anti-GHA mAbs (26). Relative GHB cross-reactivity with each mAb was estimated by dividing the amount of culture medium containing GHA that gave 50% displacement of ^{125}I-labeled hGH by the amount of GHB-containing medium required for 50% displacement and normalizing to the absolute amount of GH protein sequences present in each medium (as determined by radiolabeling above). The estimated cross-reactivity of GHB (Table 1) ranges from 1.7×10^{-2} with antibody 033 to $2.4\ 10^{-1}$ with antibody 665.

The cross-reactivities of murine and bovine GHs with the three anti-GHA mAbs were calculated by assaying a sample containing a known amount of one of these GHs with each mAb and then dividing the measured amounts by the known amount of GH present in the sample (Table 1). Although GHB has less cross-reactivity than GHA with respect to all three antibodies, the cross-reactivity of GHB is substantially higher than both murine and bovine GH. The relative specificity of the mAbs for the GHB protein as compared to mouse GH is important because it suggests that GHB expressed in the serum of a transgenic mouse at even a moderate level can be distinguished from endogenous mouse GH by using any of the mAbs.

The molecular mass of the anti-GH cross-reacting material produced by L cells transfected with either the *GHA* or *GHB* fusion gene was determined by gel filtration on Sephadex G-75 columns (data not shown). Fractions collected from the

Table 1. Relative cross-reactivities of GHB, mouse GH, rat GH, and bovine GH with anti-GHA mAbs

GH	Relative cross-reactivity with mAb		
	mAb 352	mAb 033	mAb 665
GHB vs. GHA	7.7×10^{-2}	1.7×10^{-2}	2.4×10^{-1}
Murine GH vs. GHA	5.0×10^{-5}	5.0×10^{-5}	1.5×10^{-4}
Bovine GH vs. GHA	$<5.0 \times 10^{-5}$	$<5.0 \times 10^{-5}$	6.0×10^{-5}
GHB vs. murine GH	1540	340	1600
GHB vs. bovine GH	>1540	>340	4000

GH levels were measured with a nonequilibrium radioimmunoassay using affinity-purified iodinated GHA. Relative cross-reactivities of GHB and murine and bovine BHs with the anti-GHA mAbs were determined by assaying a known amount of these GHs and then dividing the measured amounts by the known amounts (the actual amount of GHB assayed was determined by performing a radiolabeling experiment as described in the text). Relative cross-reactivities of GHB compared with murine and bovine GHs with the GHA mAbs were calculated by dividing GHB cross-reactivity with each mAb by murine and bovine cross-reactivity with each mAb.

columns were assayed with mAb 665. When GHA-containing medium was subjected to gel filtration, ≈70–75% of the GHA was recovered as a 22-kDa monomer and the remainder as an apparent dimer of ≈44 kDa. The GHB gel filtration profile was distinct from that of GHA, with only 25% recovered as monomer and the remainder as an apparent dimer. When the GHB-containing culture medium was subjected to immunoisoelectric focusing (with mAb 665), three peaks of GH immunoreactivity were found. The major peak was located at pH 8.8, and two minor peaks, most likely representing deamidation products analogous to those observed with GHA, were located at pH 8.35 and pH 8.5.

Generation and Characterization of Transgenic Mice Expressing *GHB*. To determine whether GHB can function in animals, transgenic mice containing a *Mt-1/GHB* fusion gene were generated. The *GHB* fusion gene that we have used for this purpose is contained within a 2.8-kb *Kpn* I–*Eco*RI fragment from the *Mt-1/GHB* fusion gene plasmid described in Fig. 1. The fragment contains about 700 bp of *Mt-1* 5′ flanking sequences and 2.1 kb of *GHB* structural sequences. After one set of injections and implantations, a total of 45 mice were born and subjected to further analyses.

At 3 weeks of age, a small piece of tail was removed from each mouse and used for the preparation of total genomic DNA. Hybridization to this DNA probed with an 802-bp *Sac* I fragment of the fusion gene revealed that 3 of the 45 mice were transgenic. Several blot-hybridization experiments (not shown) were performed to determine the structure of the fusion genes in these 3 mice. Total genomic digests with *Bgl* I yielded an ≈1.4-kb band that hybridized to the *Sac* I probe; the size of this band corresponds to the predicted size of the fragment expected from *Bgl* I digestion of the fusion gene itself (see Fig. 1). Based on these experiments, we conclude that the genome of each of the 3 transgenic mice contains at least one integrated and structurally intact fusion gene.

The three transgenic mice, all males, were weaned 30 days after birth and their weights were monitored for the next several weeks (Fig. 3). At the time of weaning, the three mice were significantly larger than nontransgenic (C57BL/6 × C3H)F_1 males; by two months of age, they were from 40% to 90% larger than controls. This increase in size was proportional, and in all other respects the transgenic mice appeared normal. One of the three transgenic mice was extensively bred; the *Mt-1/GHA* gene was inherited in Mendelian fashion in the resulting line, the transgenic offspring displaying the transgenic phenotype. Sera from the transgenic mice were assayed by using mAb 665 (based on a standard curve generated from the pXGH4 and pXGH5 radiolabeling experiment described above) and estimated to contain GHB at 19.1 μg/ml for mouse 5, 30.9 μg/ml for mouse 16, and 17.4 μg/ml for mouse 41. Serum from control mice contained no detectable GH, confirming the low cross-reactivity of mouse GH with mAb 665 (see Table 1). These observations are similar to those for transgenic mice expressing the *Mt-1/GHA* fusion gene (31), which have been reported to contain serum levels of GHA up to 64 μg/ml. When serum from mouse 16 was subjected to gel filtration, only the GHB dimer was recovered.

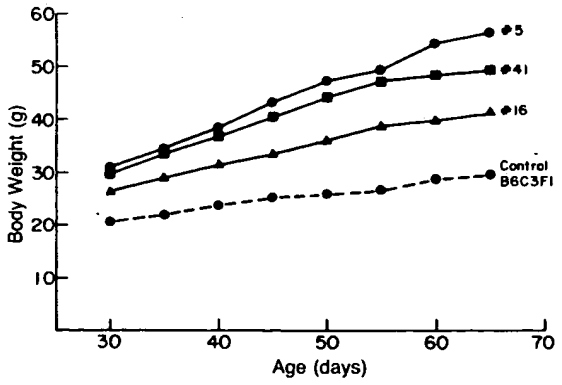

FIG. 3. Growth of transgenic mice containing the *Mt-1/GHB* fusion gene. Three of 45 mice born after one series of injections with a 2.8-kb *Kpn* I–*Eco*RI fragment containing the *Mt-1/GHB* fusion gene were found to be transgenic by Southern hybridization analysis. These 3 mice were weaned 30 days after birth and were weighed every 5th day thereafter. The dashed line represents the averaged weights of 10 (C57BL6 × C3H)F_1 males (standard errors range between 0.3 and 0.4 g for each point).

To determine the tissue specificity of fusion gene expression in these mice, RNA analyses were performed. Transgenic mouse 16 was sacrificed, and total cellular RNA was isolated from samples of several tissues by the guanidinium isothiocyanate/CsCl technique (30). RNA blot hybridizations using the 802-bp *Sac* I *Mt-1/GHB* probe showed that RNA prepared from liver (Fig. 4, lane 4) contained the most intensely hybridizing band, from brain (lane 5) and heart (lane 2) contained moderately hybridizing bands, and from kidney (lane 1) and small intestine (lane 6) contained weakly hybridizing bands. In all of these tissues, the hybridizing band was ≈900–950 nt as was expected (see above). RNA prepared from lung did not hybridize to the *Mt-1/GHB* probe. This pattern of expression is consistent with that previously reported for *Mt-1* fusion genes in transgenic mice (31–33).

DISCUSSION

We have studied the structure of GHB produced by transiently transfected cells and the function of GHB in transgenic mice. GHB in the medium of transfected cells shows moderate levels of cross-reactivity with anti-GHA mAbs—levels that are substantially higher than the cross-reactivities of murine and bovine GH with the same mAbs (Table 1). A greater fraction of GHB produced by transfection of mammalian cells with appropriate fusion genes is present as aggregates than similarly prepared GHA, and the isoelectric point of recombinant GHB is 8.8 compared with 4.9 for GHA. When expressed in the liver and other locations in transgenic mice, GHB causes a 1.4- to 1.9-fold increase in the size of the animals (Fig. 3).

The primary structure of GHB differs from that of GHA by 15 amino acid substitutions (out of a total of 191 amino acids in the mature proteins and 26 amino acids in the prese-

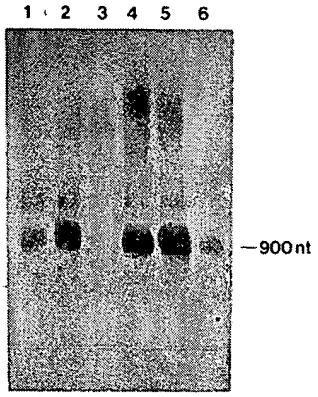

FIG. 4. Detection of Mt-1/GHB mRNA in tissues of transgenic mouse. Blot-hybridization analysis of 10 μg of total cellular RNA prepared from several tissues with the 802-bp *Sac* I *Mt-1/GHB* genomic probe was performed as described (see the Fig. 2 legend). Lanes: 1, kidney; 2, heart; 3, lung; 4, liver; 5, brain; 6, small intestine.

quence). GHB contains two fewer acidic and three more basic amino acids than GHA, and the measured isoelectric point of 8.8 for the transiently expressed protein is fully consistent with the predicted isoelectric point of 8.9 (2) based on sequence data. Although GHA and GHB have highly homologous primary structures, the mAb, isoelectric-focusing, and gel-filtration results all suggest that the two proteins have significantly different tertiary and quarternary structures.

The protein characterization we have presented and the ability to produce large quantities of GHB in the medium should facilitate the study of *GHB* expression in humans. Partially purified GHB can be used to generate mAbs, and, based on structural differences between GHA and GHB, it is reasonable to expect that some of these mAbs will bind 1–2 orders of magnitude less efficiently with GHA. The anti-GHB mAbs could then be used to assay for GHB in the serum, pituitary, placenta, and other locations in the body. If it appears that the *GHB* gene is expressed in humans, a determination of the isoelectric point of the protein should help confirm its identity.

GHB clearly functions to promote growth and development in mice. The increase in size of transgenic mice containing the *Mt-1/GHB* fusion gene is similar to that for transgenic mice containing the *Mt-1/GHA* fusion gene (31). Although GHB is growth-promoting in mice, it may not perform the same function when it is expressed in humans, or it may be expressed in a temporal and tissue-specific manner distinct from that of GHA. Patients with a homozygous deletion of only the *GHA* gene grew significantly less than average (14, 15), suggesting that *GHB* cannot by itself correct for the deficiency of *GHA* (the status of the *GHB* alleles of this patient was not studied, and it is formally possible that they were also mutant). We agree with the suggestion of Hizuka and coworkers (19) that it is possible that GHB works as a partial agonist. The possibility that a large proportion of GH oligomers found in normal human serum may be related to GHB production should also be considered.

Both GHA and GHB (19) are able to bind efficiently to GH receptors, and both promote growth in transgenic mice. A 20-kDa form of GHA, derived from alternative splicing of the GHA mRNA, has been described (34, 35), and sequence analysis shows that the GHB mRNA is also a candidate for this alternative splicing event. If the presence of GHA momomers, GHA oligomers, and the 20-kDa GHA-derived protein is in fact supplemented in humans with GHB monomers, GHB oligomers, and a 20-kDa GHB-derived protein, the study of the control of human growth and development may become even more complex than was anticipated when the existence of the five-member hGH gene family was first discovered.

This work was supported by a grant from Hoechst AG.

1. Moore, D. D., Conkling, M. A. & Goodman, H. M. (1982) *Cell* **29**, 285–287.
2. Seeburg, P. H. (1982) *DNA* **1**, 239–249.
3. Moore, D. D., Selden, R. F., Prost, E. P., Ory, D. S. & Goodman, H. M. (1986) in *Endocrine Genes*, ed. Habener, J. (Humana Press), pp. 121–135.
4. Owerbach, D., Rutter, W. J., Martial, J. A., Baxter, J. D. & Shows, T. B. (1980) *Science* **209**, 289–292.
5. Harper, M. E., Barrera-Saldana, H. A. & Saunders, G. F. (1982) *Am. J. Hum. Genet.* **34**, 227–234.
6. Martial, J. A., Hallewell, R. A., Baxter, J. D. & Goodman, H. M. (1979) *Science* **205**, 602–607.
7. Barrera-Saldana, H. A., Seeburg, P. H. & Saunders, G. F. (1983) *J. Biol. Chem.* **258**, 3787–3793.
8. Selby, M. J., Barta, A., Baxter, J., Bell, G. I. & Eberhardt, N. L. (1984) *J. Biol. Chem.* **259**, 13131–13138.
9. Seeburg, P. (1986) *Abstracts of the 68th Annual Meeting: The Endocrine Society* (Williams & Wilkins, Baltimore), p. 14.
10. Truong, A. T., Duez, C., Belayew, A., Renard, A., Pictet, R., Bell, G. I. & Martial, J. A. (1984) *EMBO J.* **3**, 429–437.
11. Kostyo, J. L. & Nutting, D. F. (1974) in *Handbook of Physiology*, eds. Greep, R. O., Astwood, E. B., Knobil, E., Sawyer, W. H. & Geiger, S. R. (Am. Physiol. Soc., Bethesda, MD), Sect. 7, Vol. 4, Part 2, pp. 187–210.
12. Goodman, H. M. & Schwartz, J. (1974) in *Handbook of Physiology*, eds. Greep, R. O., Astwood, E. B., Knobil, E., Sawyer, W. H. & Geiger, S. R. (Am. Physiol. Soc., Bethesda, MD), Sect. 7, Vol. 4, Part 2, pp. 211–231.
13. Altszuler, N. (1974) in *Handbook of Physiology*, eds. Greep, R. O., Astwood, E. B., Knobil, E., Sawyer, W. H. & Geiger, S. R. (Am. Physiol. Soc., Bethesda, MD), Sect. 7, Vol. 4, Part 2, pp. 233–252.
14. Phillips, J. A., III, Hjelle, B. L., Seeburg, P. H. & Zachmann, M. (1981) *Proc. Natl. Acad. Sci. USA* **78**, 6372–6375.
15. Laron, Z., Kelijman, M., Pertzelan, A., Keret, R., Shoffner, J. M. & Parks, J. S. (1985) *Isr. J. Med. Sci.* **21**, 999–1006.
16. Porter, D. G. (1980) *Placenta* **1**, 259–274.
17. Wurzel, J. M., Parks, J. S., Herd, J. E. & Nielson, P. V. (1982) *DNA* **1**, 251–257.
18. Pavlakis, G. N., Hizuka, N., Gorden, P., Seeburg, P. & Hamer, D. H. (1981) *Proc. Natl. Acad. Sci. USA* **78**, 7398–7402.
19. Hizuka, N., Hendricks, C. M., Pavlakis, G. N., Hamer, D. H. & Gorden, P., (1982) *J. Clin. Endocrinol. Metab.* **55**, 545–550.
20. Hamer, D. H. & Walling, M. (1982) *J. Mol. Appl. Genet.* **1**, 273–288.
21. Viera, J. & Messing, J. (1981) *Gene* **19**, 259–268.
22. Selden, R. F., Burke Howie, K., Rowe, M. E., Goodman, H. M. & Moore, D. D. (1986) *Mol. Cell. Biol.* **6**, 3173–3179.
23. Maniatis, T., Fritsch, E. F. & Sambrook, J. (1982) *Molecular Cloning: A Laboratory Manual* (Cold Spring Harbor Lab., Cold Spring Harbor, NY).
24. Lopata, M., Cleveland, D. & Sollner-Webb, B. (1984) *Nucleic Acids Res.* **12**, 5707–5717.
25. Alexander, M., Curtis, G., Avruch, J. & Goodman, H. M. (1985) *J. Biol. Chem.* **260**, 11978–11985.
26. Surowy, T. K., Bartholomew, R. M. & VanderLaan, W. P. (1984) *Mol. Immunol.* **21**, 345–352.
27. Righetti, P. G. & Drysdale, J. W. (1976) in *Laboratory Techniques in Biochemistry and Molecular Biology*, eds. Work, T. S. & Work, E. (North-Holland/American Elsevier, New York), pp. 337–348.
28. Wagner, T. E., Hoppe, P. C., Jollick, J. D., Scholl, D. R., Hodinka, R. L. & Gault, J. B. (1981) *Proc. Natl. Acad. Sci. USA* **78**, 6376–6380.
29. Rogol, A. D., Blizzard, R. M., Foley, T. P., Furllanetto, R., Selden, R., Mayo, K. & Thorner, M. O. (1985) *Pediatr. Res.* **19**, 489–492.
30. Chirgwin, J. M., Przybyla, A. E., MacDonald, R. J. & Rutter, W. J. (1979) *Biochemistry* **18**, 5294–5299.
31. Palmiter, R. D., Norstedt, G., Gelinas, R. E., Hammer, R. E. & Brinster, R. L. (1983) *Science* **222**, 809–814.
32. Palmiter, R. D., Chen, H. Y. & Brinster, R. L. (1982) *Cell* **29**, 701–710.
33. Palmiter, R. D., Brinster, R. L., Hammer, R. E., Trumbauer, M. E., Rosenfeld, M. G., Birnberg, N. C. & Evans, R. M. (1982) *Nature (London) 300*, 611–615.
34. DeNoto, F. M., Moore, D. D. & Goodman, H. M. (1981) *Nucleic Acids Res.* **9**, 3719–3730.
35. Lewis, U. J., Dunn, J. T., Bonewald, L. F., Seavey, B. K. & VanderLaan, W. P. (1978) *J. Biol. Chem.* **253**, 2679–2687.

Proc. Natl. Acad. Sci. USA
Vol. 87, pp. 968–972, February 1990
Immunology

Prevention of diabetes in nonobese diabetic mice by tumor necrosis factor (TNF): Similarities between TNF-α and interleukin 1

(insulitis/adoptive transfer/Ia expression/autoimmune disease)

CHAIM O. JACOB*, SADAKAZU AISO*, SARA A. MICHIE†, HUGH O. MCDEVITT*‡, AND HANS ACHA-ORBEA*

Departments of *Microbiology and Immunology, ‡Medicine, and †Pathology, Stanford University School of Medicine, Stanford, CA 94305

Contributed by Hugh O. McDevitt, November 1, 1989

ABSTRACT **The role of tumor necrosis factor α (TNF-α) in the pathogenesis of autoimmune diabetes mellitus was tested in the nonobese mouse (NOD) model system. The effects of TNF-α were assessed on three levels: (*i*) insulitis development, (*ii*) development of overt diabetes, (*iii*) adoptive transfer of diabetes by splenic lymphocytes. Spontaneous diabetes mellitus was blocked in NOD mice by long-term treatment with recombinant TNF-α. Treatment with TNF-α caused a significant reduction in the lymphocytic infiltration associated with the destruction of the insulin-producing beta cells. Class II major histocompatibility complex Ia expression by islet cells was not up-regulated by TNF-α. Moreover, TNF-α was able to suppress the induction of diabetes in adoptive transfer of lymphocytes from diabetic female mice to young nondiabetic male NOD mice. These activities of TNF-α were shared by interleukin 1α in this system. These studies have implications for the pathogenesis and therapy of autoimmune diabetes mellitus.**

Nonobese diabetic (NOD) mice spontaneously develop diabetes remarkably similar to human autoimmune insulin-dependent diabetes mellitus. There is increasing evidence that the human and the NOD disease result from immune destruction of the insulin-producing beta cells in the islets of Langerhans (1). The disease is characterized by progressive lymphocyte infiltration into the islets (insulitis) prior to the expression of overt diabetes and by the appearance of anti-islet cell antibodies in the serum (2). A T-cell-mediated autoimmune pathogenesis is implicated because the disease can be passively transferred with lymphocytes into irradiated prediabetic mice (3) and prevented by treatment with antibodies directed against Thy-1.2 (4) and L3T4 (5) or by treatment with cyclosporin A (6). Diabetes can also be prevented by treatment with antibodies to class II Ia antigens (7). Untreated animals develop profound glucose intolerance and ketosis and die within weeks of the onset of overt diabetes. The role of lymphokines, especially interferon γ (IFN-γ), interleukin 1 (IL-1), and tumor necrosis factor α (TNF-α), in the pathogenesis of autoimmune diabetes has received increasing attention recently (8, 9). It was shown that IFN-γ and TNF-α can induce the aberrant expression of class II major histocompatibility complex (MHC) molecules on pancreatic beta cells *in vitro*, suggesting a role for these lymphokines in the induction of the autoimmune process in diabetes (9). A different group of investigators has suggested that IL-1 is toxic to pancreatic beta cells *in vitro* and that TNF-α significantly enhances this toxicity (8). Recently we have suggested that TNF-α may play a significant role in preventing autoimmune nephritis in the (NZB × NZW)F_1 lupus nephritis model system (10). Here we present evidence that TNF-α has a major effect *in vivo* by protecting NOD mice from developing autoimmune insulitis and diabetes.

MATERIALS AND METHODS

Recombinant murine TNF-α (0.53 mg/ml; 2.6×10^7 units/ml) was kindly provided by Genentech. Recombinant human IL-1α (10^8 units/μg) was provided by Steve Gillis (Immunex, Seattle, WA). Mice were injected i.p. with 200 ng of IL-1α per injection according to Morrissey *et al.* (11) or with TNF-α, 3 μg.

Assessment of Diabetes. Diabetes development was monitored by testing the mice for urinary glucose three times weekly. Diabetes development was confirmed by hyperglycemia (fasting glycemia, >3 g/liter) and by histological examination showing destruction of at least 50% of the islets. Diabetic mice usually died within 2–8 weeks after development of glucosuria with overt diabetic symptoms, including polyuria, polydypsia, and severe weight loss.

Histopathology. Pancreas tissue was fixed in 10% buffered formalin and embedded in paraffin, and sections of pancreatic tissue were stained with hematoxylin/eosin. For immunohistochemistry of pancreatic endocrine cells, the formalin-fixed paraffin sections were deparaffinized and immunostained for insulin, glucagon, and somatostatin using an immunoperoxidase technique (DAKO PAP kit) according to Sternberg *et al.* (12). For immunohistochemistry of class II Ia expression in islets, pancreatic tissue was cut into small blocks, embedded in OCT compound (Tissue-Tek, Miles Scientific) and frozen in dry ice/isopentane without fixation. Cryosections were cut 4 μm in thickness, fixed in 4% paraformaldehyde, and immunostained with biotinylated monoclonal antibodies 40N and MKD6. 40N is reactive with NOD-I-Aβ molecules; MKD6 reacts specifically with I-$A^d\beta$ molecules (BALB/c) but not NOD. All slides were examined independently by two observers without knowledge of treatment or strain of mice from which the pancreas was taken.

Adoptive Transfer of Diabetes. Adoptive transfer experiments were done according to Wicker *et al.* (3). Recipient male NOD mice, 8–12 weeks of age, were irradiated [775 R (1 R = 0.258 mC/kg) from a ^{137}Cs source] and injected i.v. within 2 hr of irradiation with donor splenocytes suspended in 0.25 ml of phosphate-buffered saline (PBS). Diabetic donors were female NOD mice sacrificed 1–3 weeks after the onset of glycosuria. Single cell suspensions were prepared from 10–15 spleens and pooled for each experiment. Recipient mice were treated with TNF-α, IL-1α, or PBS i.p. on different time schedules as indicated.

TNF-α and IL-1 Production. Peritoneal exudate cells were obtained from NOD and SWR mice 4 days after injection of 3% thioglycolate medium. Following adherence to plastic,

The publication costs of this article were defrayed in part by page charge payment. This article must therefore be hereby marked "*advertisement*" in accordance with 18 U.S.C. §1734 solely to indicate this fact.

Abbreviations: NOD, nonobese diabetic; TNF, tumor necrosis factor; IL, interleukin; IFN, interferon; MHC, major histocompatibility complex.

macrophages were activated with 100 units of recombinant IFN-γ per ml and 1 μg of lipopolysaccharide (LPS) per ml as described (10). TNF-α and IL-1 production was assayed in the supernatants by bioassays as described (13, 14). For Northern blot analysis, peritoneal exudate cells were harvested 4 hr after mice were injected i.p. with 500 μg of LPS. Total cellular RNA was isolated by guanidine isothiocyanate extraction followed by cesium chloride density gradient centrifugation. Northern blot analysis was carried out following standard protocols. Ten micrograms of total RNA per lane was hybridized to murine TNF-α (15), murine IL-1β (16), or β-actin (17) probes.

RESULTS

Two groups of female NOD mice, 9–10 weeks of age, received recombinant murine TNF-α or equivalent volumes of PBS over a period of 3 months. As shown in Table 1, TNF-α treatment significantly reduced the incidence of diabetes. Although 55% of PBS-treated female NOD mice developed overt diabetes by 9 months of age, none of the TNF-α-treated mice showed evidence of diabetes. An age- and sex-matched BALB/c control group of mice treated similarly with TNF-α showed no effect whatsoever. No weight loss was observed in any of the mice treated with TNF-α.

Since many of the biological activities of TNF-α are shared by IL-1, we tested also the effects of recombinant IL-1α in this model. As shown in Table 1, IL-1α has protective effects similar to TNF-α.

To determine the effect of TNF-α administration on the islets, we examined histologic sections of the pancreas from control and TNF-α-treated NOD mice. As shown in Table 2 and Fig. 1, TNF-α treatment caused a significant reduction in the incidence of insulitis. Treatment for 1 month was sufficient to cause a significant reduction in insulitis, even when the pancreata were examined 5 weeks after treatment was stopped (Table 2, experiment 4). Thus, the onset of diabetes was blocked with TNF-α by preventing the development of insulitis.

In TNF-α-treated NOD mice, the islets not affected by insulitis were histologically normal without any evidence of necrosis. In experiments not shown, we have also stained pancreata from TNF-α-treated NOD mice for glucagon and somatostatin. Thus, immunohistochemical studies of these islets revealed normal numbers of insulin-, glucagon-, and somatostatin-containing cells (Fig. 1). Hematoxylin/eosin sections of peripheral lymph nodes, spleen, liver, lung, kidney, and thymus were examined (not shown). There were no differences in these organs between TNF-α-treated mice and the PBS controls. Specifically, there was no histological evidence of lymphocyte depletion in any of the lymphoid organs. Taken together, these experiments clearly show that TNF-α given *in vivo* as described here is not toxic to the pancreas or other organs.

Detectable levels of class II MHC antigens were not demonstrated on the beta cells of the islets in either PBS control NOD or TNF-α-treated mice (Fig. 1). Ia-positive cells were found in these pancreata, but these cells appeared to be inflammatory cells or interstitial cells and not endocrine cells.

Table 1. Prevention of diabetes development by long-term treatment with TNF-α or IL-1α

Mice			Incidence of diabetes		
Strain	Number	Treatment*	7 months	9 months	11 months
NOD	25	PBS	6	13	16
NOD	19	TNF-α, 3 μg	0	0	5†
BALB/c	10	TNF-α, 3 μg	0	0	0
NOD	10	IL-1α, 200 ng	0	0	3†

Female NOD and BALB/c mice received i.p. injections of TNF-α three times per week, 3 μg per injection starting at the age of 9–10 weeks and for a period of 12 weeks. Age-matched control female NOD mice received PBS, 0.3 ml per injection, three times per week for the same period of time. An age- and sex-matched NOD mouse group received IL-1α, 200 ng per injection, under similar conditions. Diabetes was diagnosed when fasting glycemia above 3 g/liter occurred.
*Three times per week.
†$P < 0.05$.

Table 2. Recombinant TNF-α prevents the development of insulitis in NOD mice

Exp.	Strain	Therapy	Dosage	Insulitis/no. of islets examined*	P
1	BALB/c	PBS	Daily	0/9 (0)	
				0/11 (0)	
				0/9 (0)	
	BALB/c	TNF-α	3 μg/day	0/19 (0)	
				0/20 (0)	
				0/12 (0)	
	NOD	PBS	0.3 ml/day	3/12 (25)	
				12/20 (60)	
				10/12 (83)	
	NOD	TNF-α	3 μg/day	1/17 (6)	<0.05
				0/12 (0)	
				0/18 (0)	
2	NOD	PBS	3× per wk	8/18 (44)	
				9/25 (36)	
				14/32 (44)	
	NOD	TNF-α	3 μg, 3× per wk	8/32 (25)	<0.05
				0/37 (0)	
				0/15 (0)	
3	NOD	PBS	3× per wk	9/22 (41)	
				11/23 (48)	
				10/25 (40)	
	NOD	TNF-α	3 μg, 3× per wk	2/29 (7)	<0.05
				1/25 (4)	
				2/33 (6)	
4	BALB/c	PBS	3× per wk	0/23 (0)	
				0/26 (0)	
	BALB/c	TNF-α	3 μg, 3× per wk	0/36 (0)	
				0/34 (0)	
				0/35 (0)	
	NOD	PBS	0.3 ml, 3× per wk	5/6 (83)	
				8/22 (36)	
				12/12 (100)	
	NOD	TNF-α	3 μg, 3× per wk	1/14 (7)	<0.05
				4/25 (16)	
				4/28 (14)	

NOD or BALB/c female mice were treated with TNF-α or PBS i.p., as indicated, for a period of 4 weeks starting at 8–9 weeks of age. In experiments 1 and 2, mice were sacrificed and the pancreas was taken for histology 4 days after treatment was stopped; in experiment 3, mice were sacrificed 2 weeks after treatment was stopped; in experiment 4, mice were sacrificed 5 weeks after stopping treatment. Sections of formalin-fixed, paraffin-embedded pancreas tissue from two or three randomly selected mice from each group were stained with hematoxylin/eosin. Several sections were examined from each pancreas for a total of at least 10 different islets. All slides were examined independently by two observers without knowledge of treatment or strain of mouse from which the pancreas was taken. Incidence of insulitis is shown as the ratio of infiltrated islets (insulitis) to total number of islets examined in each group.
*The percentage of total islets showing insulitis is given for each mouse separately in parentheses.

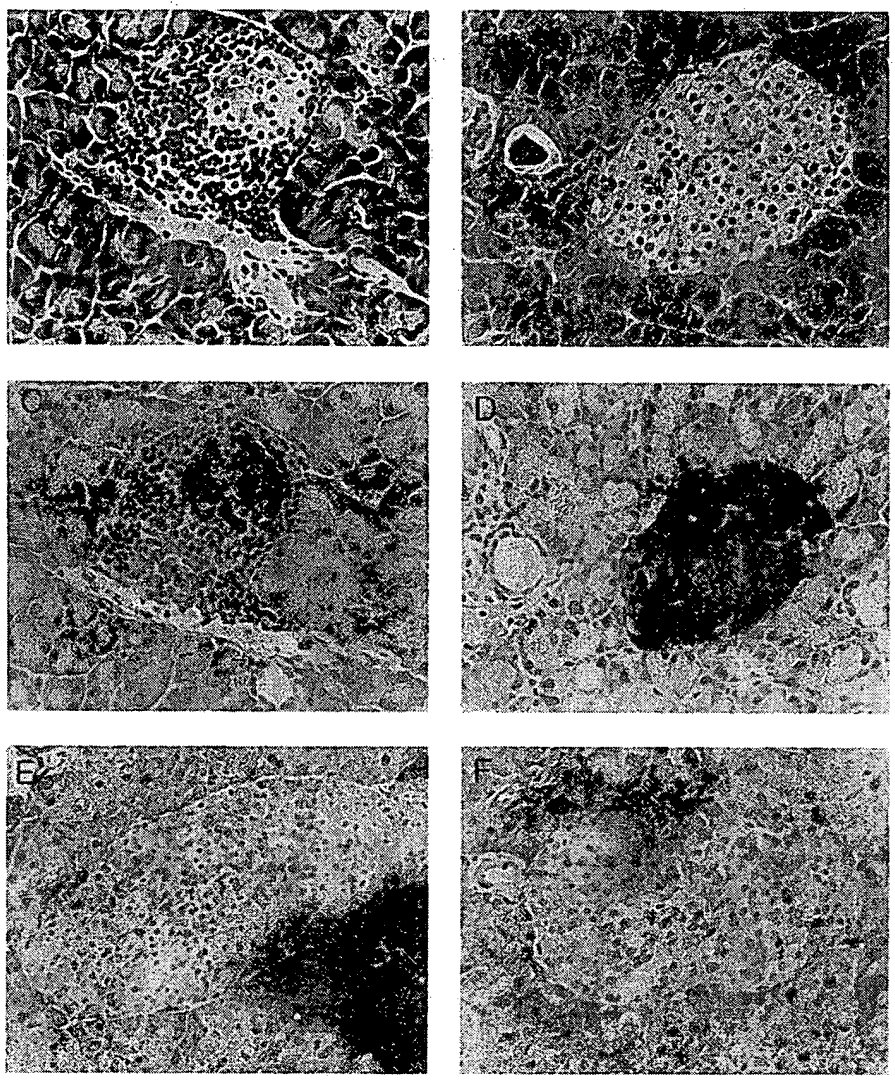

FIG. 1. Comparison of pancreatic histology of NOD mice treated with TNF-α (*Right*) and PBS-treated age- and sex-matched controls (*Left*). (*A* and *C* and *B* and *D*) Serial sections of formalin-fixed, paraffin-embedded pancreata. (*A* and *B*, stained with hematoxylin/eosin; *C* and *D*, stained with antiserum against insulin using an immunoperoxidase technique.) (*E* and *F*) Immunoperoxidase stains for Ia on frozen sections of pancreas. Randomly selected control NOD female mice older than 3 months have heavy lymphocytic infiltration of their islets (*A*), severe reduction of insulin-producing beta cells (*C*), and MHC class II Ia molecules expressed mostly on inflammatory cells with little or no Ia staining of islet cells (*E*). TNF-α-treated, age-matched female NOD mice show intact islets with no, or mild, insulitis (*B*) and normal staining of islets for insulin (*D*). There was no class II expression on islet cells of TNF-α-treated NOD mice (*F*). Note that pancreata were also stained for glucagon and somatostatin (not shown). Results of these stainings showed no decrease in glucagon- and somatostatin-producing cells in TNF-α-treated NOD mice compared with PBS-treated, age-matched, NOD female mice. (×190.)

In separate experiments we found that TNF-α is effective in preventing the adoptive transfer of diabetes by splenic lymphocytes from diabetic female NOD mice to irradiated young nondiabetic male NOD mice (Table 3). Treatment of recipient mice with TNF-α, starting 3 days after cell transfer and continuing until day 15 after transfer, significantly reduced the incidence of diabetes in the recipients. Even treatment initiated 7 days after cell transfer was still protective, although less effective than treatment starting on day 3. In preliminary experiments (not shown) we have found that TNF-α has a radioprotective effect in NOD mice [as was shown in several other mouse strains (18) if TNF-α is administered within 24 hr of irradiation]. No such protective effect could be demonstrated when TNF-α was given 72 hr or later after irradiation. We have thus selected day 3 after irradiation as the earliest time for TNF-α administration since at this point TNF-α no longer has a radioprotective effect (see control group receiving TNF-α without cells, Table 3).

Table 3. Prevention of adoptive transfer of diabetes in NOD mice by TNF-α treatment

Scheme of therapy			Cells	Diabetic recipients (+/total)			
Treatment	Frequency	Duration*	transferred	Day 26	Day 33	Day 37	Day 45
PBS, 0.3 ml	3× per wk	3–15	10^7	15/25	19/25	22/25	22/25
TNF-α, 3 μg	3× per wk	3–15	10^7	2/22†	5/22†	7/22†	9/22†
TNF-α, 3 μg	Daily	7–15	10^7	4/25‡	8/25‡	12/25‡	17/25§
TNF-α, 3 μg	3× per wk	3–15	—	¶	—	—	—
TNF-α, 3 μg	Daily	7–15	—	¶	—	—	—
PBS, 0.3 ml	3× per wk	3–15	—	¶	—	—	—
IL-1α, 200 ng	3× per wk	3–15	10^7	3/15‡	3/15‡	5/15‡	6/15‡

Incidence of diabetes is shown as the ratio of the number of diabetic mice to total number of mice in each group.
*Days after transfer during which treatment was given.
†$P < 0.005$.
‡$P < 0.01$.
§Not significant.
¶There were 8–10 mice in each of these groups. All died by day 15.

Recombinant IL-1α was also protective in these adoptive transfer experiments (Table 3), suggesting that IL-1 and TNF-α have similar activities in this system.

Peritoneal exudate cells from NOD mice produce low levels of TNF-α, similar to exudate cells from (NZB × NZW)F_1 mice (10). As shown in Fig. 2, NOD mice have three to five times lower levels of TNF-α production in comparison with SWR mice, which share with NOD mice a common derivation from a Swiss stock but are diabetes free (19). Together with the reduced TNF-α inducibility, NOD mice also have a similar reduction in their IL-1 inducibility (Fig. 2). This reduced production of TNF-α and IL-1 in NOD mice compared to SWR mice is shown on the mRNA (Fig. 2*A*) and the protein (Fig. 2*B*) levels.

DISCUSSION

TNF-α and IL-1 are members of a growing family of polypeptide mediators that orchestrate the complex processes of inflammation, immune reaction, and hemopoiesis. TNF-α and IL-1 have many biological effects that qualify them as potentially important mediators in autoimmune diseases such as type I autoimmune diabetes mellitus. The expression of MHC antigens, which is essential for initiation of immune responses, is affected by TNF-α. TNF-α induces class I MHC antigen expression (20) and synergizes with IFN-γ in the induction of class I and class II MHC mRNA and antigens (9, 21). TNF-α activates neutrophils, eosinophils, and macrophages. It induces macrophages to produce hydrogen peroxide (22), IL-1, and prostaglandin E_2 (23). Furthermore, TNF-α enhances antibody-dependent cytotoxicity and increases the number of IL-2 receptors on T cells (24). Many of these effects are shared with IL-1. However, most of these studies were done *in vitro*, and therefore their biological relevance to the homeostasis of the immune system *in vivo* remains to be determined.

The role of these cytokines in the pathogenesis of autoimmune diabetes was emphasized by several studies. The fact that infiltration of pancreatic islets by lymphocytes is the primary process that leads to the autoimmune destruction of the beta cells in type I diabetes led one group to investigate the possibility that soluble factors produced by the infiltrating cells may be involved in beta cell killing (25). Thus, IL-1 has

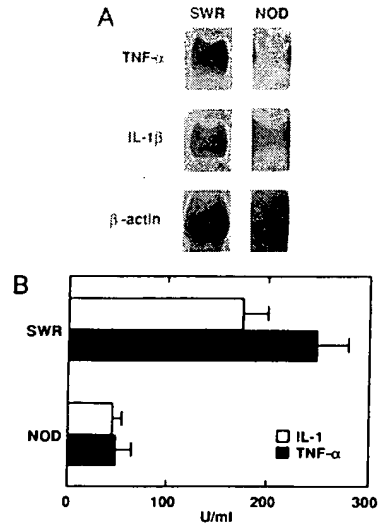

FIG. 2. Comparison between SWR and NOD mouse strains for TNF-α and IL-1 inducibility by peritoneal exudate cells. (*A*) Northern blot analysis. (*B*) Protein production. The SWR strain was chosen for comparison because these mice share with NOD a common derivation from a Swiss colony but are diabetes free (19).

been shown to be a potent suppressor of insulin production from cultured human or rat pancreatic islets. The effect was dose-dependent, with histology demonstrating disintegration of islets and cell death at the highest doses (25, 26). The effect of IL-1 was found to be significantly augmented by TNF-α (8). Thus, IL-1 and TNF-α release by infiltrating cells leading to significant beta cell damage is an attractive theory (27). The experiments described in this publication were undertaken to test the above hypothesis *in vivo*.

To our surprise, we have found that TNF-α protects NOD mice from developing insulitis as well as overt diabetes under the described *in vivo* conditions. Moreover these effects are shared by IL-1. These conclusions are based on three sets of independent experiments that clearly establish that TNF-α, rather than having a deleterious effect as predicted, is actually protecting NOD mice from developing autoimmune diabetes.

First, TNF-α was shown to reduce significantly the number of islets infiltrated by lymphocytes. This effect could be demonstrated as early after treatment as 4 weeks. Second, prolonged treatment with TNF-α for 3 months caused significant reduction in the incidence of overt diabetes development. Third, we found that TNF-α is effective in preventing the adoptive transfer of diabetes by splenic lymphocytes from diabetic female NOD mice to irradiated young nondiabetic male NOD mice.

However, our data do not necessarily contradict the previous studies. We studied the *systemic* effects of TNF-α, whereas the other group tested *in vitro* effects. It is possible that locally TNF-α and IL-1 may be toxic to pancreatic beta cells, whereas systemically they may have an immunoregulatory effect on T and/or B lymphocytes. Thus, the two mechanisms are not mutually exclusive.

It is of interest to compare the effect of TNF-α in this model system to other potential immunotherapeutics that have been suggested in the NOD mouse model. For example, in the case of treatment with monoclonal anti-L3T4, depletion of lymphocytes from islets was not observed at 1 month after initiation of treatment (5). Moreover, if treatment with anti-L3T4 was stopped after ≈100–150 days of treatment, recurrence of insulitis was observed as early as 14 days after cessation of therapy (5). In some cases a rebound phenomenon was actually described, wherein a month after stopping anti-L3T4 treatment the level of insulitis was as pronounced in the treated group as in the PBS controls (5).

In contrast, TNF-α treatment for a period of 4 weeks was sufficient to cause a significant depletion of lymphocytes from islet tissue. Even 5 weeks after cessation of TNF-α treatment (for only 4 weeks) there was still a significant reduction in insulitis [only 9 of 67 islets showed insulitis versus 25 of 40 islets in the PBS control mice ($P < 0.01$)].

Inappropriate expression of MHC class II molecules induced by INF-γ has been postulated to play a role in the initiation and development of autoimmune processes (28). These investigators have also shown that IFN-γ and TNF-α can additively induce the aberrant expression of class II MHC molecules on pancreatic beta cells *in vitro* (9), suggesting a role for these cytokines in the induction of autoimmune diabetes (9, 29). However, uncertainty persists concerning the extent and importance of aberrant expression of class II antigens on pancreatic beta cells (30). At least part of the controversy is due to the fact that Ia-positive cells can be found in the pancreas of NOD mice. However, these cells may be interstitial cells and/or inflammatory macrophages but not endocrine beta cells. Our data support the data published by Signore *et al.* (30), which showed no class II expression by endocrine cells at any age in NOD mice. Whether class II expression is, or is not, relevant to the induction of autoimmune diabetes, our observations here clearly show that TNF-α *in vivo* does not induce the expression of class II Ia molecules on pancreatic beta cells. Moreover, in experiments to be

presented elsewhere, we have found that in the (NZB × NZW)F_1 lupus mouse model, TNF-α treatment caused a reduction in class II MHC expression on peritoneal macrophages rather than induction of expression (C.O.J., G. D. Lewis, and A. M. Stall, unpublished).

Fluorescence-activated cell sorter analysis of lymphoid cells from TNF-α-treated NOD mice has not yet been done. However such a study has been done in (NZB × NZW)F_1 mice treated with TNF-α but did not prove to be informative. Thus, we have found no major effects on the frequency and the phenotype of B, T, or monocyte cell populations in different lymphoid organs during and after TNF-α treatment (C.O.J. and A. M. Stall, unpublished).

We do not know the physiological role and mechanism of the *in vivo* effect of TNF-α. However, we have found that peritoneal exudate cells from NOD mice produce low levels of TNF-α, only slightly higher than the levels of TNF-α in (NZB × NZW)F_1 mice in which TNF-α administration was also effective in preventing nephritis development (10). One possibility is that TNF-α is acting as a replacement therapy in this system. Its relevant effect could be due to the low level of TNF-α production in the NOD mice. Although (NZB × NZW)F_1 lupus-like mice have low TNF-α levels, their IL-1 production is quite high [similar to the non-autoimmune BALB/c mice (10)]; in NOD mice IL-1 and TNF-α production are similarly reduced compared to the SWR mice. This would suggest that the mechanism of TNF involvement in the pathogenesis of autoimmune diabetes might be different than in lupus nephritis. Moreover, in accordance with this proposed mechanism of a replacement therapeutic effect of TNF-α, we have found that recombinant IL-1α also reduces diabetes development in adoptive transfer experiments and in long-term administration.

It is extremely difficult at this point to discern which of the many *in vitro* activities shared by IL-1 and TNF-α are relevant to this *in vivo* system. We may suggest that TNF-α has a global regulatory effect on the immune system rather than a direct effect on the pancreatic islet cells as has been suggested previously. Alternatively, these data may imply that the effects of TNF-α on the immune system may be more relevant to the pathogenesis of the disease than direct local effects. Based on the data presented here, one should also be cautious in extrapolating the effects of TNF-α in various *in vitro* systems to the *in vivo* situation, and we must be careful not to extrapolate systemic administration effects to the local release situation. Our data also suggest that these cytokines actually have qualitatively different effects in *in vivo* versus *in vitro* situations.

1. Makino, S., Kunimoto, K., Muraoka, Y., Mizushima, Y., Katagiri, K. & Tochino, Y. (1980) *Exp. Anim.* **29**, 1–13.
2. Kanazawa, Y., Komeda, K., Sato, S., Mori, S., Akanuma, K. & Takaku, F. (1984) *Diabetologia* **27**, 113–115.
3. Wicker, L. S., Miller, B. J. & Mullen, Y. (1986) *Diabetes* **35**, 855–860.
4. Harada, M. & Makino, S. (1986) *Exp. Anim.* **35**, 501–509.
5. Shizuru, J. A., Taylor-Edwards, C., Banks, B. A., Gregory, A. K. & Fathman, C. G. (1988) *Science* **240**, 659–662.
6. Mori, Y., Suko, M., Okudaira, H., Matsuba, I., Tsuruoka, A., Sasaki, A., Yokoyama, H., Tanase, T., Shida, T., Nishimura, M., Terada, E. & Ikeda, Y. (1986) *Diabetologia* **29**, 244–247.
7. Boitard, C., Bendelac, A., Richard, M. F., Carnaud, C. & Bach, J. F. (1988) *Proc. Natl. Acad. Sci. USA* **85**, 9719–9723.
8. Mandrup-Poulsen, T., Bendtzen, K., Dinarello, C. A. & Nerup, J. (1987) *J. Immunol.* **139**, 4077–4082.
9. Pujol-Borrell, R., Todd, I., Dashi, M., Bottazzo, G. F., Sutton, R., Gray, D., Adolf, G. R. & Feldmann, M. (1987) *Nature (London)* **326**, 304–306.
10. Jacob, C. O. & McDevitt, H. O. (1988) *Nature (London)* **331**, 356–358.
11. Morrissey, P. J., Charrier, K., Alpert, A. & Bressler, L. (1988) *J. Immunol.* **141**, 1456–1463.
12. Sternberg, L. A., Hardy, P. H., Cuculis, J. J. & Meyer, H. G. (1970) *J. Histochem. Cytochem.* **18**, 315–325.
13. Mukavitz-Kramer, S. & Carver, M. E. (1986) *J. Immunol. Methods* **93**, 201–206.
14. Mizel, S. B., Oppenheim, J. J. & Rosenstreich, D. L. (1978) *J. Immunol.* **120**, 1497–1501.
15. Pennica, D., Hayflick, J. S., Bringman, T. S., Palladino, M. A. & Goeddel, D. V. (1985) *Proc. Natl. Acad. Sci. USA* **82**, 6060–6064.
16. Gray, P. W., Glaister, D., Chen, E., Goeddel, D. V. & Pennica, D. (1986) *J. Immunol.* **137**, 3644–3648.
17. Ponte, P., Ng, S. Y., Engel, J., Gunning, P. & Kedes, L. (1984) *Nucleic Acids Res.* **12**, 1687–1696.
18. Neta, R., Oppenheim, J. J. & Douches, S. D. (1988) *J. Immunol.* **140**, 108–111.
19. Serreze, D. V. & Leiter, E. H. (1988) *J. Immunol.* **140**, 3801–3807.
20. Collins, T., Lapierre, L. A., Fiers, W., Strominger, J. L. & Pober, J. S. (1986) *Proc. Natl. Acad. Sci. USA* **83**, 446–450.
21. Chang, R. J. & Lee, S. H. (1986) *J. Immunol.* **137**, 2853–2856.
22. Hoffman, M. & Weinberg, J. B. (1987) *J. Leuk. Biol.* **42**, 704–707.
23. Bachwich, P. R., Chensue, S. W., Larrick, J. W. & Kunkel, S. L. (1986) *Biochem. Biophys. Res. Commun.* **136**, 94–98.
24. Lee, J. C., Truneh, A., Smith, M. F. & Tsang, K. Y. (1987) *J. Immunol.* **139**, 1935–1938.
25. Bendtzen, K., Mandrup-Poulsen, T., Nerup, J., Nielsen, J. H., Dinarello, C. A. & Svenson, M. (1986) *Science* **232**, 1545–1547.
26. Mandrup-Poulsen, T., Egeberg, J., Nerup, J., Bendtzen, K., Nielsen, J. H. & Dinarello, C. A. (1987) *Acta Pathol. Microbiol. Immunol. Scand.* **95**, 55–63.
27. Bendtzen, K. (1989) *Autoimmunity* **2**, 177–189.
28. Bottazzo, G. F., Pujol-Borrell, R., Hanafusa, T. & Feldmann, M. (1983) *Lancet* **ii**, 1115–1119.
29. Bottazzo, G. F., Dean, B. M., McNally, J. M., MacKay, E. H., Swift, G. F. & Gamble, D. R. (1985) *N. Engl. J. Med.* **313**, 353–360.
30. Signore, A., Cooke, A., Pozilli, P., Butcher, G., Simpson, E. & Beverley, P. C. L. (1987) *Diabetologia* **30**, 902–905.

1: Biochem Biophys Res Commun. 1988 Oct 31;156(2):611-8.

Basic fibroblast growth factor (FGF) promotes cartilage repair in vivo.

Cuevas P, Burgos J, Baird A.

Ramon y Cajal Hospital, Madrid, Spain.

Although it has been clearly established that basic fibroblast growth factor (FGF) is a potent mitogen for chondrocytes in vitro, there is little evidence that it can stimulate this cell type in vivo. In an effort to address this problem, we examined the effect of an intraarticular administration of basic FGF. Alzet osmotic pumps delivering the mitogen to the site of injury promotes the healing of intra-chondrial lesions by stimulating chondrocyte proliferation and the formation of extracellular matrix. The observation that chronic infusions of basic FGF can elicit a repair response at the site of injury suggests that this growth factor may have therapeutic applications that extend beyond its capacity to induce neovascularization. The results also suggest that one of the ways that the perichondrium mediates cartilage repair may be by the local production of FGF-like mitogens.

PMID: 3190672 [PubMed - indexed for MEDLINE]

1: Biochem Biophys Res Commun. 1987 Sep 15;147(2):876-80.

An in vivo model for study of the angiogenic effects of basic fibroblast growth factor.

Hayek A, Culler FL, Beattie GM, Lopez AD, Cuevas P, Baird A.

We have investigated the angiogenic effects of basic fibroblast growth factor following its implantation in slow release beads under the kidney capsule. The presence of basic fibroblast growth factor in the subcapsular space induced a marked angiogenic response maximal at 1 microgram dose per kidney. Histological examination at the site of treatment failed to reveal evidence of an inflammatory response, thus supporting the observation that basic fibroblast growth factor alone can stimulate in vivo neovascularization. Beads pretreated with saline or with human growth hormone had no angiogenic effect. Because of the readily accessible location in the retroperitoneal space, the ease of drug delivery, and the marked vascular proliferation seen in response to FGF, our results suggest that the kidney capsule is an excellent model for study of the physiological role played by FGF and related peptides in promoting angiogenesis in vivo.

PMID: 2443140 [PubMed - indexed for MEDLINE]

Proc. Natl. Acad. Sci. USA
Vol. 90, pp. 10759–10763, November 1993
Biochemistry

Direct transfer of transforming growth factor β1 gene into arteries stimulates fibrocellular hyperplasia

(gene transfer/gene expression/extracellular matrix/cellular proliferation)

ELIZABETH G. NABEL*†, LILLIAN SHUM‡, VINCENT J. POMPILI*, ZHI-YONG YANG*§, HONG SAN*, HONG BING SHU*, SUSANNE LIPTAY*, LESLIE GOLD¶, DAVID GORDON‖, RIK DERYNCK‡, AND GARY J. NABEL*§**

Departments of *Internal Medicine, **Biological Chemistry, and ‖Pathology, §Howard Hughes Medical Institute, University of Michigan Medical Center, Ann Arbor, MI 48109-0688; ‡Departments of Growth and Development, and Anatomy Programs in Cell Biology and Developmental Biology, University of California, San Francisco, CA 94143-0640; and ¶Department of Pathology, New York University, New York, NY 10016

Communicated by J. Lawrence Oncley, July 29, 1993

ABSTRACT **The arterial wall responds to thrombosis or mechanical injury through the induction of specific gene products that increase cellular proliferation and connective tissue formation. These changes result in intimal hyperplasia that is observed in restenosis and the early phases of atherosclerosis. Transforming growth factor β1 (TGF-β1) is a secreted multifunctional protein that plays an important role in embryonal development and in repair following tissue injury. However, the function of TGF-β1 in vascular cell growth *in vivo* has not been defined. In this report, we have evaluated the role of TGF-β1 in the pathophysiology of intimal and medial hyperplasia by gene transfer of an expression plasmid encoding active TGF-β1 into porcine arteries. Expression of TGF-β1 in normal arteries resulted in substantial extracellular matrix production accompanied by intimal and medial hyperplasia. Increased procollagen, collagen, and proteoglycan synthesis in the neointima was demonstrated by immunohistochemistry relative to control transfected arteries. Expression of TGF-β1 induced a distinctly different program of gene expression and biologic response from the platelet-derived growth factor B (PDGF B) gene: procollagen synthesis induced by TGF-β1 was greater, and cellular proliferation was less prominent. These findings show that TGF-β1 differentially modulates extracellular matrix production and cellular proliferation in the arterial wall *in vivo* and could play a reparative role in the response to arterial injury.**

Transforming growth factor β (TGF-β) is a secreted factor that modulates the proliferation of many cell types, including vascular cells, and regulates their interaction with the extracellular matrix. *In vitro*, vascular smooth muscle cell growth can be stimulated or inhibited by TGF-β1, depending on cell density, cell age, coculture factors, and the concentration of TGF-β (1–3). The TGF-β-induced increase in proliferation of smooth muscle cells and connective tissue cells has been shown to be mediated by a stimulation of autocrine platelet-derived growth factor (PDGF) synthesis (4, 5). This proliferative effect of TGF-β is in contrast to its growth inhibitory effect on many other cell types such as lymphocytes (6), endothelial cells (7), and epithelial cells (8).

Besides its growth-modulatory effects, TGF-β is a potent inducer of various extracellular matrix proteins and increases the synthesis of cell adhesion receptors (9), probably leading to increased adhesion and interaction of cells with the surrounding extracellular matrix (10). TGF-β is also a chemoattractive factor for macrophages and fibroblasts (11), and disruption of the gene encoding TGF-β results in a systemic inflammatory disorder (12). Despite these multiple biological properties that have been demonstrated in cell culture, the effects of TGF-β *in vivo* and its role in cardiovascular disease have been difficult to define. To investigate the function of TGF-β1 in arteries, we transfected the human TGF-β1 gene (*TGFB1*) into porcine arteries *in vivo* and demonstrate that TGF-β1 gene expression is associated with extracellular matrix synthesis and intimal hyperplasia. The findings suggest a role for TGF-β1 in the development of vascular lesions.

MATERIALS AND METHODS

Plasmids. A plasmid expression vector β1-C_2S_2, which directs the synthesis of active human TGF-β1, has been described (13). To evaluate expression of the TGF-β1 vector, primary porcine endothelial and vascular smooth muscle cell cultures were transfected with the plasmid by using Lipofectin (BRL) (14). Transfected endothelial cells were assayed for secretion of recombinant TGF-β1 into culture supernatants with a colorimetric proliferation assay by standard methods (15).

Arterial Gene Transfer. *In vivo* arterial gene transfer was performed in 24 pigs, 9 with the recombinant human gene (*TGFB1*) encoding TGF-β1, 9 with a control reporter gene (*Escherichia coli lacZ*) encoding β-galactosidase, and 6 with a recombinant human PDGF B gene (PDGF B) (14) encoding PDGF BB. Double balloon catheters (Bard, Billerica, MA) were positioned in the iliofemoral arteries as described (16), and gene transfer was performed by using 2–5 μg of DNA and 5 μl of Lipofectin in Opti-MEM for 20 min (14). The animals were sacrificed at 4, 7, and 21 days.

Polymerase Chain Reaction (PCR) Analysis. For PCR analysis of recombinant TGF-β1 in transfected vessels, primers were synthesized from the cDNA sequence (17), which generated a 363-bp fragment: sense (25 mer): 5′-TCC ACC TGC AAG ACT ATC GAC ATG G-3′; antisense (25 mer): 5′-CAG CCG GTT GTC GAG GTA TCG CCA G-3′. The sense primer was selected from a region 50 bp upstream from the transcription start site. Samples were analyzed by ethidium bromide staining on a 1% agarose gel. TGF-β1 mRNA expression was analyzed by reverse transcription PCR and Southern blotting as described (14).

Immunohistochemistry and Staining. Recombinant TGF-β1 protein expression was analyzed by immunohistochemistry of artery segments transfected with *E. coli lacZ* or the recombinant human *TGFB1* gene. Formalin-fixed, paraffin-embedded artery segments were sectioned (6 μm), deparaffinized, rehydrated, and blocked in 3% hydrogen peroxidase and 10% nonimmune rabbit serum. Specimens were incubated with 4 μg of an affinity-purified rabbit anti-human

The publication costs of this article were defrayed in part by page charge payment. This article must therefore be hereby marked "*advertisement*" in accordance with 18 U.S.C. §1734 solely to indicate this fact.

Abbreviations: TGF-β, transforming growth factor β; PDGF, platelet-derived growth factor.

†To whom reprint requests should be addressed.

TGF-β1 antibody (18) per ml for 30 min at 37°C and were stained by standard methods with a biotinylated goat anti-rabbit IgG antibody–streptavidin–peroxidase conjugate. *TGFB1*-transfected arterial segments were also analyzed with a control first antibody, purified rabbit IgG, and these *TGFB1*-transfected arteries showed minimal background staining (data not shown).

Procollagen synthesis was analyzed by immunohistochemistry of paraffin-embedded, methyl-Carnoy-fixed arterial segments by using as primary antibody a 1:500 dilution of a monoclonal SP1.d8 aminopeptide-specific type I procollagen antibody (Developmental Studies, Hybridoma Bank, University of Iowa), a 1:1000 dilution of a monoclonal 1912 carboxypeptide-specific type I procollagen antibody (Chemicon), or a 1:400 dilution of a purified mouse IgG2b antibody (Promega) and as secondary antibody a 1:400 dilution of a biotinylated horse anti-mouse IgG2 antibody (Zymed) according to standard methods, and methyl green nuclear counterstaining was performed (19).

Reticulin staining with Snook's ammoniacal silver solution (20), alcian blue staining of proteoglycans with 3% acetic acid and 1% alcian blue solutions (21), and trichrome staining (22) were performed by standard techniques.

Morphometry. Morphometric measurements of intimal and medial thickness and measurements of cell number were determined in a blinded manner with a video imaging system (Image-1 System, Universal Imaging, Westchester, PA). In each specimen, eight random high-power (×40) fields were examined. Six specimens were counted from each group [control (*E. coli lacZ*-transfected), human *TGFB1*-transfected, or human *PDGFB*-transfected arteries]. Comparisons of cell number and intimal-to-medial ratio between *TGFB1*-transfected and control arteries were made by the two-tailed unpaired *t* test. Differences in procollagen synthesis between *TGFB1*-transfected, *PDGFB*-transfected, and control arteries were examined by analysis of variance with Dunnett's test (23, 24). Statistical significance was accepted at the 95% confidence level.

RESULTS

Expression of TGF-β1 in Arteries. To explore the function of TGF-β in the vasculature *in vivo*, we transfected an expression plasmid for secreted TGF-β1 into porcine arteries. Since TGF-β1 is normally secreted in a latent, inactive form, we used an expression vector for active human TGF-β1 in which two cysteines in the TGF-β1 precursor segment were replaced with serines (13). In addition, because the proliferative effects of TGF-β1 on mesenchymal cells are proposed to act through autocrine PDGF synthesis (4), we compared the results of PDGF B and TGF-β1 expression on arterial function *in vivo*. We transfected the pRK5-β1C2S2 expression plasmid for active human TGF-β1 into the iliofemoral arteries of nine pigs *in vivo* by direct gene transfer. Nine control pigs were similarly transfected with a plasmid expressing *E. coli lacZ*, and six pigs were transfected with a plasmid expressing *PDGFB*. The presence of the introduced TGF-β1 expression plasmid was evaluated by PCR (Fig. 1*A*). The recombinant TGF-β1 cDNA was detected in transfected iliofemoral artery segments (Fig. 1*A*, lanes 1 and 2) but not in nontransfected carotid artery segments from the same animal (Fig. 1*A*, lane 3), documenting transfer of the recombinant plasmids.

To confirm gene expression, recombinant TGF-β1 mRNA was analyzed by reverse-transcription PCR (Fig. 1*B*). Recombinant TGF-β1 mRNA was detected in transfected arterial segments (Fig. 1*B*, lane 4) compared with nontransfected arteries from the same animal (Fig. 1*B*, lane 2), confirming gene expression. Expression of recombinant TGF-β1 protein was demonstrated by immunohistochemistry using an affinity-purified TGF-β1-specific antibody that does not recognize TGF-β2 and -β3. Porcine arteries transfected with

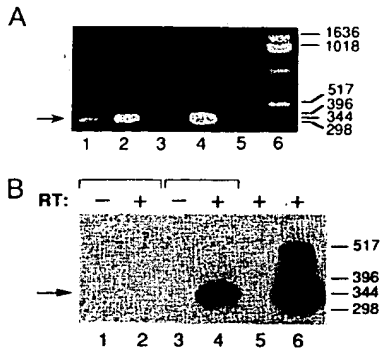

FIG. 1. Presence of recombinant human TGF-β1 in porcine arteries after direct gene transfer *in vivo*. (*A*) Recombinant human *TGFB1* was transfected into porcine right (lane 1) and left (lane 2) iliofemoral arteries and was detected by PCR 21 days after direct gene transfer. Recombinant *TGFB1* was not detected in a nontransduced carotid artery from the same pig (lane 3). Additional controls included the recombinant TGF-β1 expression plasmid (lane 4) and H_2O (lane 5). Lane 6 contains molecular size markers. (*B*) The presence of TGF-β1 mRNA was detected by using reverse-transcription PCR. RNA from *TGFB1*-transfected arteries (lanes 3 and 4) were analyzed for recombinant TGF-β1 mRNA at 5 days with (lane +) or without (lane −) reverse transcriptase (RT) compared with nontransfected arteries (lanes 1 and 2) treated with or without reverse transcriptase. Water (lane 5) and recombinant *TGFB1* plasmid (lane 6) were included as negative and positive controls, respectively.

human *TGFB1* demonstrated immunoreactive TGF-β1 protein in the intima and media, whereas TGF-β1 protein was not detectable with this method in arteries transduced with *E. coli lacZ* (Fig. 2*A*, control vs. TGF-β1). Specifically, TGF-β1 protein was prominent in the deeper layer of the intima, above the internal elastic lamina. Further immunohistochemical studies using antibodies against α-actin and porcine macrophages showed a localization of TGF-β1 protein in α-actin-staining cells in the intima and media (data not shown), suggesting that the TGF-β synthesis occurs in smooth muscle cells. In addition, infiltrating macrophages in these lesions were rare (data not shown) and insufficient to account for TGF-β1 protein production. These findings suggest that recombinant TGF-β1 was expressed largely by intimal and medial smooth muscle cells in porcine arteries *in vivo* after direct gene transfer. In human *TGFB1*-transfected arteries, a majority of cells in the deeper regions of the intima showed immunoreactive TGF-β1 protein. To determine whether a high transfection efficiency of cells in this region could account for this pattern of reactivity, experiments were performed in which arteries transfected with the reporter gene, *E. coli lacZ* for β-galactosidase, were stained with the histochemical reagent 5-bromo-4-chloro-3-indolyl β-D-galactoside (X-Gal) (25). In these arteries, β-galactosidase staining was observed in the lower regions of the intima and upper regions of the media in a small percentage (0.1–1%) of cells (data not shown). These findings suggest either that the *TGFB1*-transfected cells proliferated preferentially, or more likely, that the secreted TGF-β1 protein is retained preferentially in this region. This latter effect could be mediated by biglycan or decorin, which have been shown previously to accumulate in this region (26–28).

Generation of Intimal and Medial Hyperplasia. To evaluate the physiological response of the arterial wall to expression of recombinant TGF-β1, the artery segments transfected with *E. coli lacZ* or human *TGFB1* were analyzed by light microscopy. The iliofemoral artery segments transfected with *TGFB1* showed intimal hyperplasia in contrast to a minimal thickening of the intima in arteries transfected with *lacZ* (Fig.

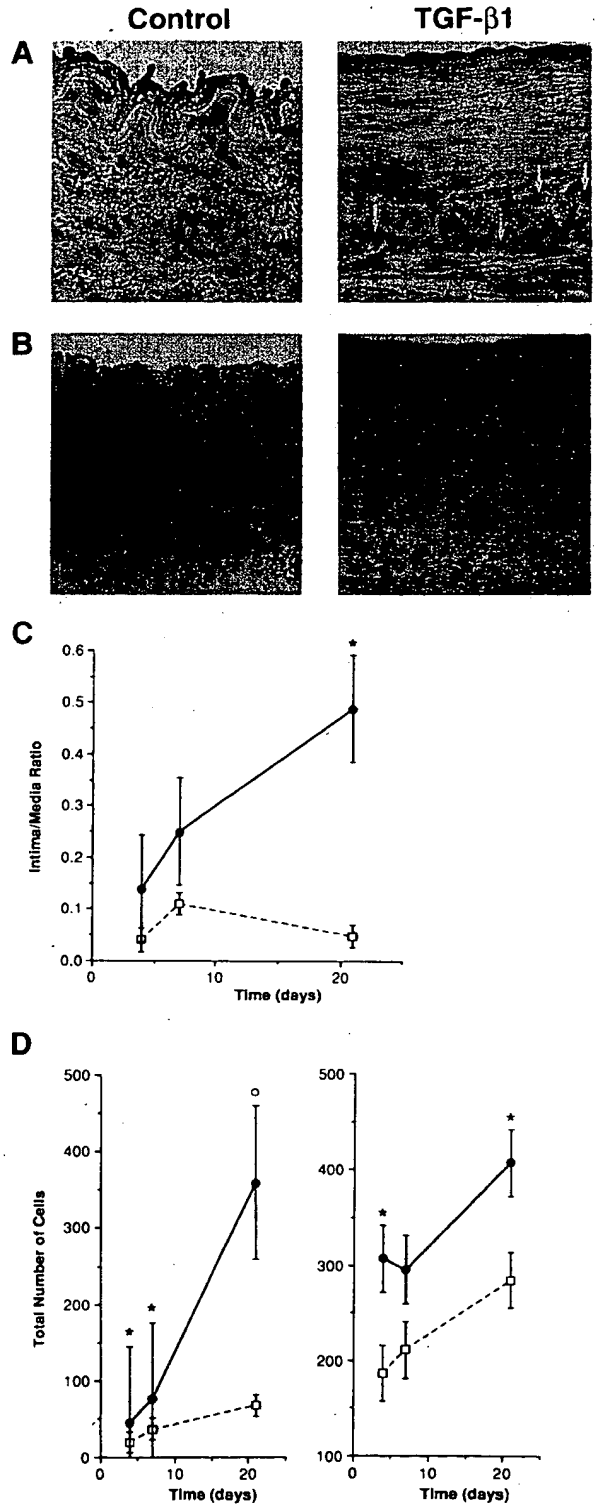

FIG. 2. Expression of recombinant TGF-β1 protein in porcine artery cells after direct gene transfer. (*A*) Immunohistochemical staining of porcine arteries transfected with *E. coli lacZ* for β-galactosidase (*Left*) or recombinant human *TGFB1* (*Right*) as indicated 21 days after gene transfer with an affinity-purified rabbit antibody to TGF-β1. The black arrowhead denotes the internal elastic lamina; the white arrows denote positive staining cells. (×170.) (*B*) Light microscopy of arterial segments transfected with *E. coli lacZ* (*Left*) or human *TGFB1* (*Right*). (×85; hematoxylin/eosin stain.) (*C*) Ratio of intimal to medial thickness in control arteries (□) and *TGFB1*-transfected arteries (●) at 4, 7, and 21 days after gene transfer. (*D*) Measurements of cell numbers in the intima and media of transfected arteries. Mean number of cells in the intima (*Left*) and media (*Right*) per eight high-power fields (×40) per specimen ($n = 4$ arteries in each group at each time point) in control arteries (□) and *TGFB1*-transfected (●) arteries at 4, 7, and 21 days. Values are expressed as means + SEM. *, $P < 0.05$; ○, $P < 0.01$, *TGFB1*-transfected vs. control arteries.

2*B*; control vs. TGF-β1). By quantitative morphometry, the intimal-to-medial ratio in the arteries that expressed TGF-β1 was significantly greater than in vessels expressing β-galactosidase at 21 days (0.49 ± 0.07 vs. 0.05 ± 0.03; $P < 0.05$) (Fig. 2*C*). To quantitate the basis for these changes, cell numbers in the intima and media were measured. The number of cells in both the intima and media of *TGFB1*-transfected arteries was significantly greater at all time points examined—4, 7 ($P < 0.05$), and 21 ($P < 0.01$) days after gene transfer (Fig. 2*D*)—compared with control arteries. These findings show that recombinant TGF-β1 stimulated increased cellular proliferation in two layers of the arterial wall after gene transfer.

Induction of Procollagen, Collagen, and Extracellular Matrix Synthesis: Comparison with PDGF BB. It has been suggested that the effects of TGF-β on smooth muscle cell proliferation are mediated by PDGF. Therefore, we compared the pattern of cellular proliferation and matrix production in *TGFB1*- and *PDGFB*-transfected arteries. Recombinant *TGFB1* expression was associated with increased procollagen production in the arterial intima and media, compared with control reporter gene and *PDGFB*-transfected vessels (Fig. 3). Procollagen synthesis in *TGFB1*-transfected vessels was observed in the intima and media at 4 days and increased in both layers at 7 days (Fig. 3*A Top* and *Middle*). By 21 days, procollagen staining had diminished in the intima and media but was still higher in *TGFB1*-transfected arteries compared with control arteries (Fig. 3*A Bottom*). In particular, at 21 days, procollagen synthesis was localized to the deeper layers of the intima and colocalized to the same region as the recombinant TGF-β1 protein (see Fig. 2*A*). The absolute number of cells staining with the procollagen antibody in the intima and media was significantly increased in *TGFB1*-transfected arteries at all time points (4, 7, and 21 days) compared with *PDGFB*-transfected arteries ($P < 0.05$) and control arteries ($P < 0.05$) (Fig. 3*B*). Staining with another monoclonal antibody to procollagen (1912) and trichrome further suggested an increase in procollagen and collagen synthesis in *TGFB1*-transfected arteries compared with *lacZ*-transfected arteries (data not shown).

The expression of human TGF-β1 in porcine arteries was also associated with different patterns of production of other matrix proteins, including reticulin and proteoglycans, compared with arteries transduced with human *PDGFB* or *lacZ* (Fig. 4). Although both TGF-β1 and PDGF BB (14) stimulated intimal hyperplasia, expression of TGF-β1 induced more reticulin (Fig. 4*A*) and a less cellular response (Fig. 4*C*) than did PDGF BB-expressing arteries when transfected arteries with comparable degrees of intimal hyperplasia were analyzed at similar time points. Both *TGFB1*- and *PDGFB*-transfected arteries demonstrated increased proteoglycan synthesis, compared with *lacZ*-transfected arteries. However, different patterns of expression were evident. Specifically, increased proteoglycan synthesis was present in the lower regions of the intima adjacent to the internal elastic lamina in *TGFB1*-transfected arteries and was colocalized to the region of TGF-β1-containing cells (see Fig. 2*A*). In *PDGFB*-transfected arteries, proteoglycan synthesis was observed in the upper intima next to the lumen and was also

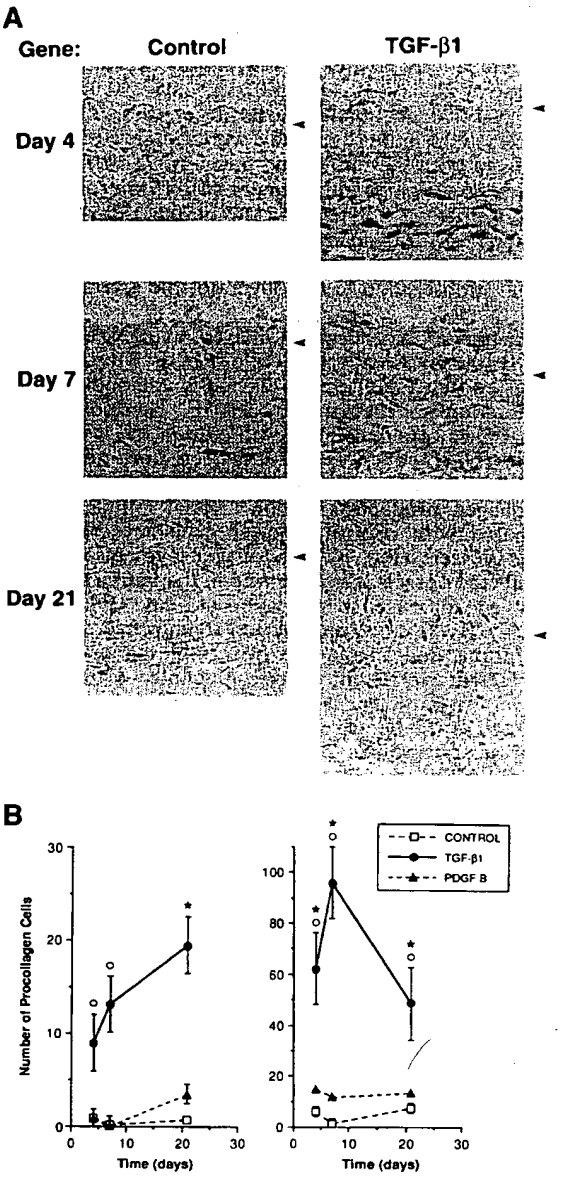

FIG. 3. Procollagen formation in porcine arteries 4, 7, and 21 days after direct gene transfer *in vivo*. (*A*) Immunohistochemical staining of porcine arteries transfected with *E. coli lacZ* (*Left*) or recombinant *TGFB1* (*Right*) at 4, 7, and 21 days after gene transfer with a monoclonal procollagen antibody (SP1.d8). The black arrowhead denotes the internal elastic lamina. (×170.) (*B*) Mean number of cells in the intima (*Left*) and media (*Right*) per eight high-power fields (×40) per specimen (n = 4 arteries in each group at each time point) that stain with a procollagen antibody in control (□), *TGFB1*-transfected (●), and *PDGFB*-transfected (▲) arteries at 4, 7, and 21 days. Values are expressed as a mean + SEM. *, $P < 0.05$ *TGFB1*-transfected vs. control arteries; ○, $P < 0.05$ *TGFB1*- vs. *PDGFB*-transfected arteries.

colocalized to regions of the intima where PDGF BB-containing cells are present (14). These findings demonstrate distinctly different biologic effects of the TGF-β1 and PDGF BB in uninjured arteries *in vivo*.

DISCUSSION

These results demonstrate that expression of active human TGF-β1 in the normal porcine artery wall results in intimal and medial hyperplasia with increased deposition of extracellular matrix proteins. The increased number of intimal and medial smooth muscle cells may be a direct stimulation of proliferation by TGF-β1, as suggested by the proliferative effect of TGF-β on smooth muscle cells in culture. Alternatively, it is also possible that as a result of TGF-β-induced extracellular matrix production, a more permissive microenvironment is created that facilitates cellular proliferation. This effect has been observed with tumor cells that are resistant to the direct growth-modulatory activities of TGF-β (13). Since there was no apparent increase in infiltrating macrophages, it is likely that observed alterations are not a consequence of factors released by macrophages.

The increased extracellular matrix production that accompanies the intimal and medial hyperplasia has not been observed following expression of other growth factor genes in the vessel wall, including genes for PDGF BB (14) and a secreted form of fibroblast growth factor 1 (FGF-1) (29). In particular, porcine arteries transfected with human *PDGFB* demonstrated intimal hyperplasia, characterized by increased numbers of intimal smooth muscle cells, but increased deposition of procollagen, as in *TGFB*-transfected arteries, was not observed. Interestingly, proteoglycan synthesis was increased in both *TGFB1*- and *PDGFB*-transfected arteries, although the patterns of expression in the intima were different. These findings suggest that these different growth factors may have discernible roles in stimulating arterial hyperplasia *in vivo*. While there may be overlapping effects, *TGFB1* has a distinct function in inducing procollagen formation, effects not observed with genes for FGF-1 or PDGF BB. This major difference in histological appearance in comparison with the *PDGFB*-transfected artery also indicates that the phenotypic changes in *TGFB1*-transfected arteries are not a mere consequence of the TGF-β-induced PDGF production by smooth muscle cells.

Recent studies have demonstrated that TGF-β1 mRNA and protein are expressed in human vascular lesions (30). TGF-β1 protein has also been detected in neointimal segments of balloon-injured rat carotid arteries after mechanical injury (31, 32). These observations are consistent with increased TGF-β1 synthesis observed after wound healing in other tissues, including tumors (33). A previous study suggested that systemic administration of TGF-β1 protein into rats with preexisting neointima could regulate further intimal growth (32), but it has not been possible previously to examine the effects of this gene product synthesized locally. Whereas these data associated TGF-β1 with vascular fibroproliferative responses, the role of local expression and activation of TGF-β1 in cellular responses in the normal artery has been unclear.

Our findings suggest that TGF-β synthesis and activation *in vivo* contributes to arterial modeling through the elaboration of cell proliferation and extracellular matrix formation. These effects may be induced, for example, as a consequence of arterial injury following balloon angioplasty. TGF-β synthesis is stimulated following injury and during wound repair in many tissues. It is likely, then, that in the context of the blood vessel wall, TGF-β1 expression induced by arterial injury may play a dominant role in the repair of the injured vessel through the synthesis of extracellular matrix. This function of TGF-β, which is not observed with PDGF B, may contribute to the reparative process following arterial injury. By stimulating the formation of extracellular matrix, it is possible that TGF-β1 could help to promote healing but limit the extensive cellular intimal hyperplasia which is observed with PDGF BB. This function of TGF-β1 in the arterial wall may prove useful in the design of molecular interventions to limit restenosis following balloon angioplasty.

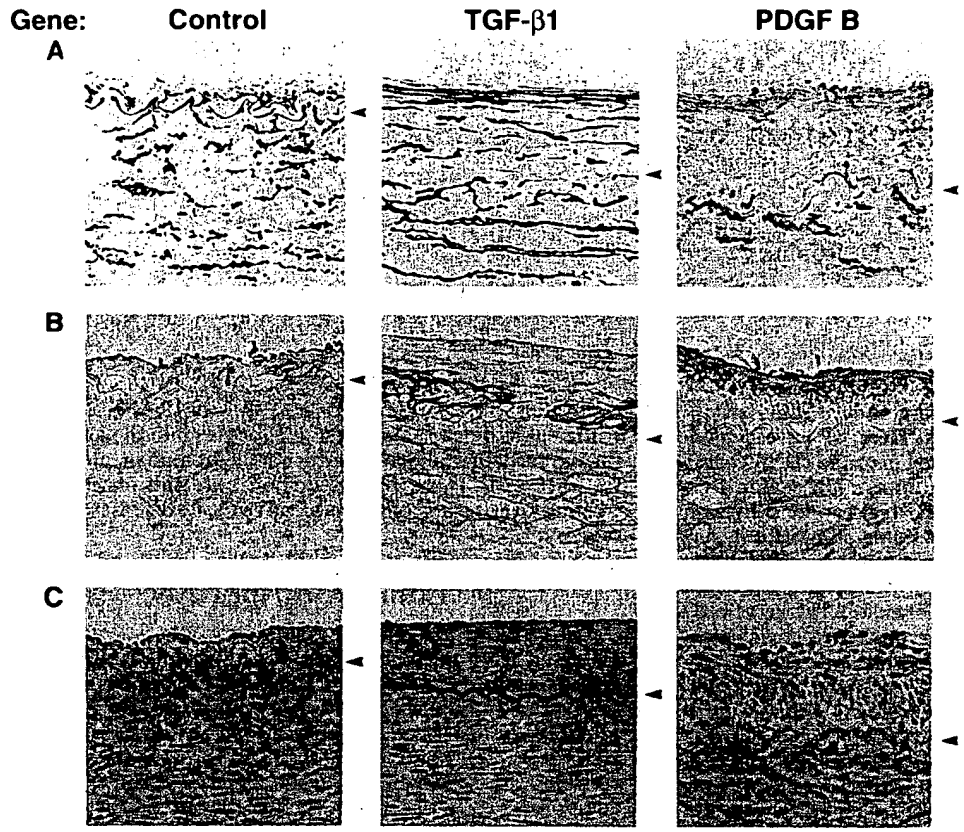

FIG. 4. Matrix proteins in transfected porcine arteries *in vivo*. Reticulin (*A*), proteoglycans (*B*), and morphology (*C*) were analyzed in porcine arteries transfected with *E. coli lacZ* (*Left*), human *TGFB1* (*Center*), and human *PDGFB* (*Right*) 21 days after direct gene transfer. The black arrowhead denotes the internal elastic lamina. [×250; Snook's reticulum stain (*A*), alcian blue stain (*B*), and hematoxylin/eosin stain (*C*).]

We are grateful to Lingling Xu for technical assistance, to Christine Enger for providing catheters, and to Mrs. Gail Reisdorph for manuscript preparation. These studies were supported by Grants DK 42706, AI 29179, and HL 43757 from the National Institutes of Health. E.G.N. is an Established Investigator of the American Heart Association. Work in the laboratory of R.D. was supported by grants from the National Institutes of Health and the American Cancer Society and by a fellowship from the Tobacco-Related Disease Research Program (California) to L.S.

1. Barnard, J. A., Lyons, R. M. & Moses, H. L. (1990) *Biochim. Biophys. Acta* **1032**, 79–87.
2. Owens, G. K., Geisterfer, A. A. T., Yang, Y. W. H. & Komoriya, A. (1988) *J. Cell Biol.* **107**, 771–780.
3. Majack, R. A. (1987) *J. Cell Biol.* **105**, 465–471.
4. Battegay, E. J., Raines, E. W., Seifert, R. A., Bowen-Pope, D. F. & Ross, R. (1990) *Cell* **63**, 515–524.
5. Majack, R. A., Majesky, M. W. & Goodman, L. V. (1990) *J. Cell Biol.* **111**, 239–247.
6. Fontana, A., Frei, K., Bodmer, S., Hofer, E., Schreier, M. H., Palladino, M. A., Jr., & Zinkernagel, R. M. (1989) *J. Immunol.* **143**, 3230–3234.
7. Takehara, K., LeRoy, E. C. & Grotendorts, G. R. (1987) *Cell* **49**, 415–422.
8. Knabbe, C., Lippman, M. E., Wakefield, L. M., Flanders, K. C., Kasid, A., Derynck, R. & Dickson, R. B. (1987) *Cell* **48**, 417–428.
9. Chen, J. K., Hoshi, H. & McKeehan, W. L. (1987) *Proc. Natl. Acad. Sci. USA* **84**, 5287–5291.
10. Edwards, D. R., Murphy, G., Reynolds, J. J., Whitham, S. E., Docherty, A. J. P., Angel, P. & Heath, J. K. (1987) *EMBO J.* **6**, 1899–1904.
11. Tsunawaki, S., Sporn, M., Ding, A. & Nathan, C. (1988) *Nature (London)* **334**, 260–262.
12. Shull, M. M., Ormsby, L., Kier, A. B., Pawlowski, S., Diebold, R. J., Yin, M., Allen, R., Sidman, C., Proetzel, G., Calvin, D., Annunziata, N. & Doetschman, T. (1992) *Nature (London)* **359**, 693–699.
13. Arrick, B. A., Lopez, A. R., Elfman, F., Ebner, R., Damsky, C. H. & Derynck, R. (1992) *J. Cell Biol.* **118**, 715–726.
14. Nabel, E. G., Yang, Z., Liptay, S., San, H., Gordon, D., Haudenschild, C. C. & Nabel, G. J. (1993) *J. Clin. Invest.* **91**, 1822–1829.
15. Mosmann, T. (1983) *J. Immunol. Methods* **65**, 55–63.
16. Nabel, E. G., Plautz, G. & Nabel, G. J. (1990) *Science* **249**, 1285–1288.
17. Derynck, R., Rhee, L., Chen, E. Y. & Van Tilburg, A. (1987) *Nucleic Acids Res.* **15**, 3188–3189.
18. Pelton, R. W., Saxena, B., Jones, M., Moses, H. L. & Gold, L. I. (1991) *J. Cell Biol.* **115**, 1091–1105.
19. Gordon, D., Reidy, M. A., Benditt, E. P. & Schwartz, S. M. (1990) *Proc. Natl. Acad. Sci. USA* **87**, 4600–4604.
20. Snook, T. (1944) *Anat. Rec.* **89**, 413.
21. Lev, R. & Spicer, S. S. (1964) *J. Histochem. Cytochem.* **12**, 309.
22. Sheehan, D. C. & Hrapchak, B. B. (1980) in *Theory and Practice of Histotechnology*, eds. Sheehan, D. C. & Hrapchak, B. B. (Battele, Columbus, OH), pp. 190–191.
23. Winer, B. J. (1971) *Statistical Principles in Experimental Design* (McGraw-Hill, New York), pp. 261–300.
24. Dunnett, C. W. (1964) *Biometrics* **20**, 482–494.
25. Dannenberg, A. M. & Suga, M. (1981) in *Methods for Studying Mononuclear Phagocytes*, eds. Adams, D. O., Edelson, P. J. & Koren, H. S. (Academic, New York), pp. 375–395.
26. Yamaguchi, Y., Mann, D. M. & Ruoslahti, E. (1990) *Nature (London)* **346**, 281–284.
27. Schonherr, E., Jarvelainen, H. T., Kinsella, M. G., Sandell, L. J. & Wight, T. N. (1993) *Arterioscler. Thromb.* **13**, 1026–1036.
28. Jarvelainen, H. T., Kinsella, M. G., Wight, T. N. & Sandell, L. J. (1991) *J. Biol. Chem.* **266**, 23274–23281.
29. Nabel, E. G., Yang, Z., Plautz, G., Forough, R., Zhan, X., Haudenschild, C. C., Maciag, T. & Nabel, G. J. (1993) *Nature (London)* **362**, 844–846.
30. Nikol, S., Isner, J. M., Pickering, J. G., Kearney, M., Leclerc, G. & Weir, L. (1992) *J. Clin. Invest.* **90**, 1582–1592.
31. Madri, J. A., Reidy, M. A., Kocher, O. & Bell, L. (1989) *Lab. Invest.* **60**, 755–764.
32. Majesky, M. W., Lindner, V., Twardzik, D. R., Schwartz, S. M. & Reidy, M. A. (1991) *J. Clin. Invest.* **88**, 904–910.
33. Sieweke, M. H., Thompson, N. L., Sporn, M. B. & Bissell, M. J. (1990) *Science* **248**, 1656–1660.

Proc. Natl. Acad. Sci. USA
Vol. 87, pp. 8437–8441, November 1990
Genetics

Temporary amelioration of hyperlipidemia in low density lipoprotein receptor-deficient rabbits transplanted with genetically modified hepatocytes

(familial hypercholesterolemia/hepatocyte transplantation/gene therapy)

JAMES M. WILSON*†, N. ROY CHOWDHURY‡, MARIANN GROSSMAN*, RENATA WAJSMAN‡, ADAM EPSTEIN‡, RICHARD C. MULLIGAN§, AND J. ROY CHOWDHURY‡

*Departments of Internal Medicine and Biological Chemistry, Howard Hughes Medical Institute, University of Michigan, Ann Arbor, MI 48109; ‡Department of Internal Medicine, Liver Research Center, Albert Einstein College of Medicine, Bronx, NY 10461; and §Department of Biology, Whitehead Institute, Massachusetts Institute of Technology, Cambridge, MA 02142

Communicated by Donald S. Fredrickson, July 20, 1990

ABSTRACT **Familial hypercholesterolemia is an inherited disease in humans that is associated with coronary artery disease and is caused by a deficiency of the receptor that mediates the internalization of low density lipoprotein (LDL). We have used an animal model for familial hypercholesterolemia, the Watanabe heritable hyperlipidemic (WHHL) rabbit, to design a therapeutic approach for this disease, which attempts to correct the hepatic defect in LDL receptor expression. Hepatocytes were harvested from WHHL rabbits, plated in primary cultures, and exposed to recombinant retroviruses capable of efficiently transferring a functional human LDL receptor gene. Genetically modified cells were harvested and infused into the portal vein of WHHL recipients, who were analyzed for metabolic consequences of human LDL receptor expression. Each animal exhibited a statistically significant decrease in total serum cholesterol 2–6 days after transplantation, with an eventual return to pretreatment levels. Proviral DNA sequences and virus-directed transcripts were detected in liver tissue 24 hr after transplantation. *In situ* hybridization demonstrated provirus expression in a small population of hepatocytes distributed in periportal sections of the liver. This study illustrates the potential of somatic gene therapy in ameliorating hyperlipidemia associated with familial hypercholesterolemia.**

Familial hypercholesterolemia (FH) is an autosomal dominant disorder in humans caused by a deficiency of the receptor that mediates the uptake of low density lipoprotein (LDL) (reviewed in ref. 1). Patients that inherit two abnormal LDL receptor alleles (i.e., homozygous deficient patients) have marked hypercholesterolemia from birth and suffer from accelerated and often life-threatening coronary artery disease in childhood. Current medical therapies are largely ineffective in improving the hypercholesterolemia or preventing the progression of coronary artery disease in these patients. Recent attempts at correcting the hepatic deficiency of LDL receptor in FH by orthotopic liver transplantation have been moderately successful (2, 3).

Another potentially effective approach to the treatment of FH is somatic gene therapy (4, 5). The liver is the primary organ responsible for the degradation of LDL and the only organ responsible for excretion of cholesterol (1), suggesting that the most appropriate target cell for LDL receptor gene transfer is the hepatocyte. Furthermore, it may be possible to achieve significant clinical improvement with only partial replacement of hepatic LDL receptor activity as suggested by the previously described correlation of residual LDL receptor activity and clinical severity of coronary artery disease in homozygous deficient patients (1, 6). Finally, the availability of an authentic animal model for FH, the Watanabe heritable hyperlipidemic (WHHL) rabbit, provides an opportunity to test experimental therapies *in vivo* (4, 7).

One approach we have considered in the design of liver-directed gene therapies is similar in concept to the well-described bone marrow-directed gene therapies. This method involves isolating hepatocytes from genetically deficient animals, transferring functional genetic material into the hepatocytes *in vitro*, and transplanting the genetically modified cells into the affected animals. In this report, we describe retrovirus-mediated gene transfer of a human LDL receptor gene into adult WHHL hepatocytes and transplantation of these genetically corrected cells into WHHL rabbits with consequent improvement in hypercholesterolemia.

MATERIALS AND METHODS

Animals. WHHL rabbits used in this study were derived from mating homozygous LDL-receptor-deficient rabbits. Wild-type New Zealand White rabbits were purchased from Dutchland Farms (Denver, PA). All animals were maintained on a Purina laboratory rabbit chow. Individual WHHL rabbits exhibited <2% variation in total serum cholesterol for a period up to 2 weeks prior to hepatocyte transplantation. In addition, baseline pretreatment serum cholesterol levels were indistinguishable between the two experimental groups: WHHL recipients transplanted with mock-infected cells (539 ± 46 mg/dl, mean ± 1 SD, n = 6) or LTR-LDLR-infected cells (543 ± 48 mg/dl, mean ± 1 SD, n = 7).

Recombinant Retrovirus. The retroviral vector (LTR-LDLR) used to produce amphotropic virus has been described (5) and is depicted in Fig. 1. The initial description of this vector stated that enhancer sequences in the 3′ long terminal repeat were replaced with homologous sequences from the myeloproliferative sarcoma virus (5). It has subsequently been discovered that, due to confusion regarding one of the DNA fragments used in the original construction of the vector, it actually contains Moloney enhancer and promoter sequences and an additional mutation (8) in the tRNA binding site; the rest of the vector is identical to the one described in the original reference (5). The original virus-producing cell line that was generated from this vector was subcloned prior to this study and shown to be free of replication-competent virus.

The publication costs of this article were defrayed in part by page charge payment. This article must therefore be hereby marked "*advertisement*" in accordance with 18 U.S.C. §1734 solely to indicate this fact.

Abbreviations: LDL, low density lipoprotein(s); WHHL, Watanabe heritable hyperlipidemic; FH, familial hypercholesterolemia; PCR, polymerase chain reaction.

†To whom reprint requests should be addressed.

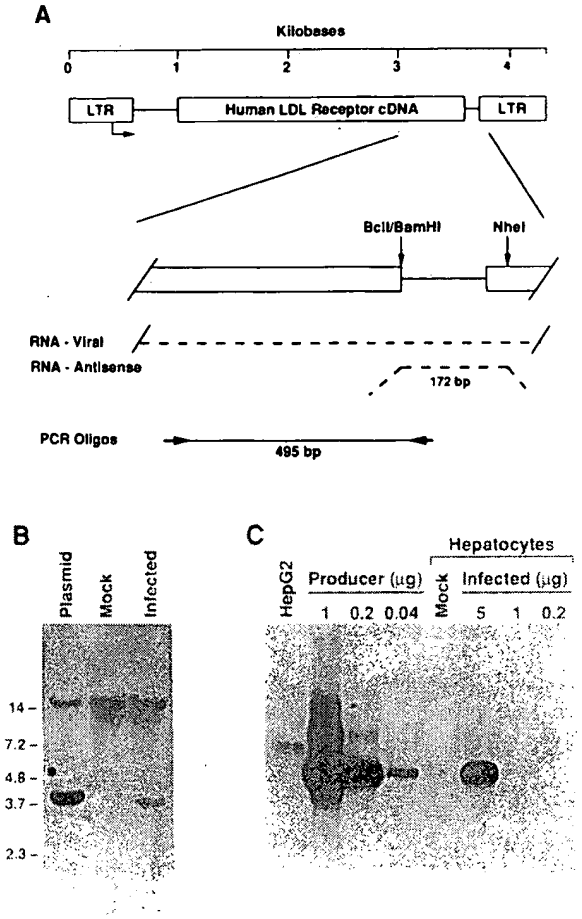

FIG. 1. Retroviral vector and *in vitro* characterization of transduced WHHL hepatocytes. (*A*) Retroviral vector. Vector sequences involved in the production of appropriate probes are expanded in the area below the vector. The RNA probe complementary to viral sequences in the recombinant transcript is noted; a 172-base-pair transcript should be protected from digestion with RNase A. The 5′ and 3′ PCR oligonucleotides (Oligos) are derived from human LDL receptor cDNA sequences and flanking viral sequences, respectively, as shown; a 495-base-pair fragment is amplified with these oligonucleotides. bp, Base pair(s); LTR, long terminal repeat sequences. (*B*) Southern blot analysis. Total cellular DNA was isolated and analyzed (10 μg per lane) for proviral sequences. Lanes: "Plasmid," DNA from mock-infected hepatocytes plus 1.25 pg of LTR-LDLR plasmid; "Mock," DNA from mock-infected hepatocytes; "Infected," DNA from hepatocytes infected with LTR-LDLR virus. Molecular size standards (in kilobases) are indicated at left. (*C*) RNA blot analysis was performed on total cellular RNA. Samples were derived from HepG2 (5 μg), the virus-producing cell line (1, 0.2, and 0.04 μg), mock-infected hepatocytes (5 μg), and hepatocytes infected with the LTR-LDLR virus (5, 1, and 0.2 μg). HepG2 cells were grown in medium containing lipoprotein-deficient serum prior to harvest for RNA.

Hepatocyte Isolation and Infection. Rabbit hepatocytes were prepared and plated in primary culture as described (5). Two days after the cultures were established, the medium was changed to virus-containing medium (supplemented with Polybrene at 8 μg/ml) that was harvested from the virus-producing cells (5). Mock-infected hepatocytes were exposed to the same type of medium supplemented with Polybrene but void of LDL receptor-expressing virus. Twelve to 18 hr later, the cells were harvested for transplantation and assayed for gene expression. Cells were detached from the tissue culture plates by incubation in 0.1% trypsin/EDTA for 10–20 min at 37°C.

Hepatocyte Transplantation. Animals were prepared for laparotomy with i.v. pentobarbital anesthesia. By using sterile surgical technique, the abdomen was opened through a 3-cm midline incision, a loop of jejunum was externalized, and a tributary of the superior mesenteric vein was identified and secured with ligatures. A prewarmed suspension of hepatocytes (1–2 × 10^8 cells in a volume of 10 ml containing 100 units of heparin) was introduced into the mesenteric vein through a 27-gauge needle over 5 min. The needle was then removed, hemostasis was achieved by tying the ligature, the loop of jejunum was returned to the abdomen, and the abdominal incision was closed in two layers. The animals received amoxicillin (5 mg/kg of body weight, subcutaneously) once daily on the day of surgery and for 5 days after the operation. Venous samples were subsequently obtained through a marginal ear vein and analyzed for total cholesterol as described (9).

Molecular Analysis of Gene Transfer and Expression. *Blot hybridization.* Total cellular RNAs and high molecular weight DNAs were prepared and analyzed by blot hybridization using human LDL receptor cDNA as the probe (5).

Polymerase chain reaction (PCR). Proviral sequences were detected in DNA isolated from liver tissue by using PCR (10). Thirty cycles of the reaction were performed with a program that included denaturation at 94°C for 1 min and annealing/elongation at 72°C for 2.5 min. Oligonucleotides used in this reaction have the following sequences: 5′ probe, AGGTCAGCTCCACAGCCGTAAGGACACAGC; 3′ probe, GGCTCGTACTCTATAGGCTTCAGCTGGTGA. Their location within the vector is illustrated in Fig. 1*A*.

RNase protection assay. RNA probes were generated from transcription plasmids constructed in the following manner. Moloney sequences in the retroviral vector between the synthetic *Bam*HI site at nucleotide 7674 and the *Nhe* I site at nucleotide 7846 (see ref. 11 for numbering) were cloned between the *Bam*HI and *Xba* I sites of pGEM-3Z (f+) (called 3Z-env); transcription from the SP6 promoter produces antisense RNA that is specific for the virus-directed transcript. This *Bam*HI–*Nhe* I fragment was also cloned into pGEM-4Z in order to produce sense RNA (4Z-env) from the same promoter. Antisense RNA spanning rabbit LDL receptor coding sequences was used as an internal control in RNase protection experiments. An *Sma* I–*Xho* I restriction fragment from a rabbit LDL receptor cDNA clone (nucleotides 2475–2572; ref. 12) was cloned between the *Sma* I and *Sal* I sites of pGEM-4Z (4Z-rLDLR). Transcription vectors were linearized by digestion with appropriate restriction endonucleases (3Z-env, *Eco*RI; 4Z-env, *Hin*dIII; and 4Z-rLDLR, *Hin*dIII) and used as templates in transcription reactions according to the recommendations of the manufacturer (Promega).

RNase protection studies were performed on total cellular RNA according to the method of Melton *et al.* (13). Radioactivity in the resulting bands was quantified with a Betascope 630 (Betagen, Waltham, MA).

In situ hybridization. In situ hybridization was performed by a modification of the method described by Pinter and Lugo (14). Linearized transcription probes were used as templates in *in vitro* transcription reactions using SP6 polymerase and uridine 5′-[α-[^{35}S]thio]triphosphate (Amersham). Radiolabeled antisense RNA probes were isolated and hybridized with cryostat sections at 45°C for 16 hr in the presence of 50% formamide. The slides were washed at high-stringency conditions, coated with Kodak emulsion NTB-2, and exposed for 4 weeks.

RESULTS

Retrovirus-Mediated Gene Transfer into Adult WHHL Hepatocytes. The recombinant virus LTR-LDLR was used in the

present studies to infect adult WHHL hepatocytes. After infection, hepatocytes were harvested for transplantation and analyzed for retrovirus transduction and human LDL receptor expression.

Southern blot analysis of total cellular DNA was used to directly measure the efficiency of gene transfer in the infected population of cells. These studies demonstrated unrearranged proviral sequences in infected hepatocytes with a relative copy number equal to 0.05–0.1 provirus per cell (Fig. 1*B*). Duplicate plates of hepatocytes were analyzed for virus-directed transcripts by using RNA transfer blots with a probe that is relatively specific for human LDL receptor RNA (Fig. 1*C*). This cDNA probe detected abundant human LDL receptor transcripts in infected WHHL hepatocytes as well as in the human hepatoblastoma cell line HepG2. The retrovirus-derived transcript is substantially shorter than the endogenous human transcript because the long 3′ untranslated region from the endogenous gene was deleted in the retroviral vector. The infected population of hepatocytes had levels of LDL receptor RNA that exceeded endogenous levels in the human hepatoblastoma cell line by 5- to 6-fold (Fig. 1*C*).

Transplantation of Genetically Modified Hepatocytes. Hepatocytes from a single WHHL rabbit were harvested, plated into culture, and mock-infected or infected with the LTR-LDLR virus. After infection, the cells were harvested and transplanted into WHHL recipients by means of the portal vein (1–2 × 10^8 cells per animal, which is 1–4% of the total number of hepatocytes found in the liver). Animals that received LTR-LDLR-infected cells (three donors into seven recipients) demonstrated significant decreases in serum cholesterol on days 2–5 following transplantation ($P < 0.001$, Student's t test) when compared to pretreatment levels (Fig. 2). The peak effect was noted 3 days after transplantation and was associated with a decline in total serum cholesterol to 70 ± 3% of pretreatment values (mean ± 1 SD, $n = 7$). Transplantation of mock-infected WHHL hepatocytes (three donors into six recipients) had no statistically significant effect on serum cholesterol ($P > 0.6$, Student's t test) when compared to pretreatment levels (Fig. 2). A direct comparison between the control group and the experimental group using the Student's t test revealed statistically significant decreases in serum cholesterol on days 2–6 of the rabbits transplanted with genetically modified hepatocytes ($P < 0.001$). Decreases in lipoproteins that are known ligands for LDL receptor (i.e., very low density lipoproteins, intermediate density lipoproteins, and LDL) contribute to the overall diminution in total cholesterol (data not shown).

Tissues were harvested from transplant recipients in order to perform detailed molecular and cellular analyses of gene transfer and expression. Separate animals were euthanized for tissue collection at 10 min, 24 hr, and 19 days after transplantation with genetically modified hepatocytes.

Liver tissues were analyzed for proviral DNA sequences by using PCR (Fig. 3) because standard hybridization techniques lacked the necessary sensitivity. Proviral DNA sequences were detected in animals transplanted with infected hepatocytes and sacrificed 10 min and 24 hr after transplantation; proviral DNA was no longer detected in liver harvested 19 days after transplantation. Similar analysis of DNA from other tissues such as lung failed to detect proviral DNA, suggesting that most of the hepatocytes seed in sinusoids (data not shown).

RNase protection analysis was used to detect and quantify the recombinant transcript in total cellular RNA from liver tissue. The recombinant RNA was detected with an antisense probe that is complementary to viral sequences in its 3′ untranslated region (Fig. 1*A*). Another probe that is specific for endogenous rabbit LDL receptor RNA was incorporated into each assay as an internal control. Analysis of RNA from LTR-LDLR-transduced murine fibroblasts demonstrated protection of the 3Z-env probe but not the 4Z-rLDLR probe (172 base pairs) (Fig. 4, lane tRNA + VP), whereas assays of control WHHL RNA revealed no protection of the 3Z-env probe but substantial protection of the 4Z-rLDLR probe (98 base pairs) (Fig. 4, lane WC). Each probe produced a band whose intensity varied in proportion to the amount of total cellular RNA used in the initial hybridization. These studies confirm the specificities of the probes and support the use of the assay for quantifying viral and endogenous LDL receptor transcripts. Infected hepatocytes expressed the recombinant transcript at levels equal to the endogenous LDL receptor transcript (data not shown). Virus-directed RNA was also

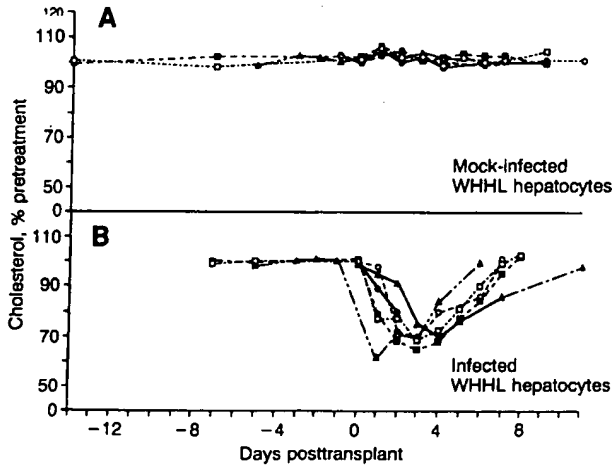

FIG. 2. Effect of hepatocyte transplantation on cholesterol metabolism in WHHL rabbits. Donor hepatocytes were transplanted into WHHL rabbits. Total serum cholesterol, presented as the % pretreatment level, was measured as a function of time following transplantation, which occurred on day 0. Data are plotted for each animal. (*A*) Mock-infected WHHL hepatocytes were transplanted into six WHHL recipients. (*B*) LTR-LDLR-infected WHHL hepatocytes were transplanted into seven recipients.

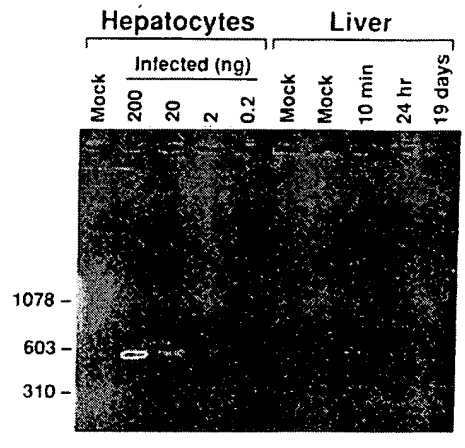

FIG. 3. Analysis of liver tissue for proviral DNA sequences by PCR. Total cellular DNA was isolated from hepatocytes and liver tissues and analyzed for proviral sequences using PCR. Hepatocyte DNA was from mock-infected (200 ng) and LTR-LDLR-infected (200, 20, 2, and 0.2 ng) hepatocytes. Liver DNA from each tissue was isolated on separate occasions with identical results; representative assays are presented. Samples were from control WHHL rabbits (Mock) and livers harvested from transplant recipients 10 min, 24 hr, and 19 days after the transplant. Sizes of the bands (in nucleotides) are indicated at left.

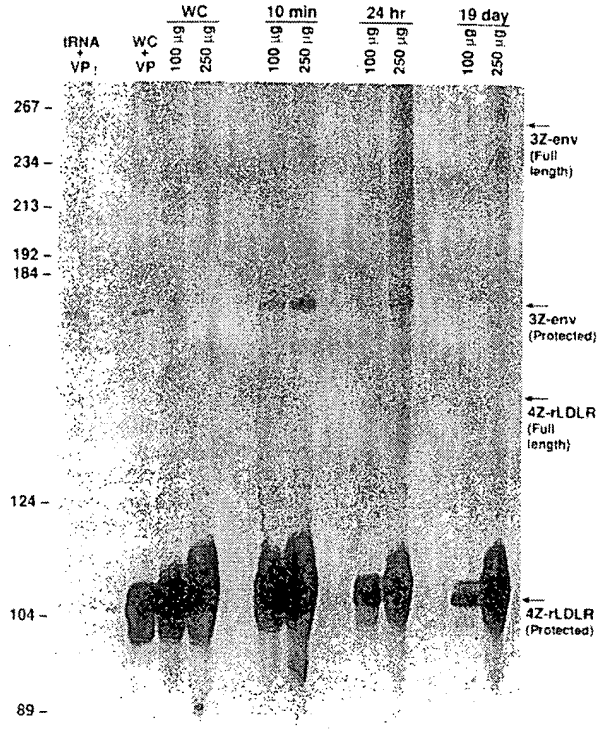

FIG. 4. RNase protection assays. Total cellular RNA samples were hybridized with ^{32}P-labeled RNA probes complementary to viral sequences (3Z-env) and endogenous LDL receptor sequences (4Z-rLDLR) and analyzed for protection from digestion with RNase A. The locations of the full-length and protected RNA probes are noted at right. Individual lanes are indicated at the top of the autoradiograph. tRNA (100 μg) was supplemented with 100 ng of viral producer (VP) RNA; RNA from the liver of a control WHHL (WC) rabbit (100 μg) was supplemented with viral producer RNA (100 ng); and liver RNA (100 μg and 250 μg) was obtained prior to transplantation (WC) as well as 10 min, 24 hr, and 19 days after transplantation with genetically modified hepatocytes. Molecular size markers (in base pairs) are indicated at left.

detected in liver tissue harvested 10 min and 24 hr after transplantation with genetically modified hepatocytes (Fig. 4). Quantitative analysis of this experiment indicated that the viral transcript was present at 1–3% of the level of endogenous LDL receptor mRNA (data not shown). No recombinant transcript was detected in liver tissue harvested at 19 days.

Recombinant gene expression was also characterized at the cellular level by *in situ* hybridization (Fig. 5). The RNA probe complementary to virus-specific sequences provided excellent specificity for this *in situ* detection of human LDL receptor mRNA. *In situ* hybridization was initially performed with the antisense probe on liver that was harvested 24 hr after transplantation of genetically modified hepatocytes. Approximately 1 in 500 to 1 in 1000 cells contained a high density of cytoplasmic grains (10- to 100-fold over background). These positive cells were distributed as single cells in the periportal areas of the liver, suggesting that the infused hepatocytes lodge in sinusoids soon after leaving the portal venule (Fig. 5 *A* and *B*). Hybridization signals were no longer detected in tissues that were analyzed 19 days after transplantation of genetically modified hepatocytes (data not shown). Specificity of this method is supported by the absence of hybridization over background when the antisense probe was hybridized with control WHHL liver (data not shown) or when the sense probe was hybridized with liver from a transplant recipient harvested 24 hr after transplantation (data not shown).

DISCUSSION

We have used an animal model of FH, the WHHL rabbit, to develop therapeutic approaches that involve the transfer of LDL receptor genes into hepatocytes. The strategy described in this report involves isolating hepatocytes from a WHHL rabbit, transducing a functional LDL receptor gene into these cells *in vitro*, and transplanting the genetically modified cells into another WHHL rabbit.

The availability of an authentic animal in combination with sensitive assays for *in vivo* gene expression provide the opportunity to critically evaluate the efficacy of this proposed therapy. The molecular basis and metabolic consequences of the WHHL mutation have been the subject of extensive investigation (4, 7, 15–20). An in-frame deletion in the LDL receptor gene leads to the expression of a dysfunctional receptor molecule that has virtually no detectable activity (15–21). Exposure of WHHL hepatocytes to the recombinant virus produced a mixed population of cells in which 10–20% of the hepatocytes expressed levels of human LDL receptor mRNA (Fig. 1) and protein (5) that exceeded normal endogenous levels by 5- to 10-fold; net expression of human LDL receptor in these cultures was equal to the normal level. Gene replacement was achieved by transplanting a small number of this mixed population of genetically modified WHHL hepatocytes (≈2% of the total hepatocytes in an adult rabbit liver). Functional replacement of LDL receptor activity therefore should be ≈2% of normal in transplant recipients. This prediction is in excellent agreement with quantitative analyses of RNA from liver harvested 10 min and 24 hr after transplantation, which detected the recombinant transcript at 1–3% of the level of the endogenous transcript. This rather modest amount of genetic correction, however, led to a substantial improvement in hypercholesterolemia to 70% of pretreatment levels. This finding is consistent with previous studies of homozygous deficient patients in which the level of residual LDL receptor activity was shown to directly correlate with serum cholesterol levels and progression of coronary artery disease (1, 6). For example, receptor-negative patients (<2% of control receptor activity) have more severe coronary disease and are less responsive to conventional therapies than receptor-defective patients (>2% control residual receptor activity). This also suggests that functionally converting a patient from receptor-negative to receptor-defective status may be metabolically and clinically efficacious.

Metabolic improvements associated with hepatocyte transplantation, however, were not permanent. There are two potential explanations for the apparent deterioration in LDL receptor function *in vivo*. There could be destruction and actual loss of the genetically modified hepatocytes. Alternatively, the cells may engraft, but expression from the recombinant gene may extinguish. In an attempt to differentiate between these possible mechanisms, the integrated provirus was used as a specific and sensitive marker of the genetically modified cells *in vivo*. Proviral DNA was detected in liver of transplant recipients prior to and during the period of metabolic improvement. The provirus was no longer detected in liver tissue after the total cholesterol returned to baseline. This suggests that cell loss is an important factor in the deterioration of *in vivo* LDL receptor function. Specific mechanisms responsible for the loss of hepatocyte engraftment remain unclear. It is possible that graft rejection due to major histocompatibility complex incompatibility of allogeneic cells may contribute to the disappearance of genetically modified cells. Alternative explanations include toxicity due to constitutive overexpression of LDL receptor or graft rejection based on an immunologic response to the human LDL receptor protein.

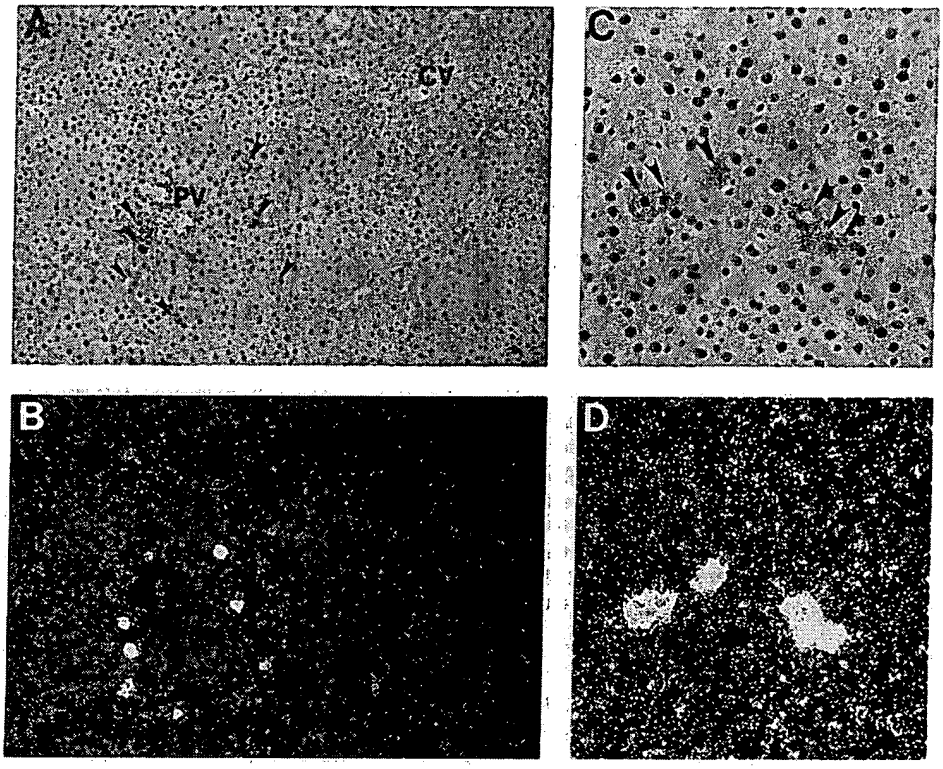

FIG. 5. *In situ* hybridization of liver from transplant recipients. Cryostat sections of liver were hybridized with the virus-specific RNA probe. These tissues were derived from a WHHL rabbit 24 hr after transplantation with LTR-LDLR-transduced hepatocytes. Slides were counter stained with hematoxylin. Bright-field (*A*) and dark-field (*B*) views of an area demonstrating periportal distribution of transplanted cells are shown. PV, portal vessels and a probable biliary ductule; CV, central vein. Cells that are clearly positive in the dark field are indicated by arrowheads in the bright field. Higher power magnification of transplanted hepatocytes visualized on a bright field (*C*) and a dark field (*D*) are shown. (*A* and *B*, ×40; *C* and *D*, ×140.)

In summary, we have used an animal model of FH, the WHHL rabbit, to develop a therapeutic approach in which a normal LDL receptor gene is introduced into genetically deficient hepatocytes, which are transplanted into recipient animals. This intervention resulted in a temporary amelioration of the profound hypercholesterolemia that is characteristic of this disorder. More complete and long-term normalization of the hyperlipidemia could potentially be accomplished with greater expression of the transgene in autologous hepatocytes.

We thank Dr. M. K. Ciechorska for assistance in animal surgery and Dr. V. Rifici for help in determination of plasma lipid subfractions. LDL receptor cDNA sequences were kindly provided by Drs. D. Russell, J. Goldstein, and M. Brown. This work was partly supported by the Howard Hughes Medical Institute (to J.M.W.) and National Institutes of Health Grants R01-DK42193 (to J.M.W.), R01-DK 34357 (to J.R.C.), R01-DK 39137 (to N.R.C.), DK 201928 (Liver Research Center), and HL 41484 (to R.C.M.).

1. Goldstein, J. L. & Brown, M. S. (1989) in *The Metabolic Basis of Inherited Disease*, eds. Scriver, C. R., Beaudeut, A. L., Sly, W. S. & Valle, D. (McGraw-Hill, New York), pp. 1215–1250.
2. Bilheimer, D. W., Goldstein, J. L., Grundy, S. M., Starzl, T. E. & Brown, M. S. (1984) *N. Engl. J. Med.* **311**, 1658–1664.
3. Hoeg, J. M., Starzl, T. E. & Brewer, H. B. (1987) *Am. J. Cardiol.* **59**, 705–707.
4. Goldstein, J. L., Kita, T. & Brown, M. S. (1983) *N. Engl. J. Med.* **309**, 288–296.
5. Wilson, J. M., Johnston, D. E., Jefferson, D. M. & Mulligan, R. C. (1988) *Proc. Natl. Acad. Sci. USA* **85**, 4421–4425.
6. Sprecher, D. L., Hoeg, J. M., Schaefer, E. J., Zech, L. A., Gregg, R. E., Lakatos, E. & Brewer, H. B., Jr. (1985) *Metabolism* **34**, 294–299.
7. Watanabe, Y. (1980) *Atherosclerosis* **36**, 261–268.
8. Barklis, E., Mulligan, R. C. & Jaenisch, R. (1986) *Cell* **47**, 391–399.
9. Trinder, P. (1974) *Ann. Clin. Biochem.* **12**, 226–228.
10. Roth, M. S., Artin, J. H., Bingham, E. L. & Ginsburg, D. (1989) *Blood* **74**, 882–885.
11. Van Beveren, C., Coffin, J. & Hughes, S. (1985) in *RNA Tumor Viruses*, eds. Weiss, R., Teich, N., Varmas, H. & Coffin, J. (Cold Spring Harbor Lab., Cold Spring Harbor, NY), 2nd Ed., pp. 766–783.
12. Yamamoto, T., Bishop, R. W., Brown, M. S., Goldstein, J. L. & Russell, D. W. (1986) *Science* **232**, 1230–1237.
13. Melton, D. A., Krieg, P. A., Rebagliati, M. R., Maniatis, T., Zinn, K. & Green, M. R. (1984) *Nucleic Acids Res.* **12**, 7035–7056.
14. Pinter, J. E. & Lugo, D. I. (1987) in *In Situ Hybridization: Applications to Neurobiology*, eds. Valentino, K. L., Eberwine, J. H. & Barchas, J. D. (Oxford Univ. Press, New York), pp. 179–196.
15. Tanzawa, K., Shimada, Y., Kuroda, M., Tsujita, Y., Arai, M. & Watanabe, H. (1980) *FEBS Lett.* **118**, 81–84.
16. Kita, T., Brown, M. S., Watanabe, Y. & Goldstein, J. L. (1981) *Proc. Natl. Acad. Sci. USA* **78**, 2268–2272.
17. Bilheimer, D. W., Watanabe, Y. & Kita, T. (1982) *Proc. Natl. Acad. Sci. USA* **79**, 3305–3309.
18. Kita, T., Brown, M. S., Bilheimer, D. W. & Goldstein, J. L. (1982) *Proc. Natl. Acad. Sci. USA* **79**, 5693–5697.
19. Pittman, R. C., Carew, T. E., Attie, A. D., Witztum, J. L., Watanabe, Y. & Steinberg, D. (1982) *J. Biol. Chem.* **257**, 7994–8000.
20. Schneider, W. J., Brown, M. S. & Goldstein, J. L (1983) *Mol. Biol. Med.* **1**, 353–367.
21. Yamamoto, T., Bishop, R. W., Brown, M. S., Goldstein, J. L. & Russell, D. W. (1986) *Science* **232**, 1230–1237.

1: Science. 1991 Dec 6;254(5037):1507-9.

Comment in:
- Science. 1991 Dec 6;254(5037):1455-6.

Systemic delivery of recombinant proteins by genetically modified myoblasts.

Barr E, Leiden JM.

Howard Hughes Medical Institute, University of Michigan Medical Center, Ann Arbor 48109.

The ability to stably deliver recombinant proteins to the systemic circulation would facilitate the treatment of a variety of acquired and inherited diseases. To explore the feasibility of the use of genetically engineered myoblasts as a recombinant protein delivery system, stable transfectants of the murine C2C12 myoblast cell line were produced that synthesize and secrete high levels of human growth hormone (hGH) in vitro. Mice injected with hGH-transfected myoblasts had significant levels of hGH in both muscle and serum that were stable for at least 3 weeks after injection. Histological examination of muscles injected with beta-galactosidase-expressing C2C12 myoblasts demonstrated that many of the injected cells had fused to form multinucleated myotubes. Thus, genetically engineered myoblasts can be used for the stable delivery of recombinant proteins into the circulation.

PMID: 1962212 [PubMed - indexed for MEDLINE]